Physics – Uspekhi **39** (9) 925 – 958 (1996)

PHYSICS OF OUR DAYS

PACS numbers: 13.30.Ce, 14.20.Dh

The neutron yesterday, today, and tomorrow

Yu A Mostovoĭ, K N Mukhin, O O Patarakin

Contents

Abstract. The current status of the study of the fundamental properties of the neutron is discussed. Experimental results on the neutron lifetime, β-decay angular correlations, electric dipole moment, and form factor are presented, and comparison with theory is made. Major experimental techniques are described. Exotic neutron features, such as the electric charge, baryon number nonconserving decays, etc., are discussed. The properties and applications of ultracold neutrons, and related problems, are discussed in detail. Some new ideas are suggested and research programs outlined.

Yu A Mostovoĭ, K N Mukhin, O O Patarakin Russian Research Center 'Kurchatov Institute', Institute of General and Nuclear Physics, pl. Kurchatova 1, 123182 Moscow, Russia
Tel. (7-095) 196 76 37, 196 75 71, 196 76 63
Fax (7-095) 196 91 33
E-mail: most@neutron.kiae.su, mukhin@chen.net.kiae.su, patarak@nuc53.kiae.su

Received 23 April 1996
Uspekhi Fizicheskikh Nauk **166** (9) 987 – 1022 (1996)
Translated by T Dumbrajs, edited by A Radzig

1. Introduction

In February 1997, it will have been 65 years since the discovery of one of the fundamental particles, the neutron. Until that discovery, the mankind did not even suspect that all objects around and people themselves consist by half of neutrons and, especially, that these particles, the base of everything that exists, can produce its destruction.

The paper is aimed at acquainting the reader with modern data on properties of a free neutron, its structure, methods of basic experiments by which the data were obtained and with the requirements of theory imposed on their accuracy in subsequent experiments. The paper is organized as follows: Section 2 is devoted to introduction to the problems considered in the paper on the theme "What we know and what we want to know about the neutron?". In particular, in Sections 2.1 and 2.2, we expound the history of the neutron

discovery and the related basic achievements in science and technology. In Section 2.3, we report the fundamental parameters of the neutron which have been determined exactly (spin, parity, etc.) and modern values of those parameters that are being defined more exactly (mass, magnetic moment), but whose more accurate determination, in our opinion, is not an urgent problem at present. Section 2.4 gives a preliminary characteristic of the neutron parameters that are most important for the theory (lifetime, angular correlations, dipole electric moment, etc.) followed with brief comments on their importance.

Section 3 is devoted to the theory of ultracold neutrons (UCN) used in many experiments to be discussed below. In this section, we consider the UCN basic properties (Section 3.1), first experiments with UCN (Section 3.2), modern methods of obtaining and investigating UCN (Section 3.3), some specific set-ups (Section 3.4), and the problem of UCN leakage (Section 3.5).

In subsequent sections, we thoroughly analyze the most essential parameters of the neutron, the procedure of their determination, and the characteristics of importance for modern theory. These are the neutron lifetime (Section 4), angular correlations in β-decay (Section 5), the electric dipole moment (EDM) (Section 6), and the form factor (Section 7). In Section 8, we briefly discuss some exotic properties of the neutron (gravitational interaction, electric charge, polarizability, decay with breaking the baryon number conservation, neutron-antineutron oscillations). In Section 9, some new problems, ideas, and projects are outlined, and conclusions are drawn in Section 10.

The paper is devoted to the 65th anniversary of the neutron discovery. Therefore, some relevant problems (the neutron discovery, UCN physics, EDM, form factor) are of necessity expounded chronologically. Since a review paper covers rather a wide range of information, it is more popular than the original works we have used. Specifically, restricted by the length of the paper, we could not always describe the procedure of data obtaining and interpret the results arrived at in detail. The readers wishing to get a deeper insight into the problem in question are referred to monographs [1 – 6]; whereas those who wish to be acquainted with elementary presentation of the procedure of determining neutron parameters such as m, $\mathbf{S}$, $\boldsymbol{\mu}$, τ, $\mathbf{d}$, angular correlations, etc., can refer to monograph [27].

In writing the review article, we have used original papers published up to the current year and some studies published in 1996. The problems raised in this review are most thoroughly analyzed in the monograph by Yu A Aleksandrov [2], we recommend to the reader. A similar review on the subject was written by A I Frank in 1982 [8].

2. What we know and what we want to know about the neutron

2.1 History of the neutron discovery

The neutron is one of the most ancient objects, as it appeared just after the Big Bang. According to the modern theory of Hot Universe, first neutrons arose during the first few minutes of the Universe's life, i.e. more than 10 billion years ago [9]. Though the first neutrons soon either decayed or were absorbed, they were all the time accompanied by still new neutrons with the properties identical to those of the primary neutrons, which is also true for the today's neutrons.

This neutron 'cycle' in the Nature can be observed in very diverse phenomena. Globally, in the scale of the Universe, these are, for instance, nucleosynthesis, formation of neutron stars or explosions of Supernovae. In the Earth's scale, this is the neutron production near the Earth surface under the action of protons of the primary cosmic component. Deep in the Earth, neutrons arise in (α, n) and (γ, n) reactions, under spontaneous and induced fission and even during the work of a natural nuclear reactor [10]. All these phenomena have started long ago and are still being continued. However, this and the very existence of the neutron have become known to people quite recently. Let us briefly recall the history of the neutron discovery.

Experimentally, neutron was discovered in early 1932 by English physicist J Chadwick, but theoretically, it was long before predicted by E Rutherford. In 1909, E Rutherford detected large-angle scattering of α-particles, and on this basis he created in 1911 the nuclear model of an atom, whereas in further experiments with α-particles, he discovered in 1919 the proton as a constituent of the nuclei and constructed the proton-electron model of a nucleus.

In the Bakerian lecture on this model in 1920, E Rutherford assumed, together with the simplest charged nucleus, the proton, the existence of the simplest neutral nucleus containing the proton and electron, that are strongly (more strongly than in a hydrogen atom) coupled with each other, and predicted its basic properties: zero electric charge, high penetration ability, and strong interaction with nuclei [11].

In his memoirs on the neutron search [12], Chadwick (who was invited by Rutherford to his laboratory as a staff member soon after the above lecture) said that Rutherford gave him convincing evidences in favour of using the neutron to overcome difficulties of the proton-electron model of the nucleus and that they carried out experiments on searching for neutrons many times. However, for some reasons, these experiments failed.

A sequence of experiments that preceded the neutron discovery and played a particularly important role in the 'preparation of the discovery' looks as follows. In 1930, continuing the Rutherford experiments with α-particles, Bothe and Becker found that when these particles irradiate light elements, for instance, Be, the latter emits, instead of protons, intensive radiation slightly absorbed by lead [13]. The measurements showed that a 1 cm thick lead layer absorbs only 20% of that radiation.

In 1931, Curie and Jolio established that the new radiation put in contact with a water-containing (hydrated) substance knocks protons out of it [14 – 16]. It would seem that both the results are consistent with the assumption that particles of the penetrating radiation are hard γ-quanta which knock out protons with the Compton effect mechanism. However, experimenters were confused by a very high energy of knocked-out protons and their large amount. Both these circumstances could not be explained by the Compton effect on a proton. Unfortunately, Curie and Jolio related this incompatibility to the experimental error; but the situation was completely different.

A correct solution to this puzzle was found by Chadwick at the beginning of 1932 who irradiated, with the radiation in question, an ionization chamber filled with hydrogen and nitrogen in turn and then analyzed the values of the energy and momentum of recoil nuclei [17]. It develops that they are consistent with the corresponding conservation laws under the assumption that the recoil nuclei are knocked out not by

massless γ-quanta but by other neutral particles with a mass close to the proton mass. In this way, the neutron was discovered, and soon, in the same 1932, Heisenberg [18] and Ivanenko [19, 20] proposed the proton-neutron model of an atomic nucleus. Both the authors interpreted the neutron as an independent elementary particle with a half-integer spin (not as a compound from the proton and electron). A nucleus with charge Z and mass number A contains Z protons and $(A-Z)$ neutrons with half-integer spins and no electrons. This interpretation removes three basic difficulties of the proton-electron model of the nucleus: inconsistency between spins and magnetic moments of a nucleus and its constituents, and 'very large sizes' of the electron for it being 'placed' in the nucleus.

2.2 Influence of the neutron discovery on the development of science and technology

The neutron discovery and creation of the proton-neutron model of an atomic nucleus initiated both a rapid development of the theory (the theory of β-decay by Fermi [21], the theory of nuclear forces by Yukawa [22], the theory of chain nuclear reaction by Zel'dovich and Khariton [23]) and experimental study of neutron properties and peculiarities of its interaction with matter (the neutron moderation and induced β-radioactivity, Fermi [24]; uranium fission, Hahn and Strassmann [25]; detection of the 93rd element, McMillan and Abelson [26]).

All these studies and discoveries resulted in widely known achievements in science and technology. This is first of all the nuclear power engineering proper for military and peace purposes: nuclear weapons, atomic electric power stations, atomic submarines and surface ships, atomic stations of heat supply, atomic electric power plants, reactors – distillers, reactors – thermal converters, high-temperature reactors for metallurgy, and research reactors. Second, this is an extended production of radioactive isotopes, specifically, for preparing the isotopic sources of current widely utilized in automatic meteorological stations, cosmic stations, satellites, etc. The neutrons are used in geology for prospecting for minerals (neutron coring), in technology (for automation), in medicine (diagnosis and treatment), in biology (genetics), and so on.

There was a tremendous growth in neutron physics that gave rise to independent sciences: neutron spectroscopy, neutron optics, neutron diffraction analysis, neutron flaw detection, neutron radiography, neutron activation analysis, etc.

We restrict ourselves to this brief list of achievements resulted from the neutron discovery. Those who wish to know about the neutrons in greater details as well as about the physics of fission, chemistry of transuranium elements and other related problems are referred, for example, to the monograph [27].

2.3 Fundamental properties of the neutron

The neutron belongs to the baryon octet of $1/2^+$ particles, i.e. it has baryon number $B=1$, spin $1/2$ (in $\hbar$ units) and positive intrinsic parity. Being a fermion, the neutron obeys the Fermi – Dirac statistics. Together with the proton, it forms an isotopic doublet of nucleons with isospin $\mathbf{T}=1/2$. The isospin projection for the neutron is $-1/2$ (for the proton, $+1/2$).

The above properties of the neutron can be considered today as determined exactly. Besides, the neutron is specified by a number of parameters (electric charge, mass, magnetic moment) whose values are known with a very high accuracy, nevertheless, still new attempts are being undertaken for their more precise determination. Among these parameters, the neutron electric charge stands by itself. Though it equals zero to a high accuracy, we will see below (see Section 8) that in this case a more precise determination is of fundamental importance (zero or still not zero!). As for the mass and magnetic moment, experimental accuracies of their determination have long exceeded theoretical possibilities for their explanation. Therefore, we shall only present brief comments on them and the corresponding modern experimental data.

Since the neutron has no electric charge, its mass can be determined by comparing it with masses of other nuclei measured by the method of mass spectrometry. Just in this way, Chadwick has first shown that the mass of the neutron approximately equals that of the proton. Precise value of the neutron mass is determined from the energy balance of nuclear reactions with neutrons involved (either as a projectile inducing reaction or as its product). The modern value of the neutron mass [28] is adopted as follows:

$$m_{\mathrm{n}} = 1.008664904(14)\ \mathrm{u} = 939.56563(28)\ \mathrm{MeV}\,. \qquad (1)$$

That the neutron has a magnetic moment was assumed soon after its discovery. From comparison of magnetic moments of the proton, deuteron, and other nuclei it followed that the neutron should possess a magnetic moment of order $-2\mu_{\mathrm{N}}$, where μ_{N} is the nuclear magneton equal to $e\hbar/2m_{\mathrm{p}}$ (e is the electric charge; $\hbar$, the Planck constant; m_{p}, the proton mass).

Experimentally, the neutron magnetic moment was measured by the nuclear magnetic resonance method. At present, its most exact value accounts for

$$\mu_{\mathrm{n}} = -1.9130428(5)\mu_{\mathrm{N}}\,. \qquad (2)$$

The minus sign ahead of the numerical value indicates that the magnetic moment of the neutron is directed opposite to its spin.

A nonzero magnetic moment of the neutron whose electric charge is zero seems to be an anomaly. The same concerns the magnitude of the proton magnetic moment ($\mu_{\mathrm{p}} \approx 2.79\mu_{\mathrm{N}}$) whose charge equals unity. It was noticed therewith that both anomalous parts of the magnetic moments are approximately equal to each other:

$$\mu_{\mathrm{p}} - 1 \approx |\mu_{\mathrm{n}} - 0|\,, \qquad (3)$$

which points to the identical nature of their origin. Though, as already mentioned, there is still no theory of the neutron magnetic moment, this equality can be understood qualitatively by assuming that the neutron (proton) exists for a certain time as the Dirac proton (neutron) surrounded by a 'cloud' of negatively (positively) charged mesons 'rotating' around it. Notice also that the ratio of magnetic moments of the proton and neutron equals $2.79/(-1.91) \approx -3/2$, which is compatible with the primary ideas of quark structure of nucleons (p = uud, n = udd)†.

And finally, the third group involves those neutron parameters whose values are still unsatisfactory for physicists, and it is just these parameters that require a more thorough discussion. They include, besides the electric charge

† At present, these ideas are further developed in the Cloudy Bag Model (see Section 8.3).

mentioned, the neutron lifetime τ_n, angular correlations between the neutron spin and momenta of its decay products, the electric dipole moment and form factor of the neutron, its polarizability, and some others. In view of their particular importance, they will be considered in detail in separate sections of the paper. However, here we consider it necessary to make short introductory comments.

2.4 Theoretical requirements on the accuracy of measuring the most important neutron parameters

The mass of the neutron ($m_n \approx 939.57\ \text{MeV} = 1838.7 m_e$) is by $2.6 m_e$ larger than that of the proton ($m_p \approx 938.27\ \text{MeV} = 1836.1 m_e$) and by $1.6 m_e$ larger than the sum of the electron and proton masses. Therefore, the β^--decay of a neutron into a proton and an electron is allowed in energy. Since spins of all the particles are half-integer, then in accordance with the angular momentum conservation law the neutron β-decay should be accompanied by emission of one more particle of half-integer spin with a very small or zero mass, according to the energy conservation law.

That this particle should exist in nature was theoretically predicted by Pauli [29, 30] from the analysis of β-spectra of radioactive nuclei at the end of 1930, i.e. a year before the neutron discovery; therefore, it was initially given that name. However, once the true neutron was discovered, Fermi, for preventing confusion, 'rechristened' the new particle as neutrino.

Besides the above properties, the neutrino possesses a zero electric charge, a zero magnetic moment, and an extremely high penetrability. Therefore, its existence was proved only in 1953 – 56 in direct experiments by Reines and Cowan [31].

Nowadays, known are three types of the neutrino: electron ν_e, muon ν_μ, and tau-neutrino ν_τ, each having an antiparticle ($\tilde{\nu}_e$, $\tilde{\nu}_\mu$, and $\tilde{\nu}_\tau$). The β-decay of the neutrino and β^--radioactive nuclei is followed by emission of the electronic antineutrino $\tilde{\nu}_e$ according to the scheme:

$$n \to p + e^- + \tilde{\nu}_e\,, \qquad (A, Z) \to (A, Z+1) + e^- + \tilde{\nu}_e\,. \quad (4)$$

The β-decay of β^+-radioactive nuclei is accompanied by transformation of a proton of a nucleus into a neutron, a positron, and an electronic neutrino:

$$p \to n + e^+ + \nu_e\,, \qquad (A, Z) \to (A, Z-1) + e^+ + \nu_e \quad (5)$$

(the first scheme in (5) is symbolical as the β^+-decay of the free proton is forbidden in energy).

Neutrinos and antineutrinos of all types participate only in weak interactions. Because of this, the study of processes with the neutrinos involved is important for constructing the theory of weak interactions. Especially important is the study of β-decay of the neutron characterized by the exactly known matrix elements that determine the β-decay probability, which in turn allows the neutron β-decay constant $\lambda^{00}_{\tau_n}$ to be estimated from the experimental lifetimes of the neutron τ_n and nuclei with $(0^+ - 0^+)$ transitions.

The β-decay by scheme (4) was first observed in 1948 – 50, practically simultaneously in three countries: the USSR, Canada, and the USA (see Section 4). First estimates of the neutron lifetime gave $\tau_n = 10 - 20$ min. Its modern value averaged over many experiments equals $\tau_n = (887 \pm 1.6)$ s, however, in view of extreme importance of this parameter, still new attempts for it to be defined more exactly are being undertaken.

A second important parameter specifying the neutron β-decay is angular correlations between the neutron spin $\mathbf{S}_n$ and momenta of an electron ($\mathbf{p}_e$) and an antineutrino ($\mathbf{p}_{\tilde{\nu}}$). To get a complete picture, 4 types of correlations, $\mathbf{p}_e\mathbf{p}_{\tilde{\nu}}$, $\boldsymbol{\sigma}_n\mathbf{p}_e$, $\boldsymbol{\sigma}_n\mathbf{p}_{\tilde{\nu}}$, and $\boldsymbol{\sigma}_n[\mathbf{p}_e\mathbf{p}_{\tilde{\nu}}]$, are studied experimentally. Coefficients of each of the first three correlations allow one to compute the β-decay constant λ_c, while the fourth one is used for verifying T-invariance. Both the constants ($\lambda^{00}_{\tau_n}$ and λ_c) should be equal to each other in the framework of the (V – A)-version of weak interaction theory, whereas their difference may suggest that the theory is to be supplemented with a small admixture of the (V + A) type ('right-handed currents') fraught with far-reaching consequences (for more details on vector (V), axial-vector (A), and other variants of weak interaction theory, see Section 5).

The accuracy of measurement of $\lambda^{00}_{\tau_n}$ and λ_c achieved by 1990 allowed one to assume a small difference between them. Therefore it is clear that both the constants should be determined still more exactly, i.e. the lifetimes of the neutron τ_n and nuclei with $(0^+ - 0^+)$ transitions as well as angular correlations between $\boldsymbol{\sigma}_n$, $\mathbf{p}_e$, and $\mathbf{p}_{\tilde{\nu}}$ have to be measured especially accurately. Besides, a more exact definition of these quantities will allow a re-estimation of limits of possible contributions of S- and T-versions into the theory of weak interactions consistent with experiments on the neutron β-decay.

One more important parameter of the neutron is the electric dipole moment $\mathbf{d}_n$. The neutron has no electric charge but, according to the quark model, it consists of three charged quarks [n = udd, where $B_u = B_d = 1/3$, $q_u = (+2/3)|e|$, $q_d = (-1/3)|e|$]. Therefore, in principle, one can admit that $d_n \neq 0$ for the neutron, the more so as a zero charge does not prevent it to possess a considerable magnetic moment.

It is important to know the quantity d_n for the theory because the knowledge of that parameter is a kind of a 'touchstone' for the test of T-invariance of various interactions and, in particular, in searching for the interaction responsible for breaking the T-invariance discovered in the K-meson decay in 1964. According to the modern theory, a particular mechanism of that breaking can be established on the basis of $\mathbf{d}_n$ value.

Constant interest of theorists is taken in one more parameter of the neutron, its form factor, that characterizes the spatial distribution of the electric charge and magnetic moment. According to modern ideas, they are both determined by the distribution of colour u and d quarks over the neutron.

At last, physicists are always interested in all sorts of exotics (which can in time become a physical reality). In this review, we decided to refer the neutron electric charge and polarizability, the decay with breaking of the baryon number conservation law ($\Delta B = 1$), and neutron-antineutron oscillations ($\Delta B = 2$) to this exotics. All above is, of course, very essential for the theory development as being related to fundamental hypotheses on the violation of conservation laws.

3. Ultracold neutrons

Experiments on the study of neutron properties expounded above cannot be carried out without a power source of neutrons, a nuclear reactor. The spectrum of neutrons emitted by a standard nuclear reactor whose core contains a moderator (a reactor on thermal neutrons) corresponds to the Maxwellian distribution over velocities for a given temperature. At temperature $T = 300$ K, the energy of neutrons

corresponding to the most probable velocity equals $\varepsilon = kT = 0.025$ eV, where $k = 0.862 \times 10^{-4}$ eV deg^{-1} is the Boltzmann constant. Neutrons with energies close to kT are referred to as thermal neutrons. Usually, the energy range for thermal neutrons is considered to be $5 \times 10^{-3} - 0.5$ eV. Neutrons with energies $\varepsilon < 5 \times 10^{-3}$ eV (conditionally, down to $\sim 10^{-4}$ eV) are called cold neutrons; whereas those with energies $\varepsilon > 0.5$ eV (conditionally, up to 10^4 eV), resonance neutrons. Below the lower limit of the region of cold neutrons (CN) there are the regions of very cold neutrons (VCN) with conditional limits $10^{-7} - 10^{-4}$ eV and ultracold neutrons (UCN) with energies of order 10^{-7} eV (Table 1).

It is easy to see that for advantageous conducting of experiments, we shall discuss in detail, neutrons as slow as possible are required because the properties of a neutron, for instance, β-decay, are studied during its movement through an experimental set-up and, consequently, it is desirable that the neutron would pass through the set-up as long as possible. The slower is the neutron, the greater is the probability of its decay inside the set-up.

First experiments were carried out on the beams of thermal neutrons with the velocity of 2200 m s^{-1}. Therefore, a neutron was inside the set-up of standard sizes (about 20 cm) approximately 10^{-4} s; and since the lifetime of the neutron $\tau_n \approx 10^3$ s, the probability of its decay inside the set-up is extremely small, 10^{-7}. One may ask, why beam experiments were not based on slower neutrons contained in the energy spectrum. The answer is rather simple: there are very few of them and it is difficult to extract them. Fraction of CN, VCN, and UCN is the smaller, the lower is the neutron energy, and for UCN it amounts only to 10^{-11}. The UCN are formed out of thermal neutrons not in consequence of their further moderation but in a very rare process of the only inelastic collision accompanied by the loss of almost the whole energy of a thermal neutron [32].

It is, in principle, possible to increase the number of neutrons with $\varepsilon < 0.025$ eV by passing the beam of reactor neutrons through an extra moderator, a container with liquid hydrogen ($T \approx 23 - 25$ K). Then in the process of further thermalization, the reactor neutrons will attain a new thermal equilibrium at the temperature of liquid hydrogen, and in consequence the Maxwellian spectrum maximum will shift to the energy range of cold neutrons whose mean velocity is around 600 – 800 m s^{-1} (a cold source).

Thus, in the CN case, there is a gain at the expense of decreasing the velocity of neutrons without losses in the beam density. Furthermore, the amount of resonance neutrons in the CN spectrum, which are in some cases extremely harmful (see Section 4), is diminished. Therefore, following first experiments on thermal neutrons, experimenters began to utilize cold neutrons, and we shall also discuss some relevant questions in this review.

However, it is clear that the fraction of VCN, and especially that of UCN, cannot be increased in this way since this requires an absolutely unattainable temperature of the extra moderator ($\sim 10^{-3}$ K for UCN). Therefore, the gain in the UCN velocity (≈ 5 m s^{-1}), as compared to the CN one, cannot be put to use in beam experiments. Again, this gain is not so large; anyhow, UCN strike, in a literal sense, across the set-up in a time of about 0.05 s. That is quite another thing if neutrons could completely be stopped inside the set-up and one could simply wait for their having decayed! This wish turns out to be not so fantastic.

3.1 Key properties of UCN

A remarkable property of UCN is their capacity for complete internal reflection from the vacuum – matter interface at any angle of incidence. In other words, though UCN cannot be stopped, they may be locked in the set-up for a long time, ideally, for all their life. In that case, the measurement of τ_n will be no more difficult than measurements with fixed radioactive targets.

Here we have drawn an ideal picture. Naturally, years and years of very hard work of scientists have been required for approaching that picture. Let us see how theoretical views about the UCN properties were developed in time, recall the first appropriate experiments, and outline the modern situation.

The UCN do really possess remarkable properties. Owing to an extremely small velocity, their de Broglie wavelength $\lambda = h/mv$ equals 10^{-5} cm, i.e. wave properties of UCN should appear not in their interaction with separate atoms and, moreover, with nuclei of characteristic sizes 10^{-8} and 10^{-12} cm, respectively, but in interaction with a substance as a whole and should be specified by properties of that substance as a neutron scatterer. These include the concentration of nuclei N and the length b of coherent scattering of neutrons from a bound nucleus (for most substances $b > 0$). In 1959, Zel'dovich showed [33] that UCN with energies $\varepsilon < E_b$, where

$$E_b = \frac{h^2 N b}{2\pi m}, \tag{6}$$

should be reflected from the substance boundary with given N and b irrespective of the incidence angle, and hence, should be accumulated in a closed cavity made of that substance (a 'neutron bottle'). The corresponding boundary velocity is defined by the formula

$$v_b = \sqrt{\frac{2E_b}{m}} = \frac{h}{m}\sqrt{\frac{Nb}{\pi}}. \tag{7}$$

In Table 2, we report the values of E_b and v_b for several materials most frequently utilized in the UCN experimental physics.

Table 1

Groups of neutrons	Energy ε, eV	Velocity v, m s^{-1}	Wavelength λ, A
Resonance	$0.5 - 10^4$	$3.8 \times 10^3 - 1.4 \times 10^6$	$2.86 \times 10^{-3} - 0.405$
Thermal	$5 \times 10^{-3} - 0.5$	$9.8 \times 10^2 - 9.8 \times 10^3$	$0.405 - 4.05$
$(kT)_{300}$	0.025	2.2×10^3	1.81
Cold	$10^{-4} - 5 \times 10^{-3}$	$1.4 \times 10^2 - 9.8 \times 10^2$	$4.05 - 28.6$
Very cold	$10^{-7} - 10^{-4}$	$4.4 - 140$	$28.6 - 904$
Ultracold (conditionally*)	$\sim 10^{-7}$	~ 4.4	~ 900

* More precisely, the UCN energy is determined by properties of a material wherewith the neutrons contact: $\varepsilon_{UCN} < E_b$ (see Table 2).

Table 2

Material	E_b, 10^{-7} eV	v_b, m s^{-1}
Al	0.55	3.2
Mg	0.605	3.36
Cu	1.72	5.7
C	1.94	6.1
Be	2.40	6.8
Fe	3.4 and 0.8	7.95 and 4.37
Co	1.66 and −0.488	5.56 and 0
Ni	2.806 and 2.074	7.23 and 6.21

We recall that, by definition, just the neutrons with kinetic energy $\varepsilon < E_b$ are said to be ultracold.

Notions of ε and E_b are tightly connected with the view of the index of refraction n for a substance with parameters N and b with respect to a neutron wave. This results from the following simple (not very rigorous) consideration†.

By analogy with geometrical optics, the refraction index is defined by the formula

$$n = \frac{\sin\varphi}{\sin\varphi'} = \frac{\cos\psi}{\sin\varphi'} = \frac{v'}{v} = \frac{K'}{K}\,, \tag{8}$$

where φ is the angle of incidence; φ', that of refraction; ψ, the glancing angle; v, K and v', K' are the velocities and wave numbers of neutrons in vacuum and matter, respectively (Fig. 1). Consequently,

$$n^2 = \frac{v'^2}{v^2} = \frac{\varepsilon'}{\varepsilon} = \frac{\varepsilon - \bar{U}_{\text{eff}}}{\varepsilon} = 1 - \frac{\bar{U}_{\text{eff}}}{\varepsilon}\,, \tag{9}$$

where ε and ε' are the neutron kinetic energies in vacuum and matter, respectively; $\bar{U}_{\text{eff}}$ is the mean effective repulsive potential characterizing interaction of neutrons with medium and which is to be naturally identified with E_b (UCN with $\varepsilon < E_b$ cannot overcome a barrier of height $\bar{U}_{\text{eff}}$ at any incidence angles). Then,

$$n^2 = 1 - \frac{E_b}{\varepsilon}\,, \tag{10}$$

which upon substitution of E_b defined by (6) gives

$$n^2 = 1 - \frac{h^2 Nb}{\pi m^2 v^2} = 1 - \frac{\lambda^2 Nb}{\pi}\,. \tag{11}$$

Now, we shall analyze the total expression

$$n^2 = \frac{\sin^2\varphi}{\sin^2\varphi'} = \frac{\cos^2\psi}{\sin^2\varphi'} = 1 - \frac{E_b}{\varepsilon} = 1 - \frac{\lambda^2 Nb}{\pi}\,. \tag{12}$$

As we are interested only in the neutrons with $\varepsilon \approx E_b$, it is clear that n^2 can assume two values, $0 < n^2 < 1$ for $\varepsilon > E_b$ and $n^2 < 0$ for $\varepsilon < E_b$ (imaginary refraction index). According to our optical analogy, the first case is pictured in Fig. 1a – c. At small incidence angles φ (Fig. 1a), the intensity of a reflected wave should be very small (a thin line in Fig. 1a), and that of a refracted wave is close to a maximum. With growing angle φ, the intensity of the reflected wave increases; while that of the refracted wave diminishes (Fig. 1b). At a certain $\varphi = \varphi_{cr}(\varepsilon)$, the angle of refraction φ' reaches the value 90°, and the refracted wave intensity vanishes, whereas the intensity of reflected wave becomes maximal, i.e. the phenomenon of total internal reflection of neutrons from the 'vacuum–medium' interface will set in and for all angles $\varphi > \varphi_{cr}(\varepsilon)$ it will be retained (Fig. 1c).

From expression (12) and Fig. 1c it is seen that φ_{cr} and ψ_{cr} obey the condition

$$\sin\varphi_{cr} = \cos\psi_{cr} = n\,, \tag{13}$$

which for small glancing angles gives

$$\psi_{cr} \approx \sqrt{1 - n^2} = \sqrt{\frac{E_b}{\varepsilon}}\,, \tag{14}$$

i.e. with increasing energy the angle ψ_{cr} decreases by the law $1/v$, and for thermal neutrons equals approximately 10′. On the contrary, at energies close to 10^{-7} eV, for instance, at $\varepsilon = 2\langle E_b\rangle \approx 4 \times 10^{-7}$ eV, when $n^2 = 0.5$ and $\cos^2\psi_{cr} = n \approx 0.7$, we get $\psi_{cr} \approx 45°$.

In the second case ($\varepsilon < E_b$, $n^2 < 0$), no matter how large is the angle of incidence, we obtain a meaningless expression $\sin^2\varphi' < 0$ that can be interpreted as the absence of the effect of refraction, i.e. as the total internal reflection of neutrons from the 'vacuum – substance' interface at any angles of incidence (Fig. 1d).

In 1960, Vladimirskiĭ pointed out that the UCN kinetic energy (around 10^{-7} eV) is comparable with the energy of interaction between the magnetic moment of a neutron $\mu_n = -1.91\mu_N = 6.03 \times 10^{-8}$ eV T^{-1} and a magnetic field with induction $B = 2$ T [34]. Therefore, UCN can be kept far from the vessel walls by establishing a nonuniform magnetic field with induction of the same order of magnitude ('a magnetic bottle'). In view of this, it is clear that for ferromagnets with the induction of saturation B the boundary energy E_b can assume two values:

$$E_b = \frac{h^2 Nb}{2\pi m} \pm |\boldsymbol{\mu}\mathbf{B}|\,. \tag{15}$$

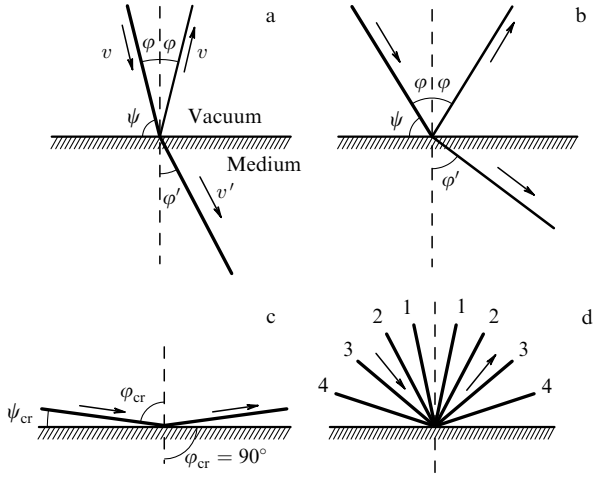

Figure 1. The scheme of refraction of a neutron wave on the 'vacuum – medium' interface: v and v' are the velocities of neutrons in vacuum and a medium, respectively; φ is the angle of incidence; φ', that of refraction; ψ, the glancing angle. (a) $\varepsilon > E_b$, small φ; (b) $\varepsilon > E_b$, intermediate φ; (c) $\varepsilon > E_b$, total internal reflection for $\varphi > \varphi_{cr}$; (d) $\varepsilon < E_b$, total internal reflection at any φ angles.

† A more strict consideration can be found, e.g., in monograph [27].

In particular, for iron $E_b^{(1)} = 3.4 \times 10^{-7}$ eV and $E_b^{(2)} = 0.8 \times 10^{-7}$ eV (whereas for Co even $E_b^{(2)} < 0$ eV, see Table 2).

Let us illustrate the role of an extra boundary energy $\pm|\boldsymbol{\mu}\mathbf{B}|$ by the example of production of polarized thermal neutrons by the method of reflection from the cobalt mirror. According to formula (14), the critical glancing angle in this case for $E_b^{(1)}$(Co) equals

$$\psi_{cr}^{Co} = \sqrt{\frac{E_b^{(1)}}{\varepsilon_{ter}}} = \sqrt{\frac{1.66 \times 10^{-7}}{2.5 \times 10^{-2}}} = 2.58 \times 10^{-3} \text{ rad} \sim 9'. \quad (16)$$

It is clear that at this angle, reflected will be only the neutrons with one of two possible directions of the spin (magnetic moment), whereas for the other direction $E_b^2(\text{Co}) < 0$, and the corresponding neutrons will not reflect from the mirror, rather, they either will pass through it or will be absorbed by it.

Formula (15) was derived under an implicit assumption that a neutron moves in a horizontal plane, for instance, along a horizontally placed neutron guide. If, nevertheless, by experimental conditions, neutrons can move upwards (downwards), their kinetic energy will decrease (increase) owing to the gravitation interaction (see Section 8.1). Clearly, for neutrons with a given (fixed) initial energy this implies one more term to appear in the expression for the boundary energy which increases (diminishes) it by mgH, where g is the acceleration due to gravity and H is the change in height. When the height is measured in meters, the value of mg should be taken as 1.03×10^{-7} eV.

So, the final expression for E_b looks as follows:

$$E_b = \frac{h^2 Nb}{2\pi m} \pm mgH \pm |\boldsymbol{\mu}\mathbf{B}|, \quad (17)$$

where the plus (minus) sign ahead of the gravitation term stands for the motion up (down). Then, instead of formula (11) for the index of refraction of neutrons with a *fixed* initial energy we obtain

$$n^2 = 1 - \frac{h^2 Nb}{\pi m^2 v^2} \pm \frac{2gH}{v^2} \pm 2\frac{|\boldsymbol{\mu}\mathbf{B}|}{mv^2}, \quad (18)$$

where the minus (plus) sign ahead of the gravitation term corresponds to the motion up (down). In this case, the neutron energy being fixed is seen from the formula itself (all terms contain the same quantity v^2).

3.2 First experiments with UCN

During the first years of the research on UCN, they were extracted from the spectrum of reactor neutrons with the use of tubes bent in a horizontal plane (neutron guides) and fabricated from a material with a sufficiently high boundary energy E_b. In this case, UCN with $\varepsilon < E_b$ will go along the tube following its bends, whereas faster neutrons will pass directly through walls of the tube (or will be absorbed in them).

To improve the parameters of the UCN beam, a small (usually, hydrogen-containing) moderator, a converter, was installed at the neutron-guide entrance. Some neutrons of those reaching the converter, upon being inelastically scattered, can lose so high part of the energy in it that they become UCN and emerge from its surface to the neutron guide. In this case, the UCN source comprises a flat thin (of an order of the mean free path) surface layer of the converter, which suited experimenters. Obviously, the converter boundary energy E_b^c should be lower than that of the neutron guide E_b^n since ε of UCN escaped from the converter grows across its surface by E_b^c †.

The first experiments on extraction of UCN from a reactor with the use of curved neutron guides, application of a converter and on the proof of the UCN storing effect (up to 30 s) in a set-up were carried out by the group of Shapiro in 1968–70 [35–38]. In subsequent studies of this group [39–41], various constructions of converters (including those with cooling) were examined, a neutron guide was employed with an elbow rotating around the horizontal axis (for changing the UCN spectrum due to gravitation interaction), the UCN yield on beams from different reactors including the one of a high flux was investigated, and so on. The UCN storage time was increased in those studies up to 250 s [40]; earlier studies have been reviewed elsewhere [32].

Another way of studying the properties of very slow neutrons was realized in 1969–71 in Münich (Germany) by Steyerl [43, 44] who constructed a long (11 m) slightly bent ($R = 35$ m) vertical channel. Clearly, the neutron energy in a channel like that should diminish with changing the height and reach the values typical of UCN at the very top.

In 1976, Antonov et al. [45] showed that except for neutron guides, the UCN can be transported from place to place directly in a 'bottle'. In this case one should be particularly careful, not accelerating, when possible, the bottle; this acceleration can supply an additional energy to neutrons and they can partly be 'tipped out' of the corked bottle through its walls.

The above-mentioned idea of the UCN magnetic storage [34] was first demonstrated experimentally in 1976 in studies by Abov et al. [46] and by Kosvintsev et al. [47] in which the UCN storage vessel was surrounded by coils with current ~ 1000 A. The storage time in these first experiments was small enough, but as far as in 1981 it was increased up to 140 s [48]; whereas in 1983, to 300 s [49].

3.3 Modern methods of producing and studying UCNs

The high-density UCN beams from research reactors of high neutron flux are obtained with the use of CN intensive sources from which UCN are extracted either directly or indirectly, through the spectral conversion of CN into UCN [50]. The CN source comprises usually a small (about 1 l) volume of an extra moderator cooled down to cryogenic temperatures and placed into the reactor domain with a maximal flux of thermal neutrons. Its operation was described at the beginning of Section 3. The fraction of UCN in the CN spectrum is about 2 orders as large as that in the spectrum of thermal neutrons and amounts to around 10^{-9}.

Studies of various moderators carried out at Gatchina [51] have shown that their efficiency as sources of UCN increases when H_2 is changed by D_2, and still better, by the mixture of 40% H_2 and 60% D_2, and when the temperature is lowered below the boiling point of a liquid. The thickness of a moderator in a cold source (about 10 cm) is, as a rule, insufficient for complete thermalization of neutrons at a new temperature; however, this does not visibly affect the effi-

† The barrier of height $U_{eff} = E_b$ exists also for neutrons emitted from a substance into vacuum. Therefore, converters with low values of $E_b < E_b^n$ are especially important when horizontal neutron guides are used as wherein there is no effect of the gravitation deceleration of CN and UCN from a reactor source (being able to have $E_b > E_b^n$).

ciency of UCN formation because an extra moderator of the cold source behaves like the above-described convertors emitting UCN from a thin surface layer.

Studies on the ways of extracting the UCN from a cold source have shown that it is preferable to employ a vertical scheme of the extraction both for the direct and indirect ways of UCN production. The experience in utilizing neutron guides of different construction has led to the conclusion that neutrons, being extracted horizontally, meet in their motion more various structural obstacles like, for instance, 'small windows' than when being extracted vertically. Besides, in view of the gravitational deceleration of neutrons in their motion upward, the vertical position of a neutron guide leads to a decrease in the number of reflections, and hence, the losses.

For the neutron guide being efficient as a conductor of CN, VCN, and UCN to the place of their utilization, of great importance is the material of the guide and quality of its surface. One of the best material is a nonmagnetic alloy of ^{58}Ni with Mo used at Gatchina [51, 52]. This alloy possesses a very high boundary velocity $v_b = 7.8$ m s^{-1} and favourable metallurgical properties. Besides, nonmagnetic materials are better than magnetic ones because there is no diffuse scattering by magnetic domains. Of no lesser importance is the progress achieved in improving the quality of surfaces of pure metallic mirrors and tubes that was possible owing to the copying technique [53] developed in Garching and Grenoble. This technique makes it possible to transfer the microscopic planeness of a glass surface onto a metal.

Before we proceed to describe concrete modern experimental apparatus for extracting and studying UCN, let us briefly dwell upon general principles laid before their construction.

Owing to the property of complete internal reflection and the growth of reaction cross sections for slow neutrons by the $1/v$ law, the UCN cannot pass through structural materials, for instance, fly out from deep within a cold source. Therefore, efficient use of the UCN requires them to be produced out of faster neutrons in the region immediately adjacent to the experimental set-up or in the neutron guide. As could be clear from all said above, this possibility may be realized by using vertical (or slightly deviated from vertical) neutron guides, converting CN into UCN with the help of special devices, and utilizing cooled converters. And, finally, UCN can be accumulated by using the principle of magnetic storage described in Section 3.1.

3.4 Some particular experimental facilities

3.4.1 Set-up (Fig. 2) for obtaining UCN and polarized CN on the VVR-M reactor at the St Petersburg Institute of Nuclear Physics (PINPh) in Gatchina [51]. The scheme of the above set-up created at Gatchina [51] is drawn in Fig. 2. The source of cold neutrons is a vessel with liquid hydrogen with a volume of about 1 l dipped into the core centre of the reactor where the flux of thermal neutrons equals $(1.5-2)\times 10^{14}$ cm^{-2} s^{-1}. Heating of a cryogenic device was reduced to an acceptable level (2 kW) through the lead shield around the source.

The vertical neutron guide for obtaining polarized cold neutrons is equipped with a solenoid for magnetizing the Co-mirrors, a shutter blocking the beam, and a flipper for the neutron spin-flip. The flux density of polarized neutrons equals 6×10^8 cm^{-2} s^{-1}, and the total cross section of the beam, 12×4 cm^2. The UCNs are extracted from the cold

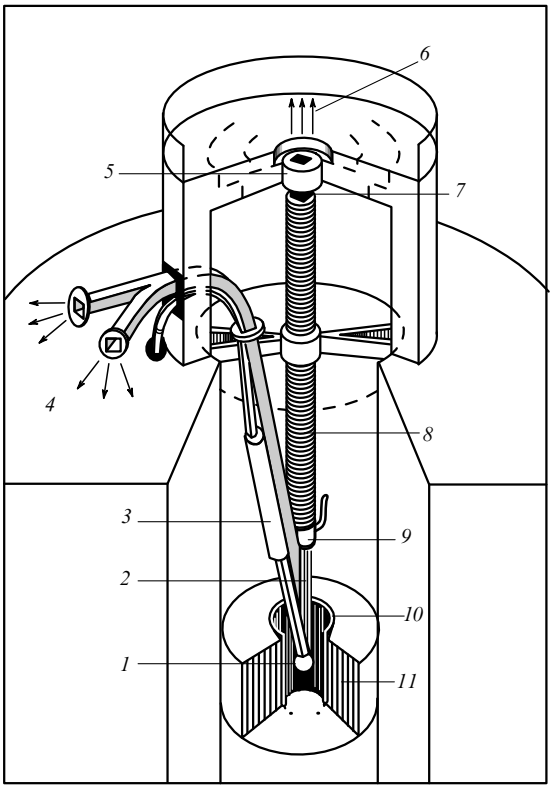

Figure 2. The scheme of the source of UCN and polarized CN on the VVR-M reactor at Gatchina: *1* — liquid-hydrogen source, *2* — foil separator of CN and UCN, *3* — H_2 heat exchanger, *4* — UCN, *5* — flipper, *6* — polarized CN, *7* — ^{6}Li shutter, *8* — solenoid, *9* — water seal, *10* — lead shield, *11* — reactor core.

source by means of the second neutron guide (slightly deviating from vertical) that is at the end splitted into two arms, each 40 cm^2. Close to its upper part, the neutron guide is highly curved ($R = 1$ m) for selecting neutrons with velocities smaller than 18 m s^{-1}. Maximal yield of UCN was obtained when the CN source was filled with liquid D_2 at a temperature of 17 K. Selection of UCN was carried out by the time-of-flight method, both with the open and closed shutter.

3.4.2 Turbine source of UCN on the high-flux reactor at the Laue – Langevin Institute (LLI) in Grenoble. The scheme of the turbine source is shown in Fig. 3a taken from Ref. [50]. Here the cold source is taken to be a vertically placed vessel with cavity of liquid D_2 in whose throat there is inserted a vertical neutron guide for conducting VCN from the cold source to the neutron turbine. In the turbine, the neutron beam of velocity 50 m s^{-1} transforms into an intensive beam of UCN by multiple total reflection of neutrons from semicircular cylindrical 'blades' mounted along the turbine circumference of diameter 1.7 m and a linear velocity 25 m s^{-1} in the direction of neutron motion (Fig. 3b). In this case, in the coordinate system coupled with a blade the neutron velocity equals 25 m s^{-1} and has the same direction. Upon about 10 successive reflections, a neutron preserving the absolute value of the velocity will fly in the same coordinate system opposite to the blade motion, i.e. it will become ultracold in the laboratory frame of reference (Fig. 3c). The UCNs leave the turbine almost perpendicular to its plane in the form of a wide-diverging (up to 2π) beam.

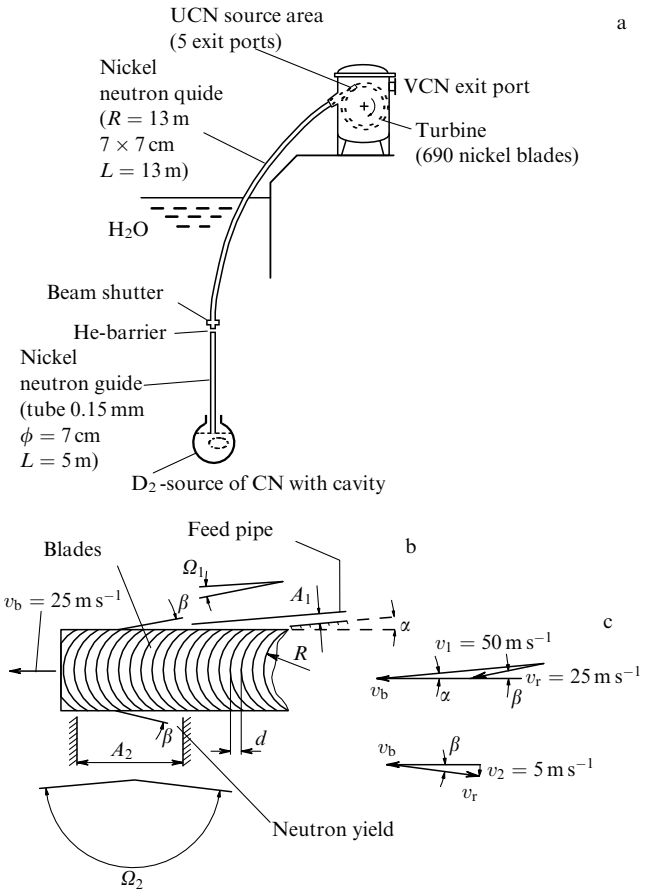

Figure 3. Turbine source of UCN on the ILL reactor: (a) general scheme of the source; (b) the idea of CN transformation into UCN ($A_{1,2}$ and $\Omega_{1,2}$ are, respectively, cross sections and angular apertures of the initial and final beams, $d = 7$ mm); (c) vector diagram of velocities: v_1 is the initial velocity of CN; v_b, the linear velocity of blades; v_r, the velocity of reflected CN; v_2, the UCN velocity.

3.4.3 Gravity spectrometer. The property of neutrons to lose their energy in up-motion, and vice versa, to gain it in down-motion was used by Scheckenhofer and Steyerl in 1977 for constructing a gravity spectrometer [55].

The scheme of the gravity spectrometer is drawn in Fig. 4. The UCNs exit from a source S (neutron turbine), ascend along an oblique neutron guide ON to the mirror M_1, pass through an entrance collimator EC that forms a horizontal beam of UCN with a velocity of $v = 3$ m s^{-1}, descend along parabolic trajectories to a system of mirrors $M_2 - M_4$, ascend to an intake collimator RC, and upon being reflected from the mirror M_5, accelerate in a vertical neutron guide VN. A detector D for UCN is a BF_3-counter with a thin aluminium window. The vertical neutron guide (together with the collimator, mirror M_5, and detector) can be moved vertically for changing the UCN energy. The resolution of the monochromator reaches 3×10^{-9} eV. A gravity spectrometer was utilized to study UCN reflections from a glass mirror, diffraction on a grating with 1,000 grooves per 1 mm and a zone plate, interference in reflections from thin films. Light optics can be used because the UCN wavelength is 5 – 10 times as short as the average wavelength of light.

3.4.4 Magnetic storage ring. In 1977, Kügler et al. [56] from the Bonn University constructed a magnetic storage ring in

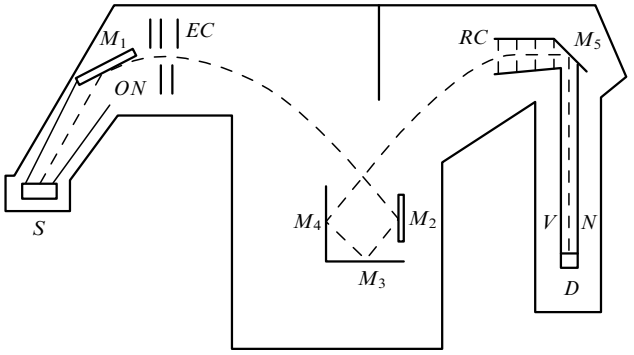

Figure 4. Scheme of a gravitational spectrometer: S — source of UCN, ON — inclined neutron guide, M_{1-5} — mirrors, EC — entrance collimator, RC — reception collimator, VN — vertical neutron guide, D — detector.

the form of a torus with diameter 1.2 m. A nonuniform magnetic field growing from the axis to edges was established by superconducting magnets with the maximal strength of 0.35 T. The magnetic field confines neutrons with definite polarization.

In late 1977, the storage ring was installed on the reactor in Grenoble. Neutrons from the reactor were periodically injected into the ring, whereas the neutrons stored in it were detected by a ^{3}He-counter which was periodically moved into the ring. The device was aimed at measuring τ_n and d_n (see Sections 4 and 6). In 1985, the same group of researchers constructed a more advanced storage ring 'NESTOR' [57] on which the record time of UCN confinement (75 min) was reached and an exact value was obtained for τ_n [58] (in more details, see Section 4.2.2).

3.5 The problem of UCN leakage during their storage and first progress in its solution

Owing to the property of total internal reflection at all angles of incidence, UCNs having got into a closed volume should be accumulated there. The UCN storage time is determined by their small absorption in medium in collisions with walls (UCN penetrate the medium for a depth of the order of wavelength λ), i.e. by a very large amount of reflections, theoretically estimated as $10^3 - 10^5$. Therefore, for large vessels and very slow UCNs ($\varepsilon < 10^{-7}$ eV), the storage time should equal many thousand seconds.

As was already mentioned, the effect of storage was for the first time proved in experimental works by Shapiro with colleagues in 1968 [35, 36]. They utilized the UCN beam of flux density 3×10^{-4} cm^{-2} s^{-1}. The obtained storage time (30 s) was a record for the first experiments but turned out to be about 100 times as small as the theoretical prediction.

In principle, the UCN losses could be caused by absorption, leakage through slits, reflections from rough surfaces, inelastic scattering, and so on. Much work was done to control these and other possible sources of the UCN losses (etching, electropolishing, degreasing and special coating of neutron guides, refining convertors and vacuum, etc.), however, all this scored only a partial success. Although quite in the short run the UCN storage time of 250 s was reached [40], the problem of anomalously large losses tortured physicists for a long time unless it was shown that the losses are due to hard-removable hydrogenous contaminations on the vessel walls. In particular, just this conclusion can be drawn by

analyzing the results of experiments by Strelkov and Hetzelt group in Dubna (1977) who showed an approximate coincidence of the storage curve for ultracold neutrons in a vessel and the curve of detected thermal neutrons beyond its walls [59]. Apparently, a part of UCN, upon inelastic collision with hydrogen, is heated up to a thermal energy, penetrates through the vessel walls, and is detected by external counters. The amount of hydrogen on the surface of a substance is sufficient, as follows from direct experiments on its detection, for the existence of the assumed effect.

Different attempts were undertaken to get rid of hydrogen on the surface of walls: by annealing of the vessel surface or its cleaning with ion bombardment, spraying with a fresh substance or deuteration. In 1982, the Morozov group from NIIAR was the first to reach the neutron storage time 920 ± 40 s comparable with the neutron lifetime in a vessel with walls covered by heavy-water ice [60]. Since then, the problem of anomalous losses of UCNs could be in main considered as solved†. In 1989, the UCN flux from the ILL reactor in Grenoble was increased up to 2.6×10^4 cm^{-2} s^{-1}, which 10^8 times exceeds the flux in first experiments, and the storage time of UCNs reached 60 min. This result was produced by the Mampe group when UCNs were stored in the vessel with walls covered by oil of fluorine compounds (without hydrogen) (see Section 4.2.1) [62]. (We already mentioned another record time of the UCN storage, 75 min, achieved on the storage ring 'NESTOR' [58].) In this case, the losses of UCNs can stem from their depolarization, heating on the acoustic 'vibration' of the field, and leakage near edges of the trap (for details, see Section 4.2.2).

4. The neutron lifetime τ_n

A free neutron constitutes a simplest nucleus with $Z = 0$. In view of its mass being different from the proton mass and due to the conservation of baryon and lepton charges, the neutron may turn into a proton: $n \to p + e + \tilde{\nu}$. This is a unique case of β-decay when a semilepton process is not influenced by nucleons in the nucleus and a weak interaction is observed without any admixtures, just in the pure state. Therefore, experimental studies on the decay of a free neutron began when there have been appeared intensive sources of neutrons, and these studies are still of great interest.

As said in Section 2.4, first measurements of the fundamental characteristic of β-decay, the neutron lifetime, were carried out at three laboratories: the Snell group in Oak Ridge [63, 64], the Robson group in Chalk-River [65, 66], and the Spivak group in Moscow [67]. Their results were of qualitative nature, however, in the fifties the accuracy better than 10 per cent was achieved. By now about 30 measurements of the neutron lifetime have been performed, and recent experiments are accurate to 0.3 per cent.

There are two essentially different types of experiments. In one of them, the lifetime is determined from appearance of the neutron decay products in the beam of neutrons escaping from the reactor; and in the other, from the decrease in the number of ultracold neutrons stored in a closed volume. Each type is characterized by its specific difficulties, therefore, consistency of corresponding results may ensure the absence of systematic errors.

† In fact, the problem of the UCN storage is still full of puzzles since the UCN losses are observed also at very low temperatures when neither of the causes listed (including 'heating' of UCNs in collisions with hydrogen) can account for them [61]. For details, see Section 9.1.

4.1 Beam method of τ_n determination

4.1.1 Essence of the method. Determination of the lifetime τ_n in beam experiments requires two independent absolute measurements: measurement of the neutron amount N in a given region of the beam, and measurement of the amount of neutron decays (dN/dt) in it. The lifetime required is determined from the ratio $\tau_n = N/(dN/dt)$.

Acts of the neutron decay are registered by the appearance of electrons or protons on the decay. Better accuracies of the lifetime measurement are produced with protons, which is due to a large difference in the electron and proton masses. Since the interval of the momentum spectra of decay products is the same, then owing to that difference, the interval of the energy spectrum of protons (0 – 751 eV) is three orders as narrow as that of electrons (0 – 782 keV). When electrons are registered, the low-energy part of the spectrum is inevitably cut off, and thus, the accuracy of dN/dt determination depends on the accuracy of cutting-off calibration and its stability. For protons, this problem does not occur since owing to their low energy they are to be accelerated up to 20 – 30 keV for registration, which makes protons almost monoenergetic.

Registration of protons is also preferable from the viewpoint of experimental background. The basis of background of the proton detector is formed by the count of electrons produced by scattered γ-quanta and neutrons. A low initial energy of protons allows it to be reliably measured because a small electric field enables the proton registration to be locked, without changing the electron part of the background. This locking is impossible for electrons as they are indistinguishable from the background.

4.1.2 Geometric selection of the decay products. A classical example of the beam experiment presents the measurement of the neutron lifetime with detection of the decay protons made in 1978 by the Spivak group [68, 69]. The scheme of the experiment is drawn in Fig. 5. In doing this, the neutron beam *2* passes through the vacuum chamber *1*; collimator *4* with two diaphragms *3* and *5* separates the region of the beam, out of which the detected protons of the decay are selected. The electrostatic filter of three grids *6* governs their passage to the detector. All this system including hemisphere *7a* is kept under voltage 25 kV accelerating and focusing protons through the hemispherical grid *7b* to the proton detector *8*. The penetrance of grids η was determined to an accuracy of fractions of per cent on the basis of transmission of α-particles. The counting rate of protons dN_p/dt was detected by a proportional counter. A narrow aperture of collimator *4* ensured focusing of all separated protons onto the counter window.

The background of a proton detector amounted to 20 per cent of the counting of decay protons. The electron component of the background was measured under a voltage of +800 V delivered to grid *6* for the proton locking. A significant fraction of the background might happen to be low-energy ions H_1^+ produced on the chamber walls by γ-quanta and fast neutrons. They were locked by a voltage of 14 V delivered to grid *6* during the experiment. The most trouble was given by the background of the decay protons scattered from the chamber walls; it was taken into account by computation.

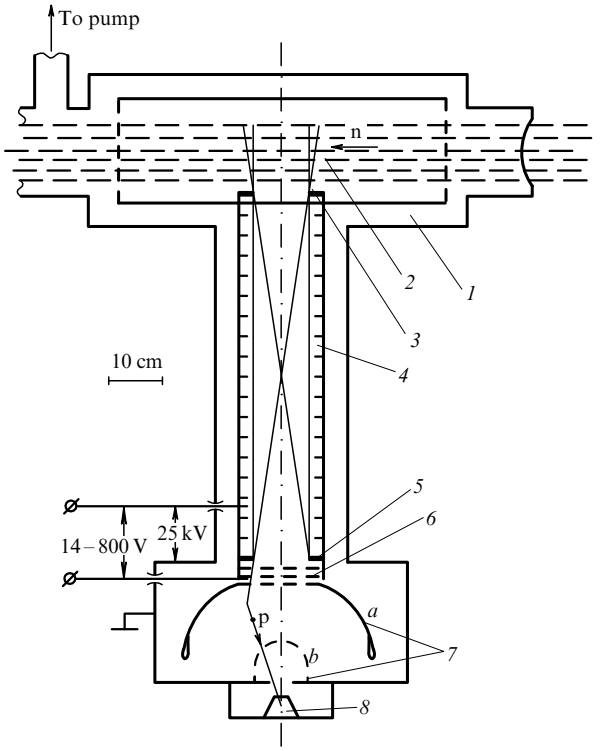

Figure 5. The scheme of experiment [69]: *1* — vacuum chamber; *2* — the neutron beam; *3, 5* — diaphragms; *4* — collimator; *6* — electrostatic filter; *7a* — hemisphere; *7b* — hemispherical grid; *8* — neutron detector.

The neutron density in the beam cross section Q was determined from activation of the golden foil. The absolute value of activity was measured by the 4π-geometry method applied to detection of $\beta\gamma$-coincidences. Gold was chosen in view of the well-known cross section of activation and high purity. Floating of the neutron flux during experiment was monitored by a highly stable fission chamber.

The size of the beam region whereout the collimator separated the decay protons, and the separated solid angle of their escaping were taken into account in the efficiency coefficient ϵ of observation.

Experiments were carried out on the IR-8 reactor of the Kurchatov Institute. The Maxwellian spectrum of neutron velocities due to incomplete thermalization was noticeably contributed with the neutrons of resonance energies.

The neutron lifetime was calculated by the formula $\tau_n = \epsilon\eta Q/(dN_p/dt)$; it amounted to $\tau_n = 891(9)$ s. Main contribution to the measurement error came from an inaccurate consideration of the resonance capture of neutrons by gold at an energy of 4.8 eV and uncertainty in the computation of the background of decay protons scattered in the chamber.

Spivak intended to increase the accuracy by 2–3 times. He prepared the apparatus to a new measurement on the beam cleaned from neutrons of resonance energies with the help of a neutron guide and introduced small constructive changes for suppressing the count of protons scattered in the chamber. Unfortunately, he had no time to make that measurement.

4.1.3 Collection of decay products with the help of fields. A basic problem of the precision measuring the neutron lifetime is to take account of the background in detecting the decay events. Even under the most optimal conditions, the average interval between the events exceeds 1 millisecond whereas the detection of every event requires 1 microsecond. Thus, 99.9 per cent of the measurement time is spent on recording the background.

An effective method of suppression of the background count was employed in the experiment [70] developed at the Sussex University under the supervision of Byrne and carried out by the English–American group of physicists at ILL, Grenoble.

A proton trap was formed by superimposing the electric and magnetic fields in the beam region. Decay protons produced in it moved along field lines wrapping around them in a spiral, and the region of their movement was confined by electrostatic mirrors locking the trap from both sides. A superconducting magnet established a uniform magnetic field of 5 T in the beam region, which provided the spiral diameter not larger than 1 mm; the trap was locked by the field of 1 kV.

Detection of protons was splitted into two stages. First, during the time $T \approx 10$ ms, the trap was closed and the produced proton was stored in it. Then, one of the reflecting field was switched off for a time of $t \approx 100$ μs and the stored proton was drawn off onto the silicon surface–barrier detector being at the potential -30 V. This regime allowed the background suppression of about 100 times. To avoid nonlinear effects of superposition of a large number of pulses in the detection, the trapping time was chosen so that the probability for three protons to be found simultaneously in the trap was negligible.

The measurements were carried out on the beam coupled, with the help of a curved neutron guide, out of a liquid-hydrogen source of cold neutrons on the ILL reactor. That beam does not practically contain fast neutrons and γ-quanta, the usual source of the detector background. As a result, the background in the experiments amounted to 0.2 per cent of the decay proton counting.

The scheme of the apparatus is shown in Fig. 6. By changing the potential pattern of ring electrodes (in total, 16) encompassing the beam, the trap length L could be changed, which allowed control of the computation accuracy for its volume.

Simultaneously, the density of neutrons was measured in the beam. For this purpose, a thin ^{10}B target was placed on the beam way after the trap, and at a fixed solid angle the counting was made of α-particles arising in the reaction (n, α). Precision measurement of the target parameters was carried out at the Central Bureau of Nuclear Measurements (Geel, Belgium).

The neutron lifetime was determined by the ratio between numbers of α-particles N_α and protons N_p detected in a measurement time, by the ratio between efficiencies of detection of protons (ϵ_p) and that of thermal neutrons from α-particles escaping out of the ^{10}B (ϵ_0) target, and also by the time of flight of a neutron through the proton trap L/v_0, where $v_0 = 2200$ m s^{-1}: $N_\alpha\epsilon_p L/(N_p\epsilon_0 v_0)$ [71]. Statistical and systematic errors in the value $\tau_n = 893.6(5.3)$ s obtained were almost the same, and the main contribution to the latter was due to the accuracy of determination of ^{10}B-target parameters.

Possibilities of the experiment discussed are far to be exhausted. Byrne continues studies of the neutron decay at ILL, and the American scientists, having installed the apparatus in duplicate, continue measurements of the lifetime in Washington.

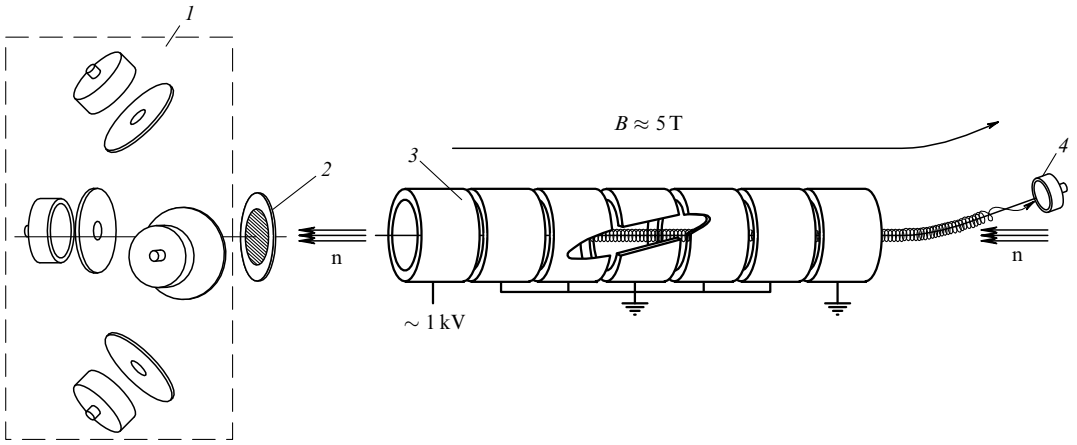

Figure 6. The scheme of experiment [70]: *1* — α-detector; *2* — ^{10}B target; *3* — ring electrodes (16, in total); *4* — proton detector.

4.1.4 Detection of decay electrons. The accuracy achieved in experiments with the detection of decay electrons [72 – 74] is worse than that of experiments with the detection of decay protons (see Table 3 in Section 4.3). Specific features of the experiments [73, 74] will be considered below, when describing measurements of the electron-spin correlation.

4.2 Determination of τ_n by the UCN storage method

If at an initial moment of time in a certain volume, where the conditions are created for the UCN storage, N_0 neutrons are isolated, then their amount will decrease in time by the law $N(t) = N_0 \exp(-t/\tau_s)$, where τ_s is the UCN-storage time in the volume. Hence it follows that to determine τ_s, it is sufficient to perform two measurements of $N(t)$ at two points in time t_1 and t_2:

$$\tau_s = \frac{t_2 - t_1}{\ln N(t_1) - \ln N(t_2)} . \tag{19}$$

For the storage with a magnetic field, conditions can be created for a narrow group of the neutron velocity vectors when there are no losses except β-decay, and the neutron storage time coincides with their lifetime, $\tau_s = \tau_n$. When material walls are used, there are, in principle, extra losses of UCN. In this case, the total probability of losses ($\Theta_s = 1/\tau_s$) is determined by the sum of the probability of the neutron decay ($\Theta_n = 1/\tau_n$) and the one of UCN leakage in the storage ($\Theta_l = 1/\tau_l$):

$$\Theta_s = \Theta_n + \Theta_l \equiv \frac{1}{\tau_s} = \frac{1}{\tau_n} + \frac{1}{\tau_l} . \tag{20}$$

To determine the neutron lifetime from the measured UCN-storage time, it is necessary either to suppress the leakage down to a negligible level, or to take it into account as accurate as possible.

4.2.1 UCN in traps with material walls. The imaginary refraction index for neutrons with energies below E_b [see formula (12)] means that the neutron wave cannot propagate inside a substance and exponentially attenuates in its thin layer. Interaction with matter in that layer gives rise to the neutron losses due to their leakage. The leakage is especially large in the hydrogen layer since it possesses a large scattering cross section, at which UCN pass into the region of thermal velocities and go freely through the vessel walls (see Section 3.5).

If a vessel is vacuumized so that the neutron leakage occurs only via collisions with walls, its probability is proportional to the collision frequency and can be varied by changing the vessel configuration. The magnitude of leakage may be characterized by the calculation factor γ proportional to the collision frequency. Extrapolation of values of the storage time measured at different γ to its value at $\gamma = 0$ eliminates the leakage contribution and allows the determination of the neutron lifetime.

In 1989 – 1993, results were published of three experiments performed with intensive UCN sources where the accuracy of about 0.3 per cent was obtained. Each of them employed its own procedure providing a high accuracy for taking account of the UCN leakage.

The first of them was the experiment of the French – English – German group supervised by Mampe [62]. As storage vessel, they utilized a vacuumized rectangular box $30 \times 40 \times 60$ cm with glass walls covered with a layer of viscous hydrogen-free oil FOMBLIN (Fig. 7a). The oil is specified by a low probability of the UCN leakage $\mu(v) = (2-3) \times 10^{-5}$ per collision and a high boundary velocity 4.55 m s^{-1}. Besides, the oil layer shut all possible slits, which allowed the use of a mobile wall to change the vessel volume.

The UCN source constituted a turbine (see Section 3.4.2). Neutrons from it filled the vessel to a standard density. Then the inlet valve was shut and after the storage time t the outlet valve was opened, and a UCN detector registered the amount of neutrons $N(t)$ retained in the vessel. The cycle of two measurements at storage times t_1 and t_2 allowed the storage time to be computed by formula (19). The required statistical accuracy was achieved by cycle repeating.

Transportation of the mobile wall changes the mean length l_{av} of the UCN free flight, which allowed a controllable change of the frequency of their collisions with walls. The kinetic theory of ideal gas, such as UCN in the vessel, connects l_{av} with the volume V and surface S of the vessel, $l_{av} = 4V/S$. The length l_{av} and the leakage probability $\mu(v)$ determine the leakage factor γ for a given velocity v. However, when the factors $\langle \gamma(v) \rangle$ averaged over the storage time in vessels with different volumes are compared, one could not obtain the accuracy of determining the leakage contribution necessary for measuring τ_n to within tenths of per cent, owing to different deformation of the velocity spectrum at a different number of UCN collisions with walls.

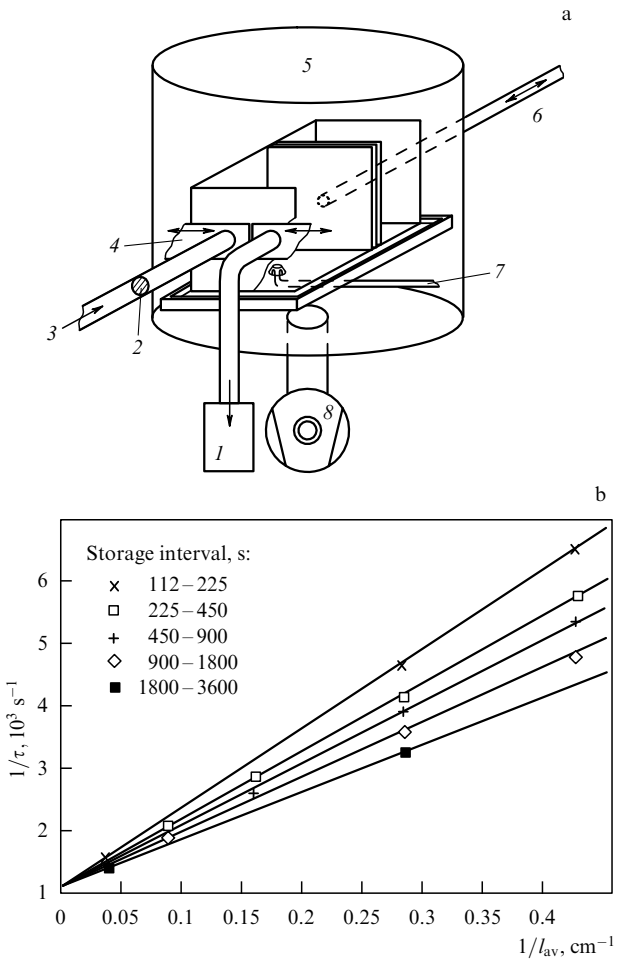

Figure 7. Experiment [62]. (a) Scheme of the apparatus: *1* — detector of UCN, *2* — foil, *3* — UCN, *4* — valve shutters, *5* — vacuum chamber, *6* — ram, *7* — FOMBLIN, *8* — vacuum pump. (b) Extrapolation of storage time at different volumes for 5 storage intervals with 2–4 volume sizes in each.

The authors used a special procedure of choosing the storage intervals which allowed them to compare the storage in vessels of different volumes at the same deformation of spectra. For this aim, when passing from volume V^i to volume V^j, the spectrum time scale was changed in proportion to the change of the mean flight length in each vessel, $t_1^i = (l_{av}^i/l_{av}^j) \times t_1^j$ and $t_2^i = (l_{av}^i/l_{av}^j) \times t_2^j$. The UCN leakage is the same in both measurements since the number of collisions with walls is the same. In this case, the difference in the number of retained UCN is determined only by the difference in the number of decays for two intervals of the storage time.

For five storage intervals, the extrapolation of the storage time for different volumes to an infinite large volume led to the same neutron lifetime 887.6(3.0) s (Fig. 7b).

Another experiment was prepared at the Kurchatov Institute under the leadership of Morozov and carried out with the participation of Mampe on the turbine source of ILL [75].

The UCN storage time was determined, as usual, via two cycles with different storage times. The difference is that the UCN leakage was not computed but it was directly measured. The main channel of leakage is an inelastic scattering moving UCN to the region of thermal velocities, therefore, the UCN leakage in a storage time can be determined from the amount of heated neutrons having passed through vessel walls and detected by counters of thermal neutrons. However, this requires a highly accurate knowledge of the ratio between efficiencies of the detection of thermal neutrons and UCNs.

Introduction of the second measurement with a changed configuration of the vessel eliminated direct calibration of the efficiencies, whereby τ_n was measured indirectly, $\tau_n = (\xi - 1)/(\Theta_{s1}\xi - \Theta_{s2})$, where Θ_{s1} and Θ_{s2} are the total probabilities of losses, and ξ is the ratio of leakage probabilities at two vessel configurations estimated from counting the UCNs and thermal neutrons in these two measurements.

Measurements at three temperatures of the vessel walls $t = +20\,^\circ$C, $-12\,^\circ$C, and $-55\,^\circ$C gave consistent results and the lifetime obtained was equal to 882.6(2.7) s.

In the experiment performed under the leadership of Serebrov at two institutes, PINPh (Gatchina) and JINR (Dubna) [76], on an intensive source of UCN at Gatchina, particular attention was given to the suppression of the UCN losses during storage. Use was made of the materials with weak absorption of neutrons. The trap was made of aluminium; its internal surface was covered with a thin layer of beryllium over which an extra pure oxygen was frozen. To suppress the UCN inelastic scattering, the trap was cooled down to 15 K. As a result, the probability of UCN losses was about 3 per cent of the decay probability.

For a correct account of the leakage factor $\gamma(v)$, the storage time was measured on narrow intervals of the UCN velocities. The construction of the storage vessel (Fig. 8) allowed it to be used as a gravitational spectrometer. The spherical form and possibility of the rotation around the horizontal axis allowed a shift of the orifice position in the

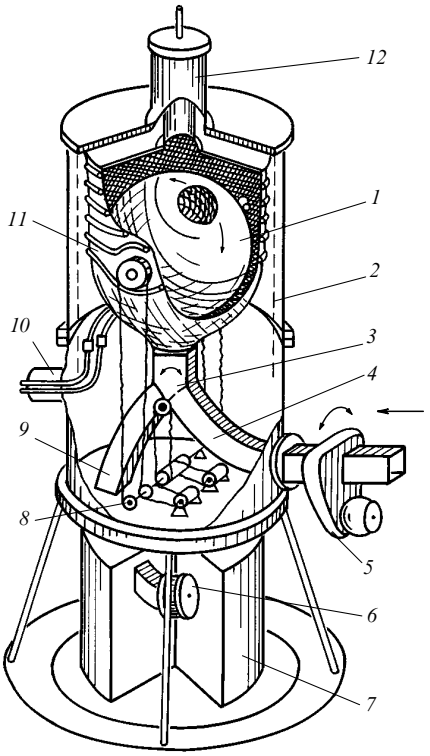

Figure 8. Set-up for measuring the neutron lifetime with a gravitational trap in the experiment [76]: *1* — UCN storage trap; *2* — nitrogen screen; *3* — distribution valve; *4, 9* — neutron guides; *5* — injection valve; *6* — UCN detector; *7* — detector shield; *8* — a system for rotation; *10* — cryopipes; *11* — cryostat; *12* — frozing system.

sphere to be made without disturbing the velocity spectrum of the UCN gas filling it. When the orifice was at the bottom, the vessel was filled; when it was at the top, the sphere worked in the storage regime, whereas switching of the distribution valve onto a detector initiated the measurement regime. Rotation of the sphere at some angle produced 'pouring out' of neutrons within a certain velocity interval onto the detector.

Measurements of the storage time for different UCN energies carried out with a cylindrical vessel instead of the sphere, which changed the leakage conditions, allowed extrapolation to its absence and the value $\tau_n = 888.4(3.3)$ s was found.

4.2.2 UCN storage in a magnetic trap. The problem of losses due to the UCN interaction with walls can be avoided if the boundary reflecting neutrons is made up by means of a magnetic field. Owing to the magnetic moment of a neutron, the magnetic field gradient depending on its orientation either accelerates neutrons and let them pass or retards them creating a potential barrier on their way without substance. As a result, neutrons with a magnetic moment antiparallel to the field gradient and with a velocity not sufficient for overcoming the barrier will be reflected from it.

A reflecting barrier of that sort rolled up into a ring was constructed on the NESTOR set-up [58]. The vacuum chamber in the shape of a torus was surrounded with a sextipole system of superconducting coils creating the magnetic barrier for the neutrons tending to fly outside, whereas their way to the torus centre was ceased by the centrifugal force of inertia. In this case, for a part of neutrons flying along the torus axis with velocities of 10–14 m s^{-1}, the motion in the chamber turned out to be very similar to that of charged particles in the cyclic accelerators. It is characterized by betatron vibrations with respect to stationary orbits corresponding to definite combinations of the particle direction and velocity. (However, unlike particles in an accelerator, neutrons can go around their orbits in both directions.)

Measurements of the neutron lifetime were performed in the following way. The VCNs were injected into the set-up with the help of a neutron guide, which was then quickly, in a time fraction of one revolution, led out of the region of stationary orbits. To measure the amount of neutrons retained in the torus in a time of storage, a neutron detector was inserted into the region of stationary orbits.

Large amplitudes of betatron vibrations resulted in the leakage of neutrons having entered a region of a weak magnetic field, where the magnetic moment can be reversed. Owing to the leakage, deviation from the exponential law of decreasing the number of stored UCNs was observed during the first 450 s. When nonstationary orbits were 'died out', there was no deviation and during the storage time from 450 to 4500 s the exponential decrease was occurred obviously.

The experiment was carried out by German physicists at ILL and they found the neutron lifetime $\tau_n = 876.7(10)$ s.

4.3 List of measurement results for τ_n

In Table 3, we report the results of the last ten measurements on the neutron lifetime; the table contains the measurement method, the obtained value of the lifetime τ_n, the constant λ calculated from it, year of publication, and references.

The mean value of τ_n averaged with allowance for the accuracy of results amounts to $\tau_n = 887.0(1.6)$ s. Distinction of almost two standard deviations is to be noted for the neutron lifetime obtained from beam experiments [$\tau_n = 894.2(4.2)$ s] and with the method of UCN storage [$\tau_n = 885.9(1.7)$ s] [78].

Table 3

Method	τ_n	λ	Year	Ref.
β	918 ± 14	-1.243 ± 0.012	1972	[72]
p	891 ± 9	-1.266 ± 0.008	1978	[69]
UCN	900 ± 11	-1.258 ± 0.009	1986	[77]
β	878 ± 31	-1.277 ± 0.027	1988	[73]
β	876 ± 21	-1.279 ± 0.019	1989	[74]
UCN	877 ± 10	-1.278 ± 0.009	1989	[58]
UCN	887.6 ± 3	-1.2684 ± 0.0027	1989	[62]
p	893.5 ± 5.3	-1.2633 ± 0.0046	1990	[70]
UCN	888.4 ± 3.3	-1.2677 ± 0.0030	1992	[76]
UCN	882.6 ± 2.7	-1.2727 ± 0.0025	1993	[75]

4.4 Determination of the β-decay constants from τ_n and $(0^+ - 0^+)$ transitions

The modern theory treats weak processes as interactions of leptons and quarks through the exchange of gauge vector bosons. In this approach, a wide range of weak and electromagnetic interactions is described within a unified theory of electroweak interaction. However, it is more convenient to consider the β-decay itself within the 'old' theory of universal 4-fermion weak interaction, i.e. at the level of hadrons and leptons, since in this case the renormalization of the hadron axial-vector current caused by strong interaction is given explicitly. This consideration is adequate to the theory of electroweak interaction since the β-decay energy (< 10 MeV) is much lower than the masses of gauge $W^{\pm}$ and Z^0 bosons (~ 90 GeV).

The universal theory is based on the (V – A) structure of a weak interaction. The notation V and A reflects the way of computing the bilinear forms in the β-decay Hamiltonian for two combinations of spins of produced leptons. When the spins are antiparallel, spin wave functions are vectors (V-version), whereas when they are parallel, the spin wave functions are axial vectors (A-version).

Replacing the antineutrino in the expression (4) by the neutrino, we reduce it to the symmetric form $n + \nu \to p + e$ and can write the Hamiltonian H as a product of hadron and lepton currents:

$$H = \frac{G_V}{\sqrt{2}} \{\widetilde{\psi}_p \gamma_\mu (1 + \lambda\gamma_5)\psi_n\} \{\widetilde{\psi}_e \gamma_\mu (1 + \gamma_5)\psi_\nu\}, \qquad (21)$$

where ψ_p, ψ_n, ψ_e, ψ_ν are the proton, neutron, electron, and neutrino wave functions, respectively; γ_μ are the Dirac matrices ($\mu = 1, 2, 3, 4$), $\gamma_5 = i\gamma_1\gamma_2\gamma_3\gamma_4$; parentheses $(1 + \gamma_5)$ and $(1 + \lambda\gamma_5)$ take account of the violation of the conservation law of spatial parity; G_V is the constant of vector weak interaction; and, finally, $\lambda = G_A/G_V$ is the ratio between the axial-vector and vector constants.

The Hamiltonian (21) allows us to connect the lifetime of a β-decaying nucleus τ with the constants G_V and λ:

$$f\tau = \frac{K}{G_V^2 |M_V|^2 + G_A^2 |M_A|^2} = \frac{K/G_V^2}{|M_V|^2 + \lambda^2 |M_A|^2}, \qquad (22)$$

where K is the combination of fundamental constants ($K_\tau = 2\pi^3\hbar^7/(m_e^5 c^4)$ or $K_t = 2\pi^3\hbar^7 \ln 2/(m_e^5 c^4)$, when use is made of the half-life $t_{1/2}$ instead of the lifetime τ); M_V and M_A are the matrix elements for vector and axial-vectors versions

of interaction, respectively; f is the factor of phase space arising in the integration of the Hamiltonian as applied to the experimental conditions.

Equation (22) contains two unknowns, G_A and G_V, therefore their determination requires two independent experiments. Traditionally, use is made of the neutron lifetime τ_n and the quantity $ft_{1/2}$ for superallowed $(0^+ - 0^+)$ transitions since their matrix elements squared are known exactly: $M_V^2 = 1$, $M_A^2 = 3$ and $M_A^2 = 0$, $M_V^2 = 2$, respectively.

Calculations of the f factors for neutron decay and for $(0^+ - 0^+)$ transitions were performed accurate to within hundredths of per cent. To this end, it was necessary to take account of the phase space change and appearance of induced 'small' terms in the Hamiltonian due to the electromagnetic interaction in the β-decay, G_A and G_V interference, and also to the nucleon size being finite [79–81].

Vector interaction is equally observed in all nuclear β-decays (the conservation of vector current). Then for nine superallowed $(0^+ - 0^+)$ transitions (nuclei $^{10}C_6$, $^{16}O_8$, $^{26}Al^m_{13}$, $^{34}Cl_{17}$, $^{38}K^m_{19}$, $^{42}Sc_{21}$, $^{46}V_{23}$, $^{50}Mn_{25}$, and $^{54}Co_{27}$) that proceed without changing the spin and parity of a nucleus, the values of $ft_{1/2}$ coincide within fractions of per cent although their half-lives $t_{1/2}$ differ more than by three orders. For them, $M_A = 0$, therefore only vector interaction is possible and the mean value of the factors $\langle (ft_{1/2}) \rangle$ allows us to determine the constant G_V:

$$(ft_{1/2})_{0^+0^+} = \frac{K_t}{2G_V^2} \,. \tag{23}$$

The modern values of $(ft_{1/2})_{0^+0^+} = 3073.3(3.5)$ and K_t lead to $G_V = 1.4149 \times 10^{-62}$ J m^3.

As for the constant G_A, it cannot be determined from the data on nuclear decays because the axial-vector weak interaction changes under the influence of strong interaction, the size of the change being dependent on a particular structure of the decaying nucleus. The fundamental quantity for the theory is the quantity $\lambda = G_A/G_V$ observable in the decay of a free neutron, when the change is due to the strong interaction inherent in the decaying nucleon itself.

When the neutron matrix elements are taken into account, expression (22) transforms into

$$f_n \tau_n = \frac{K_\tau}{G_V^2 + 3G_A^2} = \frac{K_\tau / G_V^2}{1 + 3\lambda^2} \,. \tag{24}$$

Comparison of (23) and (24) gives the relation

$$\frac{(ft_{1/2})_{0^+0^+}}{f_n \tau_n} = \frac{\ln 2}{2} \, \frac{G_V^2 + 3G_A^2}{G_V^2} \tag{25}$$

and at values $\langle \tau_n \rangle = 887.0(1.6)$ s, $f_n = 1.71465(15)$ and $\langle (ft_{1/2})_{0^+0^+} \rangle = 3073.3(3.5)$ it allows the following estimations to be made: $|G_A| = 1.7954(25) \times 10^{-62}$ J m^3 and $|\lambda^{00}_{\tau_n}| = 1.2689(16)$.

5. Angular correlations in the neutron β-decay

The β-decay phenomenological theory admits five forms of interaction obeying the requirement of relativistic invariance of the Hamiltonian: scalar (S), vector (V), tensor (T), axial-vector (A), and pseudoscalar (P) forms, but the latter is unessential for the description of the neutron β-decay. The forms realized in Nature could be chosen by measuring the angular correlations attendant on the separation of β-decay products. Unless the spatial invariance caused doubts, only the correlation of directions of electron and antineutrino momenta was considered possible. The first attempts to measure its coefficient a were not successful because of the severity of determining the antineutrino emission direction. The discovery of P-invariance nonconservation initiated studies on P-odd angular correlations between the direction of the neutron spin and momenta of an electron (A) and an antineutrino (B). These experiments are methodologically simpler and the first findings discovered in the late 50s and verified later, allowed the following conclusions that underlie the theory of universal 4-fermion (V – A) interaction to be made:

(1) major contribution to β-decay comes from vector (V) and axial-vector (A) transitions;

(2) complete violation of the P- and C-invariances is observed in weak interaction;

(3) breaking of the T-invariance is not observed.

Further increase in the accuracy of these experiments allowed the weak interaction constant to be determined only from the data on the neutron decay. At the same time, the value of the constant λ_c alternative to that of $\lambda^{00}_{\tau_n}$ determined by measuring the neutron lifetime and $(0^+ - 0^+)$ transitions, opened up possibilities for the experimental verification of the (V – A) theory validity at the level of corrections accounting for the influence of electromagnetic interaction on the process of β-decay.

5.1 Introductory remarks

The decay probability of a free neutron with a given spin direction $\boldsymbol{\sigma}$ accompanied by emissions of an electron and an antineutrino with the energies and momenta E_e, $E_{\tilde{\nu}}$, $\mathbf{p}_e$, $\mathbf{p}_{\tilde{\nu}}$, respectively, is given by the formula

$$\mathrm{d}W = G^2 F(E_e) \left\{ 1 + a \, \frac{\mathbf{p}_e \mathbf{p}_{\tilde{\nu}}}{E_e E_{\tilde{\nu}}} + \right.$$
$$\left. + \boldsymbol{\sigma} \left(A \, \frac{\mathbf{p}_e}{E_e} + B \, \frac{\mathbf{p}_{\tilde{\nu}}}{E_{\tilde{\nu}}} + D \, \frac{[\mathbf{p}_e \times \mathbf{p}_{\tilde{\nu}}]}{E_e E_{\tilde{\nu}}} \right) \right\} , \tag{26}$$

where $F(E_e)$ is the function of total electron energy; G^2 is the combination of constants G_i of weak interaction and the corresponding matrix elements M_i of the transitions ($i = S, V, T, A$); a, A, B are the coefficients of the above-mentioned correlations; D is a coefficient of the P-even but T-noninvariant three-vector correlation $\boldsymbol{\sigma}([\mathbf{p}_e \times \mathbf{p}_{\tilde{\nu}}])$ also depending on G_i and M_i [82].

Measuring the decay probabilities at different $\mathbf{p}_e$, $\mathbf{p}_{\tilde{\nu}}$, $\boldsymbol{\sigma}$, one can estimate the correlation coefficients each of which is defined by a unique value of λ in the framework of the (V – A) theory. The combination of a, A, B and τ_n values allows calculation of all four constants G_i, no matter whether the (V – A) theory is valid or not [83].

5.2 Measurements of the *a* coefficient

The difficulty in measuring the coefficient a is due to impossible direct detection of the antineutrino with the efficiency required. Information on the direction of its escape should be reconstructed on the basis of the recoil proton momentum. In doing so it is not necessary to detect the electron as the proton momentum already contains information about relative direction of the electron and antineutrino momenta, $\mathbf{p}_p = -(\mathbf{p}_e + \mathbf{p}_{\tilde{\nu}})$.

Studies carried out at ITEP (Moscow) in 1959 – 1967 [84 – 86] dealt with the measurement of the a coefficient. Detected

was the spectrum of momenta of recoil protons coincident with electrons having a limited solid angle of escaping. The choice of a narrow interval of electron energies provided a fixed value of the antineutrino momentum, and if all directions of their escaping are equally probable, the spectrum of proton momenta will be rectangular (Fig. 9). The value of a was determined from the slope of this spectrum. Despite a low intensity of the neutron beam and severe background conditions, the authors succeeded in obtaining the value $a = -0.099(39)$ sufficiently accurate for that time.

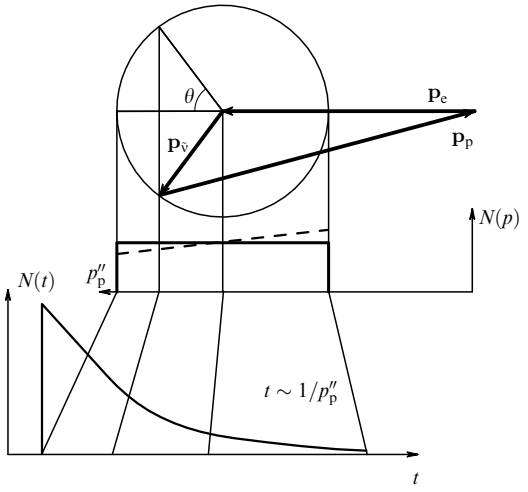

Figure 9. Vector diagram of momenta of neutron decay products. For each electron momentum $\mathbf{p}_e$, the proton retardation time determines the angle between $\mathbf{p}_{\tilde{\nu}}$ and $\mathbf{p}_e$.

Detection of the electron and proton coincidence permits the choice of experimental set-up most sensitive to a but diminishes its luminosity and requires a high accuracy in the determination of electron energies [87]. When protons are detected without coincidence with electrons, their spectrum is integrated both over all directions of the electron escaping and over all their energies, which results in high luminosity of the experiment but lowers its sensitivity to a.

The measurement of a by comparing the experimental and computed spectra of recoil protons was conducted in 1978 by Austrian physicists under the leadership of Dobrozemsky [88]. The spectrum was measured by the electrostatic spectrometer placed at the output of a vacuum tangent channel of the reactor. It contained a system of collimators that separated the recoil protons arising in the neutron decay near the active core. To ensure the identity of geometric separation in the whole proton energy interval 0–751 eV, special measures were taken for shielding the magnetic field in the channel.

In Fig. 10, we show the difference in two spectra of decay protons at $a = 0$ and $a = -0.1$ (top) and the proton-energy dependence of the factor of sensitivity of the spectrum shape $S = \{N(\varepsilon_p)_{a=-0.1}/N(\varepsilon_p)_{a=0}\} \times 100$ (bottom).

After 35 series of 24-hour measurements, the value for a was obtained with the statistical accuracy of ± 0.0019. It had to be complemented with a number of corrections: for energy calibration and resolution, for thermal motion of neutrons, charge exchange of protons on a residual gas, proton scattering in the spectrometer, as well as some relativistic and radiative corrections. In view of the uncertainty peculiar to these corrections, the final value was found to be $a_0 = -0.1017(51)$.

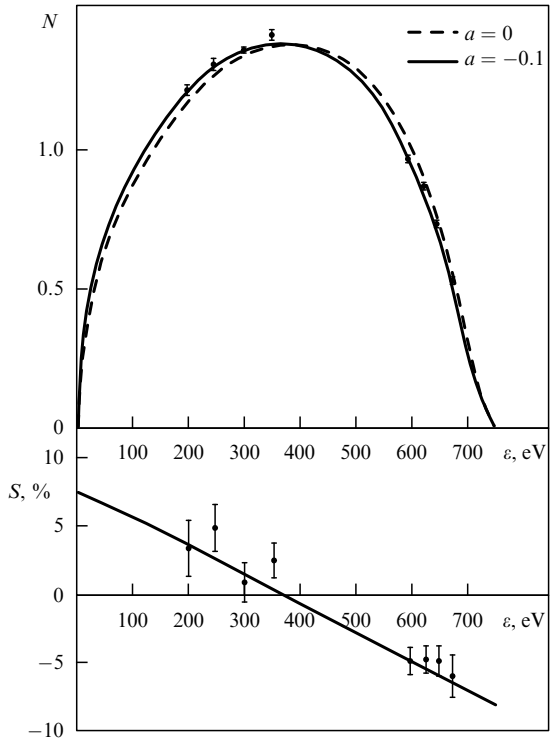

Figure 10. Sensitivity of the spectrum shape $N(\varepsilon)$ to the coefficient a and the dependence of the a-sensitive factor S on the proton energy. Experimental points are drawn for one series of experiments.

5.3 Measurements of the A coefficient

Measurement of the coefficient of the electron-spin correlation is methodologically simpler than that of the electron-antineutrino correlation because it can be carried out as a relative measurement, if under fixed conditions of the electron detection, the direction of beam polarization is reversed. As it follows from (26), the number of detected events is proportional therewith to

$$N^{\pm} \propto 1 \pm P_n A \left\langle \frac{v}{c} \cos(\mathbf{p}_e \mathbf{P}_n) \right\rangle , \tag{27}$$

where P_n is the degree of the neutron beam polarization; $\langle (v/c)\cos(\mathbf{p}_e\mathbf{P}_n)\rangle$ is the product of the electron relative velocity v/c and mean cosine of the electron escape relative to the axis of the polarization vector $\mathbf{P}_n$, which is averaged over $F(E_e)$ spectrum. (Terms ahead of factors a, B and D equal zero in view of averaging over all directions of the antineutrino emission.) Asymmetry of the electron counting $X = (N^+ - N^-)/(N^+ + N^-)$ allows one to determine the coefficient A by the formula

$$A = \frac{X}{P_n \langle (v/c)\cos(\mathbf{p}_e \mathbf{P}_n)\rangle} . \tag{28}$$

In the last three measurements of A, the accuracy better than 2 per cent was achieved.

Experiment [89] was carried out by the German – French – American group on a polarized beam of the ILL reactor with the use of a 4π-spectrometer of electrons PERKEO constructed at the Heidelberg University on the Dubbers initiative. The beam of polarized neutrons passed along the axis of a superconducting solenoid that created the field of intensity 1.6 T. Decay electrons were captured by the magnetic field in the beam region of 2 m length. At both sides of the solenoid the magnetic field was bent so as to

extract electrons from the beam onto detectors registering their energy.

Owing to two detectors connected by magnetic force lines, it was possible to eliminate the distortion of the energy spectrum of detected electrons caused by back scattering. An electron leaving only part of its energy in one detector and escaping from it in backward direction was led by the magnetic field to the second detector, and the system of detection was arranged so that when signals of two detectors coincide, their summed amplitude was attributed to the one in which a signal appeared earlier.

The coefficient A was defined by formula (28), and under the conditions of 2π-geometry of electron detection by each detector, $\langle\cos(\mathbf{p}_e\mathbf{P}_n)\rangle = 0.5$. Counting rate for the decay electrons amounted to 160 s^{-1}. The background level was measured under the beam shuttering with a ^{6}LiF absorber. The degree of the beam polarization amounted to $P_n = 97.4(0.5)\%$. In Fig. 11, the best coincidence of the experimental and calculated at $A_0 = -0.1146(19)$ dependences of asymmetries on the electron energy is shown.

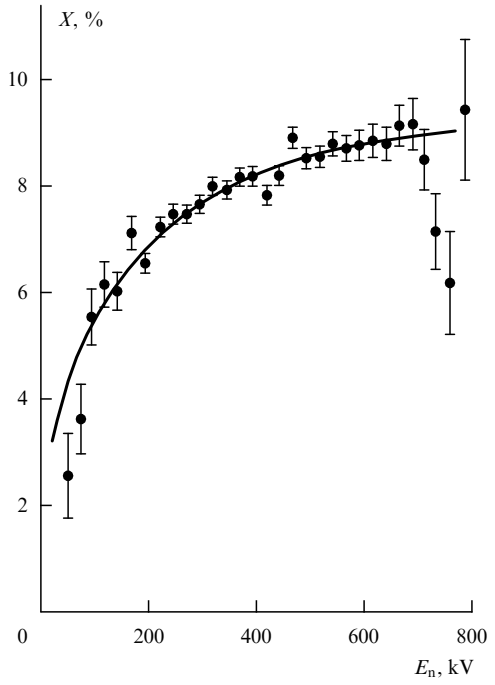

Figure 11. Asymmetry X as a function of the electron energy: experimental and calculated with the detector resolution taken into account.

The neutron lifetime was also measured with the use of PERKEO [73]. For this purpose, the apparatus was additionally supplied with a beam chopper. The decay events were registered only when the bunch of the neutron beam was entirely in the region of the solenoid magnetic field. This allowed the authors to avoid the uncertainty of gathering electrons from the positions of the beam inlet into the solenoid and exit from it. The result of measurements is presented in Table 3 (see Section 4.3).

In a joint experiment of the St Petersburg Institute of Nuclear Physics and Kurchatov Institute carried out on a polarized beam of the VVR-M reactor in Gatchina under the leadership of Erozolimskiĭ in 1990 [90] for measuring the coefficient A, coincidences of electrons with recoil protons were detected. This made it possible not only to suppress the background essentially but also to measure exactly it by the method of counting the delayed coincidences.

The experiment was run so as to provide a complete gathering of recoil protons from the beam region where decay electrons were detected, since the loss of a part of protons could admix the antineutrino-spin correlation.

The scheme of the experiment is displayed in Fig. 12. The beam of polarized neutrons restricted by ^{6}LiF diaphragms passed through a vacuum chamber *1*. Diaphragm *4* from the side of an electron detector *5* governed the size of the beam region *3* from which coincidences were registered. The electric field applied to that region drew off all the protons into the region of an accelerating field between the electrode and grid, which focused the protons onto detector *2*.

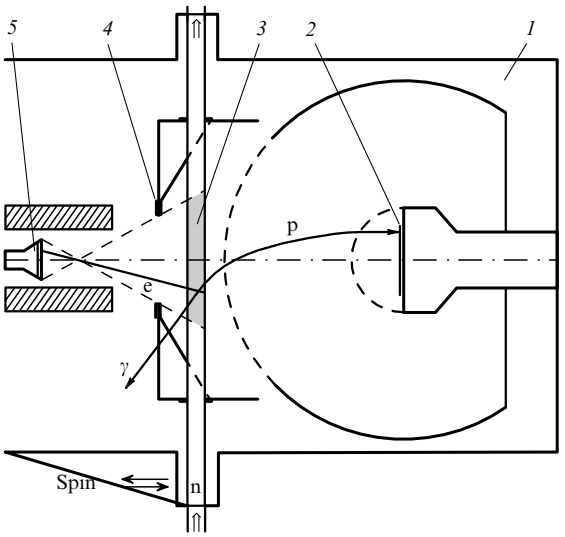

Figure 12. Scheme of the experiment [90]: *1* — vacuum chamber; *2* — detector of protons; *3* — the beam region from which coincidences were detected; *4* — diaphragm; *5* — detector of electrons.

Measurements with a miniature gun of protons [91] and the check of the size of a spot of decay protons focused on the detector confirmed the results of calculation predicting a complete collection of protons from region *3* onto a detector.

The mean cosine of the angle $\langle\cos(\mathbf{p}_e\mathbf{P}_n)\rangle = 0.970 \pm 0.004$ and the average $\langle v/c\rangle = 0.828 \pm 0.004$ entering into (27) were defined provided that the scattering of electrons in the chamber was taken into account. The degree of the beam polarization $P_n = 0.7867 \pm 0.0010$ was measured with the help of a special neutron guide whose analyzing power was calibrated by comparison with the splitting of spin components of the beam in a strong nonuniform magnetic field. With allowance made for corrections, the obtained value $A_0 = -0.1116(14)$.

The result of the latest measurement of the electron-spin correlation was published in 1995 [92]. It was carried out on the ILL reactor by the German–French group headed by Schreckenbach.

In the earlier experiment [93], a drift chamber was utilized filled with the gas mixture $^4He + CO_2$. A monoenergetic beam of neutrons reflected from the crystal RbC_8 was transmitted through the chamber. Complete information on each event fixed by the chamber was stored in the computer memory and was processed by the off-line method. Data processing restored the three-dimensional picture of electron

tracks and selected those of them which started in the beam region. Nevertheless, the background level turned out to be several times as large as the rate of decay events counting, which restricted the measurement accuracy for τ_n in 1989 [74]. In a new version of measuring A, detection of electron tracks with the drift chamber was carried out concurrently with the detection of energies of these electrons with the help of plastic scintillators, which allowed suppression of the background down to 10 per cent of the effect.

For each channel of the electron energy spectrum measured for two directions of the neutron beam polarization, asymmetry X was determined and theoretical corrections dependent on the energy E_e were introduced. Unfortunately, the space resolution in determining the direction of tracks in the drift chamber was insufficient for experimental determination of the average cosine with an accuracy required. Therefore, its value, $\langle\cos(\mathbf{p}_e\mathbf{P}_n)\rangle = 0.850 \pm 0.002$, was computed on the basis of a theoretical estimate of multiple scattering of electrons by the chamber gas. The degree of the beam polarization was $P_n = 0.981 \pm 0.003$, whereas the accuracy of its being conserved in reversing the spin amounted to 0.990 ± 0.002.

The final value obtained for the coefficient of electron-spin correlation ran into $A_0 = -0.1160 \pm 0.0015$.

5.4 Measurements of the *B* coefficient

The coefficient B weakly depends on λ, thus the value of λ_B computed on its basis cannot compete in accuracy with λ_a and λ_A calculated on the base of a and A (see Section 5.6). Measurement of B can be of interest in view of its role in estimating a possible deviation from the (V – A) theory.

In Ref. [94], the method was proposed for measuring the coefficients of correlations due to the antineutrino emission by the time lag of recoil protons with respect to electrons. It was realized in measuring B in the joint experiment of the St Petersburg Institute of Nuclear Physics and Kurchatov Institute performed on an intensive beam of polarized neutrons of the VVR-M reactor (Gatchina, 1995) [95, 96]. The set-up used for measuring A [90] was modernized. As before, coincidences of electrons and recoil protons were detected, but instead of drawing off protons from the decay region, they were given a path length free of field. To increase the accuracy of measurement of the time lag, protons were registered by a microchannel detector.

For two directions of the beam polarization, two-dimensional spectra $N^{\pm}_{i,k}$ of the electron energy E_i and lag time of protons t_k were stored in the computer memory. Asymmetry of the amount of events $X_{i,k} \equiv (N^+_{i,k} - N^-_{i,k})/(N^+_{i,k} + N^-_{i,k})$ was determined for every cell i, k; it depends on the coefficients of all three correlations:

$$X_{i,k} = \frac{P_n A\langle(v/c)\cos(\mathbf{p}_e\mathbf{P}_n)\rangle_{i,k} + P_n B\langle\cos(\mathbf{p}_\tilde{\nu}\mathbf{P}_n)\rangle_{i,k}}{1 + a\langle(v/c)\cos(\mathbf{p}_e\mathbf{p}_\tilde{\nu})\rangle_{i,k}} \quad (29)$$

The coefficients a and A can be considered as correction and their values might be taken from results of the known experiments since they are small as compared with B and their uncertainty does not affect the accuracy of B determination:

$$B = \frac{X_{i,k}\{1 + a\langle(v/c)\cos(\mathbf{p}_e\mathbf{p}_\tilde{\nu})\rangle_{i,k}\} - P_n A\langle(v/c)\cos(\mathbf{p}_e\mathbf{P}_n)\rangle_{i,k}}{P_n\langle\cos(\mathbf{p}_\tilde{\nu}\mathbf{P}_n)\rangle_{i,k}}. \quad (30)$$

As for the $\langle(v/c)\cos(\mathbf{p}_e\mathbf{p}_\tilde{\nu})\rangle_{i,k}$, $\langle(v/c)\cos(\mathbf{p}_e\mathbf{P}_n)\rangle_{i,k}$ and $\langle\cos(\mathbf{p}_\tilde{\nu}\mathbf{P}_n)\rangle_{i,k}$ averages, they were calculated with the computer model of the experiment. The calculation correctness was ensured by agreement of calculated two-dimensional spectra with those obtained experimentally and by the particular values of B derived from data at different $\langle\cos(\mathbf{p}_\tilde{\nu}\mathbf{P}_n)\rangle$ being constant.

The beam polarization (Fig. 13) measured with the method developed by Serebrov [97] amounted to $P_n = (66.88 \pm 0.22)\%$. (Decrease in polarization as compared to that obtained in Ref. [90] is due to still further worsening of properties of polarizing mirrors noted in Ref. [90].)

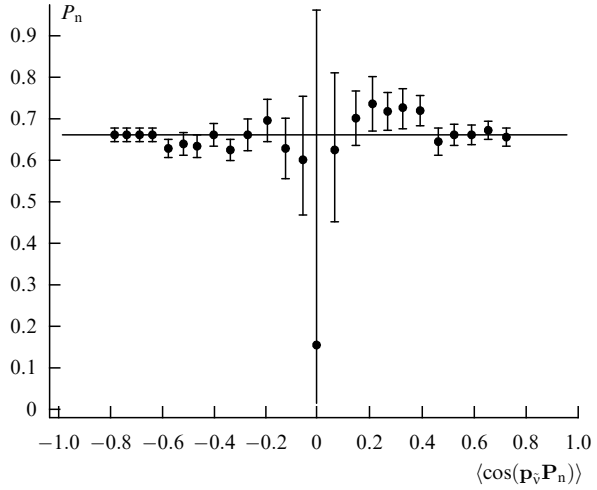

Figure 13. Experimental values of P_n obtained at different $\langle\cos(\mathbf{p}_\tilde{\nu}\mathbf{P}_n)\rangle$ [95].

The final value of B comprised 0.9894(83).

5.5 Measurement of the *D* coefficient

Up to the present, there is no theoretical understanding of the nature of the known violation of CP-invariance discovered in the decay of kaons. Search for the breaking of T-invariance that is equivalent to the CP breaking, according to the CPT-theorem, is an attempt to find an analog of this phenomenon in other processes (see Section 6). Some versions of the theory admit this violation in the decay of a free neutron. It would give a value of the coefficient D in expression (26) not larger than 10^{-3}.

To measure D, we should make the vectors $\boldsymbol{\sigma}$, $\mathbf{p}_e$ and $\mathbf{p}_\tilde{\nu}$ to be orthogonal to each other. This provides a maximum value for the T-noninvariant combination entering with D into (26), allows detection of $\mathbf{p}_p$ instead of $\mathbf{p}_\tilde{\nu}$ since $[\mathbf{p}_e \times \mathbf{p}_p] = -[\mathbf{p}_e \times \mathbf{p}_\tilde{\nu}]$, and moreover, this eliminates the P-correlations of A and B coefficients because $(\boldsymbol{\sigma}\mathbf{p}_e) = 0$ and $(\boldsymbol{\sigma}\mathbf{p}_\nu) = 0$.

Experiment [98] was carried out on a set-up with two electron and two proton detectors placed symmetrically with respect to the neutron beam. There, the direction of beam polarization and mean directions of detection of electrons and protons were made orthogonal to each other. The set-up symmetry allowed suppression of A and B correlations caused by inaccuracy in the mutual orthogonality since they are spatially odd, whereas that of D is spatially even.

This symmetry was also used later in the most accurate measurements of D and the values $D = -0.0011(17)$ [99] and $D = 0.0022(30)$ [100] were found in the process.

The present accuracy in measuring the D coefficient is not sufficient for discovering the violation of T-invariance equivalent to that of CP-invariance in the kaon decay but allows experimental restriction on the magnitude of the imaginary part of constant λ to be put: $D = (2\,\mathrm{Im}\,\lambda)/(1+3\lambda^2)$ and if λ is represented by $\lambda = |\lambda|\exp(-\mathrm{i}\phi)$, then from the average of two measurements of D it follows that $\phi = (180.07 \pm 0.19)^\circ$ [28]. This value permits further consideration of the quantity λ as real since $\mathrm{Re}\,\lambda$ differs from $|\lambda|$ no more than by $2 \times 10^{-3}\%$.

5.6 Determination of the β-decay constant λ from angular correlations

All the coefficients of two-vector correlations in the context of the (V–A) theory are expressed in terms of the single constant λ:

$$a_0 = \frac{1-\lambda^2}{1+3\lambda^2}\,, \quad A_0 = -2\,\frac{\lambda^2+\lambda}{1+3\lambda^2}\,, \quad B_0 = 2\,\frac{\lambda^2-\lambda}{1+3\lambda^2} \qquad (31)$$

(index 0 means that the coefficients contain no false corrections induced by 'small terms' in the Hamiltonian).

These relations provide estimation of sensitivity of various experiments to the determination of λ. The most sensitive is the measurement of the electron-spin correlation, $\mathrm{d}\lambda_A/\mathrm{d}A \approx 2.6$, close in sensitivity is the measurement of a, $\mathrm{d}\lambda_a/\mathrm{d}a \approx 3.3$, and the B measurement is the least sensitive, $\mathrm{d}\lambda_B/\mathrm{d}B \approx 11$ [101]. Results of the most accurate measurements of the correlation coefficients and values of λ computed by formula (31) are collected in Table 4.

Table 4

Coefficient	λ_k	Year	Ref.
$a = -0.099(39)$	$\lambda_a = -1.225(130)$	1967	[86]
$a_0 = -0.1017(51)$	$\lambda_a = -1.259(17)$	1978	[88]
$A_0 = -0.1116(60)$	$\lambda_A = -1.254(16)$	1975	[102]
$A_0 = -0.1126(50)$	$\lambda_A = -1.257(13)$	1979	[91]
$A_0 = -0.1146(19)$	$\lambda_A = -1.262(5)$	1986	[89]
$A_0 = -0.1116(14)$	$\lambda_A = -1.254(4)$	1990	[90]
$A_0 = -0.1160(15)$	$\lambda_A = -1.266(4)$	1995	[92]
$B = 1.01(5)$		1970	[103]
$B = 0.9950(350)$		1970	[104]
$B = 0.9894(81)$	$\lambda_B = -1.245(96)$	1994	[95]

If the (V–A) version of the weak interaction theory is strictly valid, the correlation coefficients are defined by the single decay constant λ and they should be connected by the expressions [105]

$$1 + A_0 - B_0 - a_0 \equiv 0\,, \qquad a_0 B_0 - A_0 - A_0^2 \equiv 0\,. \qquad (32)$$

Although two most accurate results of measuring the A coefficient differ by more than two standard deviations, the relations (32) for averaged modern data on the coefficients are fulfilled with a high accuracy, which testifies to consistency of the results of correlation experiments with the theory:

$$1 + A_0 - B_0 - a_0 = 0.0016 \pm 0.0096 a_0 B_0 - A_0 - A_0^2 = 0.025 \pm 0.036\,. \qquad (33)$$

This method of comparison with theory was developed in Ref. [100]. It was shown that if λ_{av} is obtained from λ_a, λ_A and λ_B by averaging with the weight inversely proportional to their standard deviations substituted into (31), then this leads to the most probable, within limits $\pm\sigma_a$, $\pm\sigma_A$ and $\pm\sigma_B$, combination of the coefficients $a_\lambda = -0.1021$, $A_\lambda = -0.1139$, $B_\lambda = 0.9882$ corresponding to a single $\lambda = -1.2605$. The probability of a combination like that provides estimation for consistency of a series of experiments with the (V–A) theory. It is a product of probabilities of evaluating a_λ, A_λ and B_λ and amounts to 0.99.

At the same time, the inclusion of data on the neutron lifetime and $(0^+ - 0^+)$ transitions leads to the most probable combination $\tau_\lambda = 890.1$, $a_\lambda = -0.1038$, $A_\lambda = -0.1160$, $B_\lambda = 0.9878$ corresponding to a single $\lambda = -1.2662$. The probability of that combination equals 0.007 resulting in the discrepancy with the theory by more than three standard errors.

5.7 Comparison of the results of measuring the lifetime and angular correlations

The above discrepancy is also observed when comparing the values of $\lambda_{\tau_\mathrm{n}}^{00}$ (from τ_n and $(0^+ - 0^+)$ transitions) and λ_c (from averages of correlation experiments). Usually, use is made of the value of λ_A as the most accurate.

For averaged results of eight measurements published until 1990, $\langle A_0 \rangle = -0.1142(17)$ and $\langle \tau_\mathrm{n} \rangle = 888.6(2.6)$ s, the difference between values of $\lambda_A = -1.2613(45)$ and $\lambda_{\tau_\mathrm{n}}^{00} = -1.2669(23)$ was of an order of their total inaccuracy [109]. The result of Ref. [90] published in 1990 noticeably changed the average value of A: $\langle A_0 \rangle = -0.1126(11)$ so that the values of $\lambda_A = -1.2571(29)$ and $\lambda_{\tau_\mathrm{n}}^{00}$ became still more different, which stimulated a search for possible reasons of the discrepancy.

These reasons could be as follows: deviation from the (V–A) theory, errors in the calculation of theoretical corrections or factors not considered in the experiments.

As shown in Ref. [90], the admixture of S- and T-variants of the theory would alternate the sign of the difference between λ.

In Refs [106–108], a detailed analysis was given for the possibility of admixture of (V + A) interaction carried by a right-handed W_R-boson. The contribution of right-handed currents changes λ_A and $\lambda_{\tau_\mathrm{n}}^{00}$ in a different way so that their discrepancy gives information on the W_R-boson parameters. The limitation on its mass $M_{\mathrm{W}_R} \geqslant 500$ GeV s^{-2} has been obtained from a joint analysis of the data on the neutron and muon decays and $(0^+ - 0^+)$ transitions [107]. At the same time, the analysis of Ref. [108], which included also data on the ^{19}Ne decay, predicted that the mass $M_{\mathrm{W}_R} \approx 230$ GeV s^{-2} is possible.

When the quantities λ were compared, data on the neutron decay were mixed with the ones on $(0^+ - 0^+)$ transitions. In Ref. [109], the method of determining G_A and G_V from the neutron data only was suggested. The idea consists in simultaneous solution of two equations, (24) and $\lambda_A = G_\mathrm{A}/G_\mathrm{V}$. Equation (24) defines an ellipse in coordinates G_A, G_V; whereas the λ_A quantity, an oblique line (see the insert to Fig. 14). Their intersection near the vertical line G_V^{00} determines the magnitudes of G_A and G_V. On the basis of data of 1990, $G_\mathrm{A} = -1.7908(22) \times 10^{-62}$ J m^3 and $G_\mathrm{V} = 1.4156(6) \times 10^{-62}$ J m^3 were obtained, the latter comparable in accuracy with $G_\mathrm{V}^{00} = 1.4149(8) \times 10^{-62}$ J m^3 from $(0^+ - 0^+)$ transitions.

This approach provides a clear interpretation of the problem of λ discrepancy in terms of disagreement between three experimental quantities. The point of intersection in Fig. 14 is shown on a large scale so that one can clearly see the width of ellipse and straight lines caused by experimental

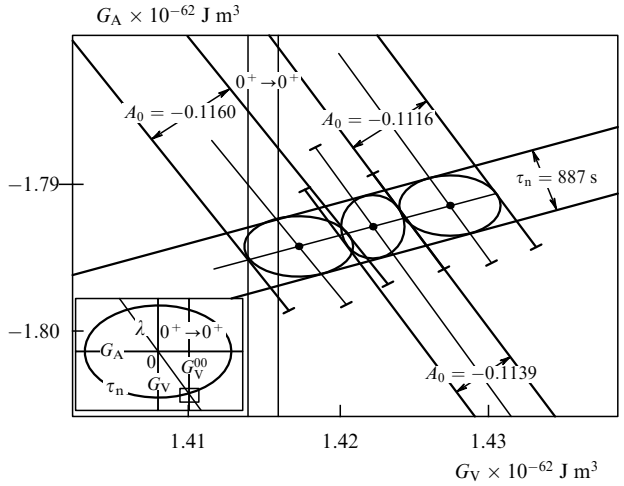

Figure 14. In the insert: the ellipse of G_A, G_V values determined by the value of τ_n; the oblique line $G_A/G_V = \lambda$ determined by the value of A and the vertical line G_V^{00} determined by the value of $(ft_{1/2})^{00}$. In the figure, the place of intersection is seen on a large scale. The width is clearly seen of the ellipse and straight lines caused by experimental uncertainties. Three oblique lines for three A_0 are drawn. Centers of their intersections with the ellipse define the values of G_A, G_V. Ovals inscribed into the regions of intersection characterize the determination uncertainty.

uncertainties, $\tau_n \pm \sigma_{\tau_n}$, $A \pm \sigma_A$ and $(ft_{1/2})^{00} \pm \sigma_{(ft_{1/2})^{00}}$. Presented are also three oblique lines for three A_0. Centres of their intersections with the ellipse determine the values of G_A, G_V whose uncertainty is characterized by ovals inscribed into the region of intersection. Disposition of the ovals relative to the G_V^{00} band indicates the degree of agreement between the experiments and (V – A) theory, and there is well seen the role of each of the three quantities τ_n, A_0 and ft_{00}: to improve the agreement, the quantities τ_n and $|A_0|$ are to be larger; whereas $(ft_{1/2})^{00}$, smaller.

Analysis of corrections to $(ft_{1/2})^{00}$ [81] led to increase in the error of $\sigma_{(ft_{1/2})^{00}}$ by about 1.5 times due to uncertainty in the choice of the calculable model for the structure correction as to compound nuclei. Theoretical corrections to τ_n and A_0 are on the scale of σ_τ and σ_A but they produce no doubts since they are defined with a high accuracy. By and large, to explain the discrepancy by errors of corrections seems to be impossible.

To establish inaccuracy of the experiments, they are to be repeated. Since 1990, there appeared five other experiments:

two measurements of τ_n [75, 76], one of which confirmed the average $\langle\tau_n\rangle$, and the other slightly diminished it;

measurement of B_0 [95] imposed the restriction on the mass $M_{W_R} \geqslant 350$ GeV s^{-2}, in contradiction with [108] but in agreement with [107];

measurement of $A_0 = -0.1160(15)$, $\lambda_A = -1.26610(40)$ [92] is in good agreement with the modern value $\lambda\langle\tau_n\rangle = -1.2689(16)$ (see Section 4.4) but in poor agreement with other correlation experiments since the average over all measurements retains the discrepancy with $\langle\tau_n\rangle$ in two standard errors [$\langle A_0\rangle = -0.1139(9)$, $\lambda_A = -1.2603(24)$] and even without [90], in one error [$\langle A_0\rangle = -0.1152(11)$, $\lambda_A = -1.2640(29)$];

measurement of $(ft_{1/2})^{00} = 3076.7(6.0)$ for ^{10}C [110] slightly increased the $\langle(ft_{1/2})^{00}\rangle$ average.

The situation resembles the one that developed in the early 70s with measurements of the lifetime, when the most accurate results differed almost by three standard errors. The problem was solved with new more accurate experiments. Totality of the present data seems to evidence in favour of experimental errors being the origin of the discrepancy in λ. Verification of this statement requires to increase the accuracy of measurement of correlation coefficients in new experiments. One of them can be the measurement of the A and B coefficients on the same beam planned jointly at the St Petersburg Institute of Nuclear Physics and Kurchatov Institute. From (31) it easily follows that the combination $(A - B)/(A + B)$ equals λ. It can be determined without knowing the degree of the beam polarization P_n since

$$\lambda = \frac{A - B}{A + B} = \frac{P_n A - P_n B}{P_n A + P_n B}\,.$$

Besides, λ_A can be determined from A by the traditional method if the beam polarization is taken into consideration. Further information: coincidence or difference between λ_A and λ_{AB}, their comparison with λ_τ, and comparison of the measured B with B calculated from λ_{AB}, can help to make choice between the right-handed currents and experimental error as possible causes of the discrepancy [111].

6. Electric dipole moment $\mathbf{d}_n$ of the neutron

6.1 Possibility of the $d_n \neq 0$ existence and its estimations

As known, the magnetic moment of the neutron is a dipole characteristic of its magnetic properties, whereas it possesses no monopole characteristic, the magnetic charge†. Apparently, the neutron has no monopole electric characteristic, the electric charge, too, although we cannot still exclude its extremely small magnitude. One would like to know what can be said about the dipole electric characteristic of the neutron, its electric dipole moment (EDM). Is it or no? Should it exist or not?

At present this question may be answered as follows: the neutron EDM (d_n) has not yet been found but, probably, it should exist although how large being it is still unknown. This intricate and not very definite answer to seemingly quite a simple question is not accidental because, as a matter of fact, that question is not so simple, which can be seen from the following clear reasoning.

Let us assume that $d_n \neq 0$ exists. Then as being a quantum-mechanical vector it should be oriented along the neutron spin $\boldsymbol{\sigma}_n$ considering that the spin is the only distinguished direction of a free particle:

$$\mathbf{d}_n = k\boldsymbol{\sigma}_n\,. \tag{34}$$

† Strictly speaking, it is not quite correct to identify the magnetic moment of the neutron as a magnetic dipole. Originally, the source of magnetic properties of magnetics was considered to be the magnetic charges of two opposite signs. When it became clear that they cannot be separated, the elementary particle of magnetism was considered to be a point magnetic dipole, the system of nonseparably connected magnetic charges equal in magnitude and opposite in sign. This model was proposed by Bloch in 1936 [112]. Practically simultaneously, in 1937, Schwinger put forward another, current model of the neutron magnetic moment [113], where it was assumed to originate from the distribution of current in the neutron.

In the Bloch model, the energy of magnetic interaction with an effective magnetic field equals $-\boldsymbol{\mu}\mathbf{H}$; whereas in the Schwinger model, $-\boldsymbol{\mu}\mathbf{B}$. Experiments on the neutron magnetic scattering testified to the validity of the Schwinger model. Therefore, it is more correctly to identify the neutron magnetic moment with a current element rather than a dipole (for details, see Ref. [4]).

Assume further that $\mathbf{d}_n$ and $\boldsymbol{\sigma}_n$ are parallel to each other ($k > 0$) and perform specular reflection (changing the x, y, z to $-x, -y, -z$). Then the polar vector $\mathbf{d}_n = e\boldsymbol{\delta}$ (δ is the distance between charges in the dipole) changes sign, whereas the axial vector $\boldsymbol{\sigma}$, whose mechanical analog is $m[\mathbf{vr}]$, remains unchanged, i.e. $\mathbf{d}_n$ and $\boldsymbol{\sigma}_n$ will become antiparallel ($k < 0$). If there exists invariance under specular reflection, then both the possibilities ($k < 0$ and $k > 0$) are to be on equal status, i.e. $\langle k \rangle = 0$ and the observed value of the neutron EDM should be $d_n = 0$. In other words, in order that $d_n \neq 0$, mirror symmetry should be broken (the conservation law of space parity is violated, $P \neq 1$). In view of this, before the discovery of the violation of that law in weak interactions in 1956 it was thought that $\mathbf{d}_n \equiv 0$, whereas upon the discovery researchers began to search actively for it. However, very soon they understood that the value $d_n = 0$ is also possible for $P \neq 1$ provided that there exists time invariance (T = 1). Indeed, it is easily seen that if t is replaced by $-t$, then the vector $\mathbf{d}_n$ in expression (34) does not change, whereas the vector $\mathbf{S}_n$ changes its sign. If T-invariance holds anew, then $k = 0$ and $\mathbf{d}_n = 0$, i.e. in order that $\mathbf{d}_n \neq 0$, the parity conservation law and T-invariance have to be broken simultaneously [114]. As a result, interest in the search for $d_n \neq 0$ dropped again and this continued up to 1964, when the discovery was made of a small violation of CP-invariance in the K_L^0-decay which is, in accordance with the CPT-theorem, equivalent to the violation of T-invariance.

It turned out that a K_L^0-meson, besides the decay into three π-mesons allowed by CP-invariance, decays rarely ($\varepsilon_K = 2.26 \times 10^{-3}$) over a CP-forbidden channel into 2 pions. Using the value of ε_K one can calculate the quantity ε', the ratio of CP-breaking interaction to a weak interaction [115]. Also, the quantity ε' was determined from direct measurements performed by two groups in 1991, which gave the average of ε' close to the calculated value [116]:

$$\varepsilon' = (3.3 \pm 1.1) \times 10^{-6}\,. \tag{35}$$

Considering that weak interaction forces are 10^7 times as weak as strong ones, one finds that the CP-breaking interaction is $10^7/(3.3 \times 10^{-6}) = 3 \times 10^{12}$ times weaker than the strong interaction. Discovery of this small CP-violation allowed again the assumption to be made that $\mathbf{d}_n \neq 0$. The latter conclusion is valid if it is assumed that CP $\neq 1$ discovered for K^0-mesons extends to a neutron as well. The difficulty is that a direct search for the CP-violation in any processes except for the K^0-decay was unsuccessful. However, there is an indirect but very convincing reasoning relative to possible violation of the CP-invariance just in *baryon* processes which can be tied to the problem of existence of the neutron EDM.

In 1967, Sakharov supposed [117] that because of small violation of the CP-invariance, not all baryons and antibaryons mutually annihilated at the end of the nonequilibrium stage of an early Universe evolution (their amounts were originally equal), but there remained a small excess of baryons (1 per 10^9 baryon-antibaryon pairs), out of which just the whole massive matter surrounding us was in time formed.

Based on the magnitude of CP-violation necessary for the Sakharov's hypothesis being valid, Ellis et al. [118], upon examining several different mechanisms of the CP-violation, showed that d_n can take the values within the limits:

$$3 \times 10^{-28} \leqslant d_n \leqslant 2 \times 10^{-25}\ e\ \text{cm}\,, \tag{36}$$

i.e. the upper and lower bounds of possible d_n values differ by 3 orders. This is a very wide scatter and, unfortunately, this drawback is characteristic of many other theoretical predictions. We will cite them following the works by Pendlebury [119] and Steyerl and Malik [61], by starting with two optimistic estimates.

In 1965, Bernstein, Feinberg, and Lee [120] put forward the hypothesis of strong violation of the CP-invariance in electromagnetic interaction that gave an assessment for d_n of an order of 10^{-20} e cm [121, 122]. However, this prediction was soon ruled out by the experiment (Fig. 15 of Ref. [119]) that gave $d_n < 3 \times 10^{-22}$ e cm [123].

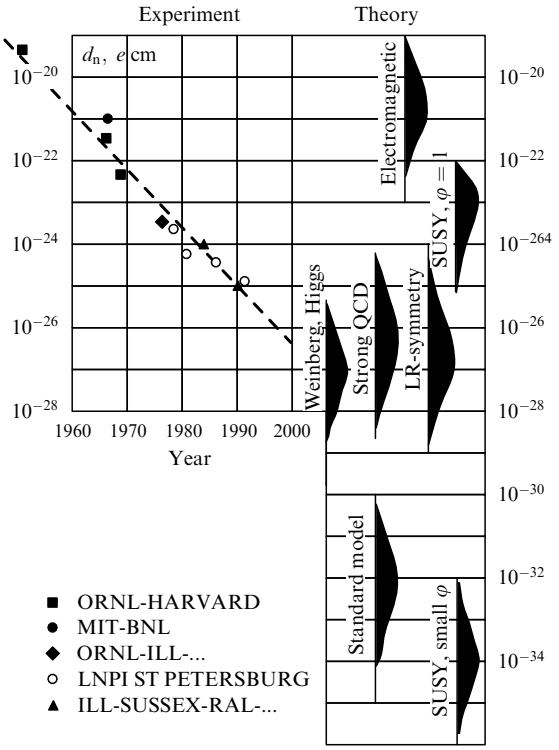

Figure 15. Comparison of experimental estimates of d_n with theoretical predictions.

Considerably smaller value of d_n but quite closer to modern experimental feasibilities is predicted by the following pictorial 'strong' QCD-model of the neutron EDM.

The neutron is known to consist of three quarks (n = udd) with fractional baryon ($B_u = B_d = 1/3$) and electric ($q_u = (+2/3)e$, $q_d = (-1/3)e$) charges. Therefore, in principle, if one ignores the reasoning about P- and CP-symmetry, a system of different-charged quarks placed at a distance of an order of the neutron size r_n and having a huge EDM

$$d_n = qr_n = \frac{e}{3}\,10^{-13} \approx 3 \times 10^{-12}\ e\ \text{cm} \tag{37}$$

could be framed. This estimate is, of course, wrong since, according to quantum chromodynamics, quarks in a neutron do not form a dipole but are uniformly distributed over its volume. However, if we assume that the above-discussed CP-breaking interaction can induce the corresponding dipolarity in a neutron, then for the neutron EDM we

obtain the value

$$d_{\rm n} = \frac{3 \times 10^{-14}}{3 \times 10^{12}} \approx 10^{-26}\ e\ \text{cm} \qquad (38)$$

close to the upper bound defined by (36).

Now we shall proceed to less optimistic estimates for $d_{\rm n}$. The standard model of electroweak interaction (that contributes to $d_{\rm n}$ only through the second-order terms) predicts the magnitude $d_{\rm n} \approx 10^{-32}\ e$ cm (the model of left-right symmetry increases this estimate up to $10^{-26}\ e$ cm). Still smaller value, $d_{\rm n} \approx 10^{-33}\ e$ cm, is forecasted by a model of supersymmetry (SUSY) when using a 'weak' (squark) mechanism of CP-violation, although when a 'strong' (gluon) mechanism is in use, the model gives $d_{\rm n} \approx 3 \times 10^{-27}\ e$ cm, and when employing the Weinberg mechanism of exchange by Higgs particles [124], even $10^{-26}\ e$ cm.

By this means, a very wide scatter is really observed in the predictions but, nevertheless, most of them are concentrated around the values $10^{-27} - 10^{-26}\ e$ cm, which are approximated in the modern experiments (see Fig. 15). To be aware of whether there is in near future a possibility to still closer approach the theoretical predictions, consider the methods of $d_{\rm n}$ measurements and prospects of their improvement.

6.2 Beam method of $d_{\rm n}$ experimental evaluation and the results obtained

In a relatively small paper, it is very difficult to describe exhaustively the complex set-ups utilized for estimating $d_{\rm n}$. Therefore, we shall rely on the reader's acquaintance (at least, with a similar procedure of determining the neutron magnetic moment, physicists dealt with during almost 60 years) and on his willingness to consult more serious sources recommended at the beginning of the paper. Here we shall only mention the basic procedure and briefly describe a pair of set-ups corresponding to two different measurement methods.

The idea of experimental estimation of $d_{\rm n}$ consists in an attempt to detect the change $\Delta\nu$ of the resonance Larmor frequency ν of a neutron moving in magnetic and electric fields under the inversion of the electric field $\mathbf{E}$:

$$\nu = \frac{2}{h}(\boldsymbol{\mu}_{\rm n}\mathbf{B} \pm \mathbf{d}_{\rm n}\mathbf{E})\,, \qquad (39)$$

$$\Delta\nu = \frac{4\mathbf{d}_{\rm n}\mathbf{E}}{h}\,, \qquad (40)$$

where $\boldsymbol{\mu}_{\rm n}$ is the neutron magnetic moment; $\mathbf{B}$ is the magnetic field induction; h is the Planck constant.

The neutron EDM, like its lifetime, is determined by two methods, the beam method and the UCN storage method. A set-up for measuring $d_{\rm n}$ by the beam method [125] is drawn in Fig.16, taken from Ref. [6]. The main part of the set-up is a magnetic-resonance neutron spectrometer earlier used for measuring the neutron magnetic moment $\mu_{\rm n}$ [126]. The spectrometer consists of a permanent magnet creating a uniform magnetic field of strength 20 mGs, a polarizer and an analyzer (magnetized iron mirrors), two radio-frequency coils spaced 2 m apart which produce an oscillating magnetic field, and a detector of neutrons, a glass plate covered with a ^{6}Li layer and glued on a photomultiplier. The measurement procedure was reduced to the determination of the resonance frequency ν whereat there occurs the neutron spin flip, which in turn is detected by the change in the counting rate of the detector.

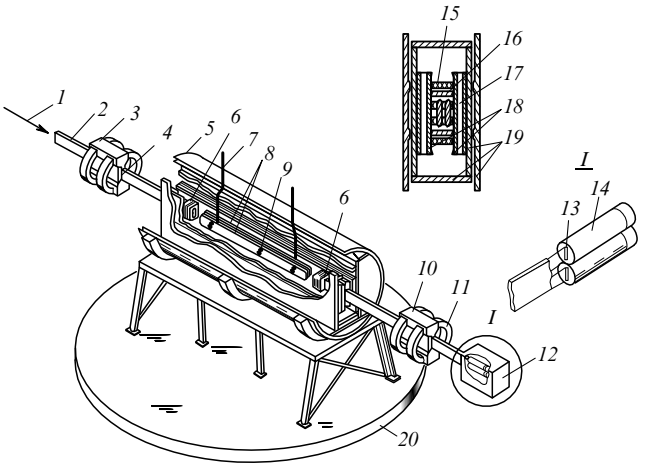

Figure 16. Scheme of the set-up for measuring $d_{\rm n}$ by the beam method: *1* — neutron beam; *2* — neutron guide; *3* — polarizer; *4* — polished iron mirrors; *5* — double magnetic shield made up of molypermalloy; *6* — radio-frequency coil; *7* — electric field source; *8* — condenser plates; *9* — insulators; *10* — analyzer; *11* — magnets made of Alnico alloy; *12* — detector; *13* — strips of scintillating glass; *14* — photomultipliers; *15* — quartz spacers; *16* — vacuum chamber walls; *17* — permanent magnets made of Alnico alloy; *18* — poles made of molypermalloy; *19* — soft iron; *20* — turntable.

For searching $d_{\rm n}$, the spectrometer was supplied with an electrostatic capacitor creating the electric field of strength 100 kV cm^{-1}. Basic requirements for a set-up are as follows: a high uniformity of the magnetic field throughout the whole beam region, its stability in time, and the magnetic and electric fields being as parallel as possible. If these conditions are not fulfilled, this would lead to further inaccuracy and a false effect (for details, see Ref. [6]). We call attention to the fact that the $\mathbf{dE}$ interaction is extremely small as compared to the $\boldsymbol{\mu}\mathbf{B}$ interaction. Therefore, at a fixed frequency of the oscillating magnetic field the change in the resonance Larmor frequency at the expense of the $\mathbf{E}$ re-orientation *can* be revealed only as a small shift of the resonance curve and related change in the detector counting rate.

By means of the above set-up, the upper bound of the neutron EDM

$$d_{\rm n} < 3 \times 10^{-24}\ e\ \text{cm} \qquad (41)$$

was determined, and it was the best estimate accessible for the beam method. More accurate estimates for $d_{\rm n}$ cannot be obtained by this method because it is impossible to improve mutual parallelism of the electric and magnetic fields (in the experiment [125], $\mathbf{B}$ and $\mathbf{E}$ nonparallelism was smaller than 0.01°).

6.3 Estimation of $d_{\rm n}$ by the UCN storage method. Modern magnitudes

Another method which has already given results better by an order of magnitude is the UCN storage method or, more properly, the method of magnetic-resonance UCN spin flip. This method employs the main property of UCN, their ability to be in the trap for a long time, which allows a careful examination of them. The idea of the method of magnetic-resonance spin flip is conserved in the process. As before, $d_{\rm n}$ is estimated by the change in the frequency $\Delta\nu$, when the direction of the electric filed is reversed: $\Delta\nu = 4\mathbf{dE}/h$. By

this method, the ILL group in 1990 arrived at the following result [127]:

$$d_n = (-3 \pm 2 \pm 4) \times 10^{-26}\ e\ \text{cm}\,, \tag{42}$$

whereas the Gatchina group found in 1992 [128] that

$$d_n = (2.6 \pm 4.2 \pm 1.6) \times 10^{-26}\ e\ \text{cm}\,. \tag{43}$$

Both the results list first systematic errors and then statistical errors.

The scheme of the ILL set-up is shown in Fig.17, taken from Ref. [119]. The measurement procedure is as follows: UCN fly up in the direction of a storage trap of volume 22 l being polarized along their way when passing a magnetized iron foil 2000 A thick. Once the trap is filled, the UCNs are isolated there for a storage time of order 150 s and are subject to the action of uniform magnetic and electric fields and a high-frequency field that flips the spin. The strength of the electric field **E** is kept in the process as high as possible at the level where there are no breakdowns and leakage currents are small. It is also important that the change of the **E** direction does not alter **B**. Therefore, the **B** quantity was simultaneously controlled with a quantum magnetometer (Rb–Cs pairs). A final direction of the spin is determined by the change in the counting rate of the detector when UCNs are allowed to escape from the trap and pass again through the foil that is now an analyzer. The value of Δv_0 is estimated from the change of counting rate in the detector. When d_n is measured, the difference in values of v corresponding to two directions of **E** is so small that for its estimation the operating point is to be chosen in the place of maximum slope of the magnetic resonance curve. Then the neutron EDM (d_n) is estimated by the shift of the operating point under the E reorientation.

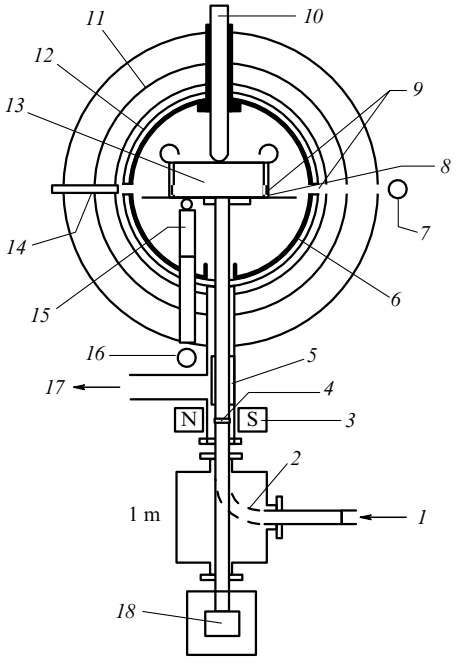

Figure 17. Scheme of the set-up for measuring d_n by the UCN storage method: *1* — UCN, *2* — neutron guide with switching, *3* — magnet, *4* — foil for polarization of UCN, *5* — high-frequency coil for spin reorientation, *6* — vacuum wall, *7* — ultraviolet Hg-lamp, *8* — aluminum insulating cylinder, *9* — windows for spectroscopy, *10* — input of high voltage, *11* — four-layer shield made of μ-metal, *12* — magnetic coil creating a field of 10 mGs strength, *13* — basic storage site, *14* — detector of ultraviolet radiation of Hg-lamp, *15* — cell of preliminary polarizations of Hg atoms, *16* — ultraviolet Hg-lamp, *17* — to vacuum pump, *18* — detector of UCN.

The uncertainty in measuring d_n is given by the expression

$$\sigma(d_n) = \frac{\hbar}{2\alpha E T\sqrt{N}}\,, \tag{44}$$

where E is the electric field strength; N is the total number of neutrons counted for a time of the whole experiment at both signs of E; T is the duration of the spin precession measured over one cycle; $\alpha = (C_1 - C_2)/(C_1 + C_2)$, where C_1 and C_2 are the counting rates at a maximum and minimum of the resonance curve near the operating point.

From formula (44) it follows that the experiments described above provide extremely possible accuracy of the d_n estimation, and to increase it, further improvements in the measurement procedure are necessary. We shall touch them in Section 9.3.

7. The neutron form factor

Now it is common knowledge that the neutron is not a point particle but possesses the finite size $r_n \approx 0.8 \times 10^{-13}$ cm and the structure, i.e. it consists of three valence quarks (n = udd) and a 'sea' of quark-antiquark pairs and gluons. As also known, the neutron charge Z_n equals zero and its magnetic moment $\mu_n \approx -1.91\mu_N$. However, details of the neutron structure, i.e. the distribution of the electric charge and magnetic moment over its volume, are ill known, and the combination of $Z_n = 0$ and $\mu_n \neq 0$ itself looks quite mysterious. Why is an uncharged neutron so strongly 'magnetized'? How should *charged* quarks be distributed over the neutron in order to provide $Z_n = 0$ and $\mu_n \neq 0$ simultaneously? And so that this distribution would not contradict the above situation with the neutron EDM and an approximate equality of the anomalous part of the proton magnetic moment to the absolute value of the neutron magnetic moment.

A bulk of information about the neutron structure was obtained from experiments on the electron scattering. The choice of the electron as a test particle is not accidental. First, it is a point particle†. Second, the strongest interaction for it is an electromagnetic interaction, the theory of which (quantum electrodynamics) features one of the most exact sciences.

Obviously, in order that an electron could probe the internal structure of a neutron, it should possess a sufficiently high energy, i.e. its de Broglie wavelength is to be much smaller than the neutron radius, $\lambda_e \ll r_n$. Otherwise, that probing can provide only some idea of the neutron external parameters: its radius, charge, and magnetic moment.

7.1 Notion of the neutron form factor and history of the problem

Since it is impossible to produce a neutron target for investigating the neutron structure, independent studies are carried out on the electron scattering from a deuteron and a proton, and the 'difference' of both the experimental results is

† The electron being a point particle was verified by agreement of experimental results with quantum-electrodynamic computations up to the distances of order 10^{-16} cm. The electron-positron-photon cloud of radius $\lambda_e^{com} = 3.85 \times 10^{-11}$ cm around the electron should not worry since its density is of order $\alpha = e^2/\hbar c = 1/137$.

separated and analyzed under certain assumptions on the deuteron structure. Let us consider the theoretical scheme of those studies for the case of studying the proton structure.

In 1950, Rosenbluth proposed the formula for the differential cross section of fast electrons scattering by a *point* proton [129]:

$$\left(\frac{\mathrm{d}\sigma(\Theta)}{\mathrm{d}\Omega}\right)_{\mathrm{Ros}} = \left(\frac{\mathrm{d}\sigma(\Theta)}{\mathrm{d}\Omega}\right)_{\mathrm{Mot}} \times \left\{1 + \left(\frac{hq}{2mc}\right)^2 \left[2(1+\mu_{\mathrm{an}})^2 \tan^2\frac{\Theta}{2} + \mu_{\mathrm{an}}^2\right]\right\}, \quad (45)$$

where $\left(\mathrm{d}\sigma(\Theta)/\mathrm{d}\Omega\right)_{\mathrm{Mot}}$ is the well-known Mott formula derived for the case $\sigma_{\mathrm{p}} = \mu_{\mathrm{p}} = 0$; Θ is the scattering angle in the laboratory system of coordinates; μ_{an} is the proton anomalous magnetic moment.

Comparison of the Rosenbluth formula with the experimental data at high energies of electrons gives

$$\left(\frac{\mathrm{d}\sigma(\Theta)}{\mathrm{d}\Omega}\right)_{\mathrm{ex}} < \left(\frac{\mathrm{d}\sigma(\Theta)}{\mathrm{d}\Omega}\right)_{\mathrm{Ros}}, \quad (46)$$

which points to the proton being not a point particle. To take the proton structure into consideration, two form factors are introduced: the Dirac form factor $F_1^{\mathrm{p}}(q)$ describing the distribution of the charge and the normal part of the magnetic moment ($\mu_{\mathrm{norm}}^{\mathrm{p}} = 1\mu_{\mathrm{N}}$), and the Pauli form factor $F_2^{\mathrm{p}}(q)$ that describes the distribution of the anomalous part of the magnetic moment ($\mu_{\mathrm{an}}^{\mathrm{p}} = 1.79\mu_{\mathrm{N}}$):

$$\frac{\mathrm{d}\sigma(\Theta)}{\mathrm{d}\Omega} = \left(\frac{\mathrm{d}\sigma(\Theta)}{\mathrm{d}\Omega}\right)_{\mathrm{Mot}} \left\{(F_1^{\mathrm{p}})^2 + \left(\frac{hq}{2mc}\right)^2 \times \left[2(F_1^{\mathrm{p}} + \mu_{\mathrm{an}}F_2^{\mathrm{p}})^2 \tan^2\frac{\Theta}{2} + \mu_{\mathrm{an}}^2 (F_2^{\mathrm{p}})^2\right]\right\}, \quad (47)$$

where

$$F_1^{\mathrm{p}}(q) = \frac{1}{e}\int \rho_{\mathrm{e}}(r)\exp(\mathrm{i}\mathbf{qr})\,\mathrm{d}^3 r\,, \qquad F_1^{\mathrm{p}}(0) = 1\,, \quad (48)$$

$$F_2^{\mathrm{p}}(q) = \frac{1}{\mu_{\mathrm{an}}}\int \mu(r)\exp(\mathrm{i}\mathbf{qr})\,\mathrm{d}^3 r\,, \qquad F_2^{\mathrm{p}}(0) = 1\,, \quad (49)$$

q is the momentum transferred; $\rho_{\mathrm{e}}(r)$ and $\mu(r)$ are, respectively, the distribution functions of the electric charge and magnetic moment over the proton volume.

Expression (47) is a second-order equation in $F_1(q)$ and $F_2(q)$. Therefore, to estimate $F_1(q)$ and $F_2(q)$ from it, the cross section $\mathrm{d}\sigma(\Theta)/\mathrm{d}\Omega$ is to be measured, at least, for two pairs of Θ and ε values corresponding to the same q.

Neutron form factors are obtained in a similar way by comparing the results of measurement on the electron scattering by a deuteron and proton. The neutron form factors are normalized as follows:

$$F_1^{\mathrm{n}}(0) = 0\,, \qquad F_2^{\mathrm{n}}(0) = 1\,. \quad (50)$$

The behaviour of form factors versus q reflects the nature of the charge and magnetic moment distributions. If a nucleon refers to a point particle, then $F(q) = 1$ at all values of q. The decrease of $F(q)$ with growing q is indicative of the charge (magnetic moment) being smeared out the more, the steeper is the curve.

A quantitative idea of the electric and magnetic structure of nucleons can be obtained by using the first Born approximation for the form factor $F(q)$:

$$F(q) = \int \rho(r)\exp(\mathrm{i}\mathbf{qr})\,\mathrm{d}^3 r = \frac{4\pi}{q}\int \rho(r)\sin(qr)r\,\mathrm{d}r\,, \quad (51)$$

whose expansion in a series in powers of qr gives

$$F(q) = F(0) - \frac{1}{6}\,q^2\langle r^2\rangle + \ldots\,. \quad (52)$$

As a result, one gets

$$\langle r^2\rangle \propto \frac{\mathrm{d}F(q^2)}{\mathrm{d}q^2}\,. \quad (53)$$

7.2 Experimental study of electron scattering. The scale law and values for $\langle r^2\rangle_N$

Experimental study of the electron scattering was carried out on a magnetic spectrometer consisting of two magnets which deviated the electrons scattered by a liquid-hydrogen or a liquid-deuteron target in horizontal (the measure of the scattering angle) and vertical (the momentum measure) directions. Detectors were taken to be hundreds of stripes of a semitransparent plastic scanned by photomultipliers connected to a computer.

The first results of the experimental study on electron scattering with energies up to 1.3 GeV by protons and deuterons were obtained by Hofstadter in 1955–61 [130]. They gave the values for proton and neutron form factors in the q^2 interval, $0 \leqslant q^2 \leqslant 40\ \mathrm{fm}^{-2}$, which resulted in the root-mean-square radii $a = \sqrt{\langle r^2\rangle}$ of the charge and magnetic moment distributions over a proton and neutron:

$$a_{\mathrm{E}}^{\mathrm{p}} = a_{\mathrm{M}}^{\mathrm{p}} = a_{\mathrm{M}}^{\mathrm{n}} \approx 0.8\times 10^{-13}\ \mathrm{cm}\,; \qquad a_{\mathrm{E}}^{\mathrm{n}} = 0\,. \quad (54)$$

Owing to a not very high accuracy of the experimental results in the region of maximum accessible q, it was assumed that the curves $F_1(q)$ at large q reach a plateau (which was not confirmed in subsequent measurements). It was natural to interpret such a behaviour of the curves as a peculiar 'revival"of the nucleon being point near its centre, which allowed one to propose a very plausible hypothesis about the nucleon structure. According to this hypothesis, the centre of both the nucleons contains a positively charged core of a very small radius (about 0.2 fm) whose charge in the neutron is compensated by a negatively charged pion cloud. This hypothesis was consistent with the principle of isotopic invariance and explained an approximate equality of anomalous parts of the nucleon magnetic moments, however, as for the core it failed.

In 1963, results were obtained for q^2 up to $125\ \mathrm{fm}^{-2}$ from which it followed that the form factors at large q^2 smoothly tend to zero by the $1/q^2$ law. This behaviour points to an exponential change of the density of the charge and magnetic moment in the proton and the magnetic moment in the neutron, with the previous value of the root-mean-square radius of 0.8 fm. It was more difficult to interpret the distribution of the charge density over the neutron, in view of insufficient accuracy of the data, but it was certainly found that both the nucleons have no cores.

Principal theoretical achievement of that stage of electron scattering studies was the vector-dominance model that predicted a group of vector mesons with spin and parity 1^- and masses $m = 5.5-7.5m_\pi$ (ρ-, ω- and φ-mesons).

Almost at the same period of time, the so-called charge and magnetic form factors were introduced instead of F_1 and F_2 for interpretation convenience:

$$G_E = F_1 + \tau\mu_{an}F_2 \quad \text{and} \quad G_M = F_1 + \mu_{an}F_2\,, \tag{55}$$

where

$$\tau = \frac{q^2}{4m_n^2}\,, \quad \mu_{an}^p = 1.79\,, \quad \mu_{an}^n = -1.91\,, \tag{56}$$

with the normalization

$$G_E^p(0) = 1\,, \quad G_E^n(0) = 0\,,$$
$$G_M^p(0) = 2.79\,, \quad G_M^n(0) = -1.91\,. \tag{57}$$

New form factors were more suitable because $\left(d\sigma(\Theta)/d\Omega\right)_{ex}$ was expressed through them in an extremely simple way:

$$\left(\frac{d\sigma(\Theta)}{d\Omega}\right)_{ex} = \left(\frac{d\sigma(\Theta)}{d\Omega}\right)_{Mot}\left(\frac{G_E^2 + \tau G_M^2}{1+\tau} + \tau G_M^2 \tan^2\frac{\Theta}{2}\right). \tag{58}$$

When $q = \text{const}$, this formula becomes

$$\left(\frac{d\sigma(\Theta)}{d\Omega}\right)_{ex} = \left(\frac{d\sigma(\Theta)}{d\Omega}\right)_{Mot}\left(a + b\tan^2\frac{\Theta}{2}\right), \tag{59}$$

where a and b are the constants, which attests to the linear dependence of $\left(d\sigma(\Theta)/d\Omega\right)_{ex}/\left(d\sigma(\Theta)/d\Omega\right)_{Mot}$ on $\tan^2(\Theta/2)$. From parameters of that curve it is easy to determine G_E and G_M.

In terms of the new form factors, basic results were formulated for the third stage of electron scattering studies started in 1966, in which the interval of accessible q^2 was extended up to 175 fm^{-2}. It turned out that

$$G_E^p = \frac{G_M^p}{|\mu_p|} = \frac{G_M^n}{|\mu_n|} = G(q^2) = \left(\frac{1}{1 + q^2/0.71}\right)^2; \quad G_E^n = 0 \tag{60}$$

(scale law or scaling).

From relation (60) it follows that the electric charge of a proton and magnetic moments of a proton and neutron are distributed by the law

$$f(r) = 3.06\exp(-4.25r)\,, \tag{61}$$

which gives

$$1)\ a_E^p = a_M^p = a_M^n = \sqrt{\langle r^2\rangle} = 0.815\times 10^{-13}\ \text{cm}\,, \quad a_E^n = 0\,; \tag{62}$$

$$2)\ G(q^2) \propto \frac{1}{q^4}\,, \tag{63}$$

in agreement with the quark model that predicts for hadrons

$$G(q^2) \propto q^{-2(n-1)}\,, \tag{64}$$

where n is the minimal number of quarks, constituents of an hadron. For a nucleon $n = 3$, which gives $G(q^2) \propto q^{-4}$. Later on, with increasing the accuracy of measurements of electron scattering by protons, deviations were revealed from formula (60) whereon we cannot dwell on here (see monograph [2] and references therein). We only mention that a new value was obtained for the proton root-mean-square radius

$$a_E^p = (0.83 \pm 0.03)\times 10^{-13}\ \text{cm} \tag{65}$$

on the basis of the refined data.

7.3 The problem of electric radius of a neutron

As before, it is still difficult to interpret the electric charge distribution over a neutron. On the one hand, the experiments on electron scattering by deuterons produce small positive values of $G_E^n \approx 0.05$ in the interval of the momentum transferred squared (5–25) fm^{-2} (Fig. 18a); on the other hand, the experiments on pion electroproduction in reactions $e^-p \to e^-p\pi^0$ and $e^-p \to e^-n\pi^+$ give zeroth and negative values (Fig. 18b). As a result, the experimental value of G_E^n averaged over many (about 10) works is close to zero.

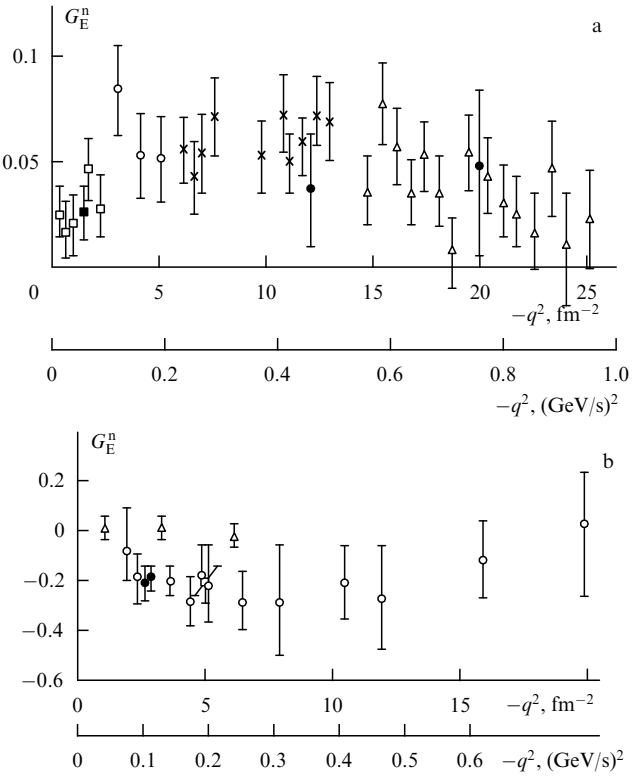

Figure 18. Experimental dependence of $G_{E_n}(q^2)$: (a) from experiments on ed-scattering; (b) from experiments on pion electroproduction on nucleons.

The result obtained is difficult to interpret for several reasons. First, it is unclear why G_E^n behaves independently of the behaviour of G_M^n altogether, whereas G_E^p and G_M^p behave equally. Second, if $G_E^n \neq G_E^p$, then why G_M^n behaves similarly to G_M^p? It turns out that for a completely different distribution of the electric charge over a proton and neutron, the distribution of currents in them is the same. And third, the equality $G_E^n = 0$ most likely points to a zero electric charge of a neutron ($a_E^n = 0$), whereas experimentally it was established that $(dG_E^n/dq^2)_{q^2=0} \neq 0$, which, according to formula (53), testifies to $a_E^n \neq 0$. Neither of these questions have been answered yet. New experiments and a more rigorous theory of the form factor are required.

Experimental uncertainty in the G_E^n and a_E^n quantities is due to the fact that, as mentioned above, basic information on these quantities is obtained as the 'difference' of the results for two experiments, electron scattering by a deuteron and a proton. The matter is not only that the error of the difference of two quantities is larger than that of each of them, but also that the deuteron however simple it looks is, nevertheless, a complex system whose structure is not yet known in detail.

Another more direct method of estimating the neutron electric charge is based on the results of experimental studies of low-energy neutron scattering from bound electrons in an atom. In this case, the measured interaction of neutrons with an atom is a sum of two parts, the interaction of the neutron magnetic moment with the Coulomb field of electrons and a nucleus (the so-called Foldy interaction) and the Coulomb interaction of the supposed electric charge of a neutron. Since the Foldy interaction can be calculated, the second term results again from the difference of the experimental and calculated findings.

Unfortunately, now the difference is the most insidious, it gives a two-valued result. The matter is that the experimental estimation of neutron interaction with an atom was given by two experimental groups with almost the same and sufficiently high accuracy but with different numerical values. One of them is larger than the subtracted calculable value of the Foldy interaction, whereas the other is smaller. Therefore, the difference expressed as the value of $\langle r_E^2 \rangle$ is either positive or negative†. Positive result for $\langle r_E^2 \rangle$ was obtained in Argonne and Garching; and the negative one

$$\left|\langle r_E^2 \rangle_n\right|^{1/2} = (0.11 \pm 0.02) \text{ fm}\,, \qquad \langle r_E^2 \rangle_n < 0\,, \tag{66}$$

by the Aleksandrov group in Dubna [2]. The most recent experimental data for $\langle r_E^2 \rangle_n$ are presented in the report by Samosvat [132] who, based on Ref. [133], also reports two values of $\langle r_E^2 \rangle_n$ different in sign:

$$\langle r_E^2 \rangle_n = -0.010 \text{ fm}^2 \quad \text{and} \quad \langle r_E^2 \rangle_n = 0.013 \text{ fm}^2\,. \tag{67}$$

Although both the pictorial nucleon model and the old meson and new quantum-chromodynamical theories prefer the negative‡ value of $\langle r_E^2 \rangle_n$, still more accurate experiments are required to finish in the argument. For now, the puzzle of the neutron electric charge cannot be considered solved§.

8. Exotic properties of the neutron

8.1 Gravitational interaction

At present, it is doubtful whether the neutron gravitational interaction can be considered as an exotic property, in particular, once we have examined the vertical neutron guides and a gravity spectrometer. However, not so long ago when only thermal neutrons were accessible to physicists, the possibility to verify the universality of the acceleration of free fall g with an *elementary particle* seemed to be rather a wonderful and very involved problem.

In fact, at the time, an attempt could be made to solve this problem by measuring the 'fall' of the beam of thermal neutrons at the end of the horizontal path of a reasonable length (about 10 m). However, by using the elementary formulae of school physics it was easy to show that this deviation would be negligible (around 0.01 cm). Again, like in all beam experiments, an extremely high velocity of thermal neutrons posed obstacles. Only later when cold neutrons (which were initially obtained by filtration of thermal neutrons through a BeO-like polycrystalline substance¶) appeared at physicists' disposal, the situation was significantly improved. For a cold neutron, the fall in a gravitational field when moving in the horizontal direction became already measurable.

The first experiment on determining the neutron gravitational interaction was carried out by McReynolds in 1951 [135] who observed that cold neutrons at the end of 12 m path were deviated down from the horizontal line by several mm. Recalculation to the acceleration due to gravity gave

$$g = (935 \pm 70) \text{ cm s}^{-2}\,. \tag{68}$$

In 1962, analogous measurement was performed by Dabbs et al.[136] on a path length of 180 m (Fig. 19) at the end of which the beam of cold neutrons sank with respect to thermal ones by 14.5 cm. Such a large 'splitting' of beams of thermal and cold neutrons gave rise to an essential increase in the accuracy of g measurement and provided the value

$$g = (975.4 \pm 3.1) \text{ cm s}^{-2} \tag{69}$$

that is very close to the universal one $g_0 = 979.74$ cm s^{-2} for given latitude and longitude. The neutron fall is especially clearly demonstrated at Dubna where still greater path length is available.

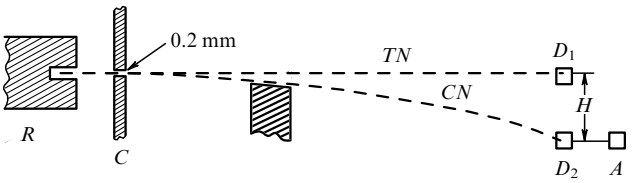

Figure 19. Scheme of the experimental study on the neutron gravitational interaction: R — reactor; C — collimator; TN — trajectory of thermal neutrons; CN — trajectory of cold neutrons; $D_{1,2}$ — detectors; A — analyzer of the beams divergence; H — shift between beams.

To summarize, we note that accurate measurements according to Eötvös approach carried out for two macroscopic bodies with different Z/A came to a conclusion of the g values equality for the neutron and proton to within experimental error of 2×10^{-9} and of the equality between the inert and gravitational masses within the error of 10^{-12}.

† By definition, $\langle r_E^2 \rangle = \int \rho(\mathbf{r}) r^2 \, d^3r$; thus, $\langle r_E^2 \rangle$ can be both positive and negative.

‡ For instance, one of the bag models, the cloudy bag model (see Section 8.3) gives $\left|\langle r_E^2 \rangle_n\right|^{1/2} \approx 0.35$ fm with negative sign [2].

§ For more details on the formalism of form factors, see monographs [2] and [131], and on the modern status of the problem and essence of the above dispute, monograph [2] and report [134].

¶ According to the Bragg–Wulf formula $n\lambda = 2d \sin\Theta$ (where n is the order of reflection; d is the distance between planes; Θ is the angle of reflection), the first-order reflection of neutrons with $\lambda > 2d$ is impossible at any angles, i.e. such neutrons do pass through a polycrystalline substance.

As for the exotics in the neutron gravitational interaction, conceivably it may be noticed in the following two experimental projects:

(1) According to General Relativity, a gravitational field established by a body changes when the body rotates around its own axis. A neutron possesses spin, i.e. it participates in a kind of quantum-mechanical 'rotation'. Therefore, gravitational forces acting on the neutron should depend on the orientation of its spin relative to the direction of the gravitational field though, of course, this effect cannot be at all noticeable. In 1967, McReynolds [137] found the absence of that effect within the limits of experimental error.

(2) In the sixties, the problem of existence of antigravitation for antiparticles was intensively discussed (see, e.g., Ref. [138]). In this connection, it would be interesting to test the behaviour of the antineutron beam in a gravitational field, though it can be said *a priori* that there will be nothing unexpected as the equality of masses of particles and antiparticles is a consequence of the fundamental CPT-theorem, and for other particles, e.g., antiprotons, it has been verified experimentally.

8.2 Electric charge of the neutron

In 1959, Feinberg and Goldhaber [139] showed that although the conservation laws being applied to nuclear reactions involving neutron give zero electric charge for it, nevertheless, this cannot be stated as an indisputable truth. The theory does not forbid a nonzero electric charge for the neutron. The reason is that the conservation laws for electric, baryon, and three lepton charges are fulfilled not only for conventional values of the corresponding quantum numbers ($Z = 0, \pm 1$; $B = 0, \pm 1$; $L_e = L_\mu = L_\tau = 0, \pm 1$), but also for other values being their linear combinations. It then follows that one cannot unambiguously define the relation between electric charges of all the elementary particles. Specifically, this is valid for the neutron that can possess a nonzero electric charge. There exist also reasons of cosmological character which admit the electric charge for a neutron at the scale

$$Q_n = \Delta q = Q_p - |Q_e| \approx (10^{-19} - 10^{-18})|Q_e| , \tag{70}$$

where Q_p is the proton charge, and Q_e is the electron charge (for details, see [2, 140]). In this connection, experiments on search for $Q_n \neq 0$ are highly appreciated.

An earlier direct experiment was conducted by Shapiro and Estulin in 1956 [141], who tried to detect the deviation of the beam of slow neutrons in a strong transverse electrostatic field. They estimated the upper bound of the neutron charge:

$$Q_n < 6 \times 10^{-12}|Q_e| . \tag{71}$$

In 1966, Shull et al. [142] performed a more accurate direct measurement of Q_n by the procedure of double Bragg reflection on a two-crystal spectrometer with a long (1.5 m) plane-parallel capacitor ($E = 225000$ V cm^{-1}) between crystals and obtained the value

$$Q_n = (-1.9 \pm 3.7) \times 10^{-18}|Q_e| . \tag{72}$$

Still more accurate were indirect experiments of 1957–63 on the search for the charge of un-ionized atoms and molecules [143–145] based on the measurement of the quantity

$$Q_a = Z\Delta q + NQ_n = (Z + N)Q_n , \tag{73}$$

where Z is the number of electron-proton pairs, and N is the number of neutrons in an atom, which gave the following estimate:

$$Q_n < 3 \times 10^{-20}|Q_e| . \tag{74}$$

Finally, in 1987, Baumann et al. [146] arrived at the best estimate for

$$Q_n = (-0.4 \pm 1.1) \times 10^{-21}|Q_e| \tag{75}$$

by the direct method with the use of neutron optics of cold neutrons. A similar result was obtained by Borisov et al. [147] with the use of UCN:

$$Q_n = (-4.3 \pm 7.1) \times 10^{-21}|Q_e| . \tag{76}$$

8.3 Polarizability

The neutron takes part in all four types of interaction: strong, electromagnetic, weak and gravitational. In accordance with the modern quantum field theory, it should be surrounded by a 'cloud' of quanta of the corresponding interactions. The cloud density is the larger, the stronger is the interaction. Analogously, effects induced by the cloud grow in the same order. The largest influence on the neutron properties comes from the meson cloud formed by quanta of strong interaction (mainly, by pions). We already mentioned it when discussing the problem of existence of the magnetic charge for an uncharged neutron†

The cloud is so called because it is not rigid and easily deformable. Deformation of the meson cloud under the action of an electric or/and a magnetic field is referred to as polarizability. The electric polarizability α is defined in the following way [147]:

$$\boldsymbol{\alpha}_E = \alpha \mathbf{E} , \tag{77}$$

where $\boldsymbol{\alpha}_E$ is the induced (dynamic) EDM, and $\mathbf{E}$ is an external static electric field. The magnetic polarizability β is given by

$$\mathbf{d}_M = \beta \mathbf{H} , \tag{78}$$

where $\mathbf{d}_M$ is the induced magnetic dipole moment, and $\mathbf{H}$ is an external magnetic field. Appearance of neutron polarizability changes its energy in electric or/and magnetic fields and therefore this polarizability can be determined from that change.

The induced dipole moment can arise, for instance, in interaction of γ-quanta with deuterons or in scattering of neutrons by heavy nuclei. We shall present below several estimates of the neutron polarizability based on the data from the above-mentioned report by Aleksandrov [134].

Processing of data on the cross section of deuteron photoabsorption gives

$$\bar{\alpha}_n + \bar{\beta}_n = (15.8 \pm 0.5) \times 10^{-4} \text{ fm}^3 . \tag{79}$$

Similar calculable estimates follow from a simple quark model as well as from a bag model, the Cloudy Bag Model

† More details on the meson theory of nuclear forces, quarks and some allied problems associated with the function of the nonnucleonic degrees of freedom can be found in introductory text to papers published in this journal, for instance, Refs [148, 149].

(CBM), in which the polarizability is determined by the distortion of the pion cloud†.

In 1990, from measurements of the quasi-free Compton scattering by a neutron bound in a deuteron, Rose et al. [134] obtained the value

$$\bar{\alpha}_n = (11.7^{+4.3}_{-11.7}) \times 10^{-4} \text{ fm}^3 , \tag{80}$$

i.e., actually, an upper bound. A similar result was found in studying the angular distribution of neutron elastic scattering by lead nuclei [134]:

$$(-5 < \bar{\alpha}_n < 6) \times 10^{-3} \text{ fm}^3 . \tag{81}$$

A nonzero value of α_n was derived from measurements of σ_{tot} for neutrons scattering by ^{208}Pb performed by Schmiedmayer et al.[150] in 1991:

$$\bar{\alpha}_n = (1.20 \pm 0.15 \pm 0.20) \times 10^{-3} \text{ fm}^3 , \tag{82}$$

where the first error is statistical, and the second one is systematic. However, in a subsequent discussion it was assumed that the result obtained also gives only the upper bound for α_n:

$$\bar{\alpha}_n < 2 \times 10^{-3} \text{ fm}^3 . \tag{83}$$

8.4 Neutron decay with violation of the baryon number conservation ($\Delta B = 1$)

The theory whose equations are invariant under special transformations is said to be symmetric with respect to these transformations. Thus, the special theory of relativity is relativistically invariant, i.e. it is symmetric with respect to the Lorentz transformations. Physical laws described by this theory do not depend on the velocity with which an observer is moving if it is constant (the laws do not depend on the choice of an inertial reference system).

This symmetry appears global because the relative velocity of motion of two inertial systems does not depend on time and coordinates. If the velocity does depend on time and coordinates (the motion with acceleration), the global symmetry is broken (for instance, acceleration of a spaceship), but it can be restored at the violation site by introducing the compensating (gauge) gravitational field (the local Lorentz symmetry).

In 1954, Yang and Mills made out that local invariance of a theory should always result in some extra compensating fields with new quanta, gauge bosons; and like quantum electrodynamics, gauge theories turn out to be renormalizable.

At present, it is known that strong, weak, and electromagnetic interactions obey this general principle of local gauge symmetry (supplemented with the ideas of its spontaneous breakdown in weak interactions and of quark confinement in strong interactions). Gauge bosons of a strong interaction are 8 colour gluons; whereas those of a weak-electric interaction, intermediate $W^{\pm}$- and Z^0-bosons and a photon.

Common gauge nature of all three interactions makes us hopeful of constructing a unified theory of strong, weak, and electromagnetic interactions. This theory called Grand Unification should be related to a wider group of symmetry [possibly, SU(5)] than those used in the above-mentioned theories [for instance, SU(2) under isotopic symmetry, SU(3) under octet symmetry, SU(2) × U1 in the weak interaction theory].

The group SU(5) contains both the quarks and leptons on equal status between which transitions become possible. In other words, the conservation law of the baryon and lepton numbers ($\Delta B = 1$, $\Delta L = -1$) can be violated in the corresponding theory but the difference $B - L$ is conserved, for instance, in the processes

$$p \to e^+\pi^0 , \qquad p \to e^+\pi^+\pi^- . \tag{84}$$

In both the processes, $B - L = 1 - 0$ on the left, $B - L = 0 + 1$ on the right, i.e. $\Delta(B - L) = 0$. For processes (84) the theory gives the estimate of the proton lifetime of $10^{31} - 10^{33}$ years.

Analogous reasoning is valid also for neutrons bound in nuclei for which decay processes of the type

$$n \to e^+\pi^- , \qquad n \to \pi^0\tilde{\nu}_e \tag{85}$$

can be expected. Search for the processes of that type is carried out at deep (to 7.6 km of water equivalent) underground laboratories well screened from cosmic background and with the use of detectors whose mass reaches several thousand tons. The principle of operation of one of the detector varieties is the detection of the Cherenkov effect, arising in the motion with superlight velocity of charged particles from the nucleon decay in water, with the help of several thousand photomultipliers. The genuine decay of a nucleon can be distinguished from background events (that have been thus far detected only) in terms of kinematics. The studies are advanced at about ten laboratories throughout the world (see, for instance, [151]). The data of these experiments provide the following estimate for the decay time of a neutron with $\Delta B = 1$:

$$\tau_n^{\Delta B=1} > 10^{32} \text{ years.} \tag{86}$$

This is, of course, highly optimistic estimate according to which a human being (consisting of about 4×10^{28} nucleons) should live around 2500 years till he will lose, as a result of decay, just one nucleon. However, for a physicist, a more tempting result would be the registration of such a unique decay in a huge detector because this would be a genuine exotics and would testify to the violation of the baryon number conservation with far-reaching consequences for the theory.

8.5 Neutron-antineutron oscillations ($\Delta B = 2$)

In 1956, on the bevatron in Berkeley (USA) Cork, Lambertson, Piccioni, and Wentzel discovered the neutron antiparticle, antineutron $\tilde{n}$. Antineutrons were produced in the process of charge exchange of antiprotons $\tilde{p}$ discovered on the same accelerator in 1955 [152]:

$$\tilde{p} + p \to \tilde{n} + n , \qquad \tilde{p} + n \to \tilde{n} + n + \pi^- . \tag{87}$$

† According to the CBM, the neutron consists of three color quarks (udd) confined inside a 'bag' out of which they cannot escape (confinement). Quarks undergo the action of strong forces whose quanta are the color gluons. Outside the bag these forces are not observed (the neutron is colorless), and interaction with other hadrons proceeds through ordinary nuclear (meson) forces. Hence, this model preserves the old clear picture with a π^--meson cloud surrounding the neutron 'bag', which allows the use of former phenomenological ideas of the origin of the neutron magnetic moment and the distribution of the electric charge over the neutron volume.

The antiproton channel of the accelerator ejected 5–10 antiprotons per minute. In reaction (87), 0.003ñ was produced per one p̃.

The basic property of an antineutron (like an antiproton) is its annihilation on colliding with a nucleon and release of a huge energy $2m_Nc^2 \approx 1900$ MeV. By using this property, antineutron events were separated from a large background of events induced by other neutral particles.

Other properties of ñ are as follows:

$$B=-1\,,\quad Z=0\,,\quad m_{\tilde{n}}=m_n\,,\quad \boldsymbol{\sigma}_{\tilde{n}}=\frac{1}{2}\,,$$

$$\boldsymbol{\mu}_{\tilde{n}}=-\boldsymbol{\mu}_n\,,\quad P=-1\,,\quad \mathbf{T}=\frac{1}{2}\,,\quad T_3=+\frac{1}{2}\,; \qquad (88)$$

the scheme of radioactive decay and half-life are also given:

$$\tilde{n}\to\tilde{p}+e^+ +\nu_e\,,\qquad T_{1/2}(\tilde{n})=T_{1/2}(n)\,. \qquad (89)$$

Annihilation is accompanied by production of 5 pions, on the average (in 95% cases), and of a pair of K-mesons (in 5% cases).

Owing to masses of n and ñ being equal, the energy levels characterizing their values are degenerate and even in superweak interaction they can mix, i.e., in principle, we may say that there exist processes of n transition into ñ and back (neutron-antineutron oscillations in vacuum)†.

The nñ oscillations should be accompanied by the change of the baryon number by 2:

$$\Delta B_{n\tilde{n}}=2\,. \qquad (90)$$

Therefore, they are forbidden in the Grand Unification model related with the symmetry group SU(5) that allows transitions with $\Delta B=1, \Delta L=-1$ (decay of a nucleon). However, some other models of Grand Unification allow interactions changing B by 2.

Besides nñ oscillations in vacuum, the change of B by 2 can occur also in a simultaneous decay of two neutrons of a nucleus. However, the theory predicts that the second process should proceed much more slowly than the first one:

$$\tau_{dec}=m_n(\tau_{os})^2\,, \qquad (91)$$

where $m_n \approx 10^{24}$ s^{-1} (in the system of units $c=\hbar=1$).

Assuming that $\tau_{dec} > 10^{32}$ years, for τ_{os} we arrive at the estimate:

$$\tau_{os} > 5\times 10^7 \text{ s}\,, \qquad (92)$$

i.e. about 1.5 years. Such a comparatively not very rare process can be observed in intensive beams of neutrons emitted by nuclear reactors. The process of nñ oscillation will be manifested by the appearance of an antineutron in the neutron beam, which can be detected through the process of annihilation. Similar experiments were already prepared and are even conducted, for instance, on the beam of cold neutrons of the ILL reactor in Grenoble. Basic units of the set-up are: the CN source giving the flux 5×10^{11} s^{-1}, path length of 74 m, annihilation target 100 μm thick, and a detector for registering annihilation products of sizes $6\times 7\times 6$ m. The path length is protected from the Earth's magnetic field by magnetic shields, and the detector is connected in the scheme of anticoincidence with a system of counters screening it from the cosmic background. Similar parameters of the set-up allow one to believe in the possibility of discovering the nñ oscillations if $\tau_{os} < 10^8$ s. In 1990, on this set-up, the estimate $\tau_{os} > 10^7$ s was obtained [153], and in 1995, even more accurate prediction was made [134]:

$$\tau_{os} \geqslant 0.86\times 10^8 \text{ s}\,. \qquad (93)$$

The intensity of neutron beams from modern reactors and meson factories makes us hope for detecting nñ oscillations even if $\tau_{os} > 10^9$ s [154]. However, it is to be remembered that the upper bound of theoretical estimates‡ equals $\tau_{os}=10^{37}$ s.

9. New problems, ideas, and projects

9.1 UCN storage anomalies

9.1.1 'Revival' of the UCN leakage. In Section 3.5, we tried to picture a joyful sense of the physicists relief when the main origin of the UCN leakage in material traps was revealed: it was the heating of UCN up to thermal energies in inelastic collisions with hydrogen nuclei that are invisibly present on the trap walls and subsequent escape of thermal neutrons through the walls. This achievement moved the UCN physics onto a new level, and many brilliant results were obtained. However, triumph turned out to be premature.

In September, 1995, at the VIIth School on Neutron Physics in Dubna, Steyerl and Malik [61] reported that in recent years information was provided on an anomalously small number of β-decays of UCNs stored in material traps at low ($\sim$ 10 K) temperatures as compared to theoretical predictions. In other words, the observed number of UCN collisions up to their disappearance is many fewer (hundreds of times) than that resulted from the theory. Any reasonable explanation of that effect, such as it being caused by large cross sections of absorption and inelastic scattering for nuclei of the wall material or possible contaminations (including boron and nitrogen), microscopic cracks in walls, roughness of the walls or their vibrations, failed. Any of these causes could explain a negligible part of the effect (1/40–1/30); and all of them, no more than 10 per cent. Thus, the problem of UCN leakage sprung up again (at another level) and in so incomprehensible form that it is now referred to as the anomaly of UCN storage. As main sources of information on the present anomaly of UCN storage, the authors of report [61] named the studies performed at Dubna and Gatchina by Strelkov [156], Alfimenkov et al. [157], and by Nesvizhevskii et al. [158].

The most clear and convincing illustration of the UCN storage anomaly at low temperatures can be seen in Fig. 20 showing the results of experiments carried out by Alfimenkov et al. [157] at Gatchina. Two types of curves are drawn in the figure. Curves *1c–4c* describe the behaviour of the UCN loss cross section versus temperature of traps various in shape and with different treatments of their walls. Curves *1a–3a* characterize the behaviour of the loss cross section when measurement is made on transmission of faster neutrons ($v=8$–15 m s^{-1}) through thin Be samples prepared by

† Information on the oscillations of K^0-mesons similar in the mathematical formalism and further details on antineutron properties can be found, e.g., in Ref. [131].

‡ For details, see [2, 155].

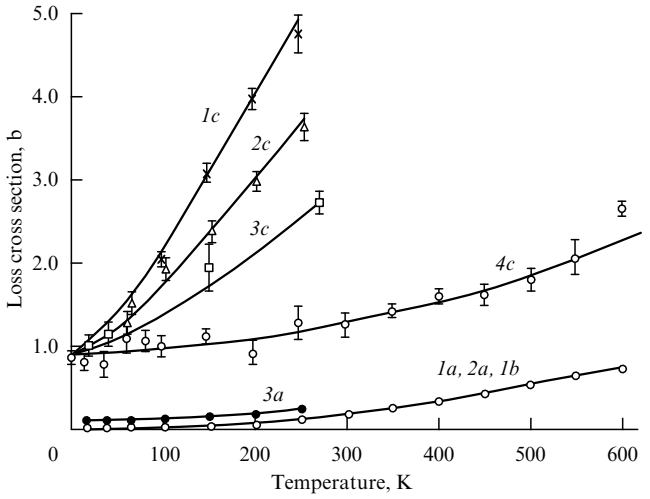

Figure 20. UCN storage anomaly at low temperatures: *1a–3a* — curves of the loss cross section obtained by the method of neutrons transmission through different Be samples (*1a* — sample obtained by melting; *2a* — quasi-monocrystalline sample; *3a* — pressed sample); *1b* — theoretical curve; *1c–4c* — curves of loss cross section in the UCN storage (*1c* — spherical trap with deposited nondegasified Be; *2c* — cylindrical trap with deposited Be degasified at 250 °C for 5 h; *3c* — any Be trap degasified at 300 °C for 8 h; *4c* — spherical trap with deposited Be degasified for 28 h at 350 °C and purified with He and D_2).

different technology. Besides, the figure shows a theoretical curve *1b*, the temperature-dependent total cross section of absorption and inelastic scattering $\sigma_a + \sigma_{in}$ calculated with the Debye model.

In experiments on the UCN storage in Be traps, the loss cross section σ was derived as the difference of measured losses in storage and the ones caused merely by β-decay. These extra losses were classified with losses from collisions with walls and were expressed as the cross section at a standard velocity of neutrons (2200 m s^{-1}).

Basic conclusions drawn from analysis of Fig. 20 are as follows.

The loss cross sections obtained in measurements of the neutron transmission are compatible with the calculated curve (apart from that for pressed Be sample, which is explained by its specific structure) and at extremely low temperature of 10 K are very small, 0.008 b.

Unlike the previous case, the loss cross sections at high temperatures measured in UCN storage experiments 'sense' the shape of a trap and the method of treating its walls, but all four curves tend to the same value, $\sigma = 0.9$ b, at a temperature of 10 K. This value is about 100 times as large as the calculated one and experimental values obtained in the previous case, and, as it follows from the comparison of curves *4c* and *1b*, it is temperature-independent.

The effect described possesses so remarkable properties ('wall' character of manifestation, a huge magnitude and independence from temperature) that it can be really called anomalous, and the corresponding value of the loss cross section, $\sigma = 0.9$ b, as the anomalous loss cross section σ_{an}.

To summarize, several comments are to the point.

The authors of Refs [156–158] noted that the anomalous effect they discovered for the Be trap was, apparently, detected still earlier by Ageron et al. [159], however, as Ignatovich suggested [5], they used a wrong value of the cross section for Be in interpreting the results.

Apart from Be, the anomalous behaviour of the UCN leakage was also observed for other wall materials with a very small nuclear absorption. Kosvintsev et al. [160] and Morozov [161] investigated D_2O; Alfimenkov et al. [157], O_2 and CO_2. In all the cases, experimentally detected losses at low temperatures exceeded the calculated value, like for Be, by about 100 times.

Finally, we will present most interesting observation. Extraordinariness of the anomalous effect struck physicists to such a great extent that they proposed the quantum-mechanical subbarier penetration of UCN through trap walls as a possible way of its explanation (except for those listed at the beginning of this section). However, the experiment did not confirm this hypothesis. So, the anomalous effect of the UCN storage is still waiting for its complete explanation†.

9.1.2 Anomalous cooling of UCN on their storage. In 1979, Kosvintsev et al. [162] studied a conjectural heating of UCN of very low energies [$E = (6-29) \times 10^{-9}$ eV] in quasi-elastic scattering initiated by vibration of walls. Neutrons were stored in a copper trap at room temperature. The UCN spectrum was regulated by introducing a polyethylene disk into the trap from the top. When the disk was at height h from the bottom of the trap, the spectrum of stored UCN was restricted from above by the energy of those neutrons whose height of 'jump' was smaller than h. The measuring procedure reduced to the change of height h and determination of the spectrum for two different time lags t_W between filling the trap and lowering the disk to a given height h: (a) $t_W = 0$, and (b) $t_W = 140$ s. The spectrum (b) was corrected for the losses due to β-decay and for the wall effect. From comparison of the corrected spectrum (b) with the spectrum (a) it turned out that the whole spectrum of UCN for the time lag 140 s shifted towards lower energies by the value of $\Delta\varepsilon$ equivalent to the change in height by $\Delta h = 2-3$ cm.

Like the anomaly considered in the previous section, the effect of UCN cooling caused by interaction with the wall that is 10^5 times warmer than UCN looks as a great puzzle for the authors of report [61], although the authors of the very observation are inclined to explain the effect of 'cooling' by a natural broadening of the spectrum through quasi-elastic scattering initiated by vibrations of walls.

9.2 Ideas of constructing the new sources of cold and ultracold neutrons

Projects of new experiments on more accurate measurements of neutron fundamental parameters require to increase the intensity of CN, VCN, and UCN sources. Steyerl and Malik [50] presented several ways for increasing the intensity of those sources.

(1) Further improvement of the liquid-helium source that can provide, as Kilvington et al. [163] showed, a high density of UCN inside the converter with liquid helium. It is quite difficult to realize this project owing to extremely high requirements to the apparatus for extracting UCN from the converter: transparency for UCN, impenetrability for helium, and reliable thermal shield. Some possibilities to overcome these difficulties were considered in studies by Golub and

† Not long before sending the manuscript for publication, Morozov informed us that about half (~ 40%) the observed anomalous effect of the UCN storage is explained through the capture of neutrons by wall protons with production of γ-quanta.

Boning [164] and Yoshiku et al. [165] on the use of the liquid-helium neutron source in beams of fission neutrons. Besides, as shown by Kilvington et al. [163] and Golub [166], there exist interesting possibilities for carrying out physical studies without extracting UCN from the source as well (see the next section).

(2) Another possibility of producing the intensive source of UCN is connected with future use of the peak intensity of pulsed reactors. It is known, for example, that the pulse reactor IBR-2 at Dubna has a very high peak flux 7×10^{15} $cm^{-2}\ s^{-1}$ against the neutron flux $10^{13}\ cm^{-2}\ s^{-1}$ averaged over time. If we succeed in extracting UCN from the neutron beam at the instant of the peak power of the reactor, the density of UCN captured in the trap will be proportional to that power. To realize this idea, Novopol'tsev et al. [167] proposed to utilize a cold converter with a fast magnetic shutter transmitting UCN (in a certain energy range) only during the neutron burst of 300 μs.

(3) One more idea of obtaining the intensive source of UCN from the pulse reactor has been developed by Brun et al. [168] where the so-called crystalline turbine was presented. This instrument makes up a rotating arm 1.2 m long on which a crystal is mounted and used as a reflector moving away from neutrons. The principle of operation of this instrument is similar to that of the neutron turbine described in Section 3.4.2. In this instance, however, the crystal running away from the beam transforms the neutron energy through the Doppler effect. Realization of this project is made difficult in view of the absence of crystals with a high reflecting power for the whole interval of velocities of incident neutrons necessary for obtaining the whole spectrum of UCN.

As for items 2 and 3, it is instructive to mention that one difficulty common for them may exist owing to the time of establishing the equilibrium spectra of VCN and UCN being larger than duration of the initial neutron flash, which can diminish the intensity of VCN and UCN sources. A way for overcoming this difficulty is 'to poison' the moderator through the absorber which should reduce the source efficiency.

(4) Finally, there exists one more obvious, so to say, 'frontal' method of increasing the intensity of VCN and UCN sources, namely, the increase of the power of stationary reactors which will lead to the growth in the intensity of the initial neutron beam, and hence, of the CN, VCN, and UCN beams. However, this method could hardly produce a gain larger than 10.

9.3 Projects of new experiments on search for d_n and measurements of τ_n and angular correlations

9.3.1 Further search for the neutron dipole electric moment. We saw in Section 6.1 that the Sakharov – Ellis model predicts the value of d_n within the limits $3 \times 10^{-28} - 2 \times 10^{-25}\ e$ cm. Though the sensitivity of modern experiments is almost sufficient to reach the upper bound of those values, as follows from formula (44), to reach the lower bound, it is to be increased by about a factor of 1000. In accordance with formula (44), this can be done by increasing E, T, and N (as well as through general refinement of the measurement procedure).

We shall list below some particular recommendations on the improvement of the procedure of searching for d_n (part of which was already realized) by taking advantage of papers by Schreckenbach and Mampe [169] and report by Steyerl and Malik [61].

(1) Increasing the volume of the UCN storage trap (increase of the counting rate).

(2) Using as the magnetometers the substances (for instance, ^{199}Hg) introduced directly into the trap volume (diminishing the systematic error).

(3) Filling the trap by ^4He with admixture of polarized ^3He, which promises a particularly large gain for following reasons [166, 167]:

(a) owing to an effective lowering of the energy of cold neutrons in superfluid ^4He, the density of UCN will significantly increase, which can give the gain in sensitivity by a factor of 100;

(b) charged particles emitted in the process of neutron absorption will initiate scintillations in ^4He, which can be easily detected (upon conversion of ultraviolet radiation into visible light); this phenomenon makes it possible to carry out measurements inside the trap;

(c) owing to the measurements inside the trap, the UCN losses decrease by a factor of 3;

(d) by virtue of the presence of helium between electrodes, it is possible to increase (about 5 times) considerably the intensity of the electric field;

(e) since polarized ^3He nuclei can absorb neutrons only with opposite spins, substantial polarization of neutrons is to be observed;

(f) ^3He, like ^{199}Hg, can serve as a volume magnetometer.

Thus, according to the above listed estimates, the total gain in sensitivity can really reach 1000, which will allow us to get to the lower bound ($3 \times 10^{-28}\ e$ cm) of the neutron EDM as estimated by the Sakharov – Ellis hypothesis. However, the theoretical value ($10^{-32}\ e$ cm) predicted by the standard model of weak interaction is still inaccessible. Since there appear much more optimistic estimates than pessimistic ones (see Section 6.1), we will hope that the finish of pursuit of $d_n \neq 0$ is not far off.

9.3.2 A new project of measuring the neutron lifetime with an increased accuracy. In 1994, Doyle and Lamoreaux [171] proposed a new experimental procedure for measuring the neutron lifetime with the use of UCN produced and stored in a three-dimensional magnetic trap filled with helium. The method is based on the regime of formation and storage of UCN in inelastic scattering of cold (8.9 A) neutrons in a superfluid ^4He [163, 172, 173].

The neutron β-decay should be detected almost with 100 per cent efficiency through scintillations in helium induced by fast charged particles, the decay products. The neutron lifetime is directly determined by measuring the counting rate of scintillations as a function of time.

The experimental procedure suggested possesses three principal advantages as compared to the previous experiments with a magnetic storage: a higher stored density of UCN on their production in superfluid helium, a direct detection of the number of neutrons in a trap, and removal of the losses generated by betatron oscillations.

It is expected that the total systematic error resulting from the UCN leakage near the trap brims, absorption by admixtures (in particular, by ^3He), and from energy-upward inelastic scattering will not exceed 0.001 per cent, thus providing at least the 50-fold increase in the measurement accuracy of the neutron lifetime.

9.3.3 Projects of some other new experiments. We shall briefly outline some other new projects and experiments under way.

(1) Erozolimskiĭ [174] proposed the project of simultaneous measurement of the constant B and ratio a/A with the help of two detectors in the 180°-geometry with very small solid angles of detection. Analysis of the project shows that this experiment does not require the precision spectrometry of the particles, which should diminish the systematic error. Computer calculations performed in 1994 prove its being realizable.

(2) In the same report [174], information is conveyed about new measurements of τ_n performed by Morozov group and about τ_n data processing at NIST (USA) made by the Bern method. Expected accuracy in both the studies is $\pm(1-2.5)$ s.

(3) At the St Petersburg Institute of Nuclear Physics and Russian Research Centre 'Kurchatov Institute', on the one hand [175], and at NIST (USA), on the other hand (private communication by Dewey from NIST), the set-up was prepared for measuring a three-vector correlation within accuracy of $\pm 2 \times 10^{-4}$.

Progress in experimental accuracy of measuring the three-vector correlation, besides the statistical accuracy, is due to increase in the symmetry of utilized set-ups for suppressing false effects. In particular, the experiment planned at NIST will have four pairs of detectors. In the experiment organized by the collaboration of PINPh and Kurchatov Institute, two pairs of detectors are kept but a slow rotation is provided for the systems of extraction and detection of decay protons during experimentation. This rotation will allow physical averaging of azimuthal nonuniformities of the proton losses in their detection, which can imitate the asymmetry searched for.

10. Conclusions

For the sixty five years past since the discovery of a neutron, we learned very much about its properties but still not less remained indecipherable. Let us judge by ourselves:

(1) Being predicted and discovered as particles highly penetrating through matter, the neutrons displayed later an opposite property, their prolonged storage in vessels with material walls, but still later it turned out that part of the stored neutrons, nevertheless, somewhere disappears, and this riddle is still far from being solved.

(2) For a comparatively long time it became known that the neutron consists of three colour valence quarks (n = udd) with electric charges ($q_u = (+2/3)|e|, q_d = (-1/3)|e|$) but it is still unknown how they are distributed over its volume (what is the neutron electric radius?) and even the problem of the magnitude of the neutron total electric charge (is it nonzero?) has not been solved yet.

(3) That the neutron has a large magnetic moment remains also a mystery. If the magnetic moment constitutes an elementary current, then how should the charged quarks move in order that they, on the one hand, create the magnetic moment and, on the other hand, produce neither total electric charge, nor positive and negative its parts distributed over the neutron volume. And why the magnetic radius of the neutron coincides both with the electric and magnetic radii of the proton?

Willy-nilly, there arise nostalgic memories about the model proposed by Schopper in 1961 [176] for the nucleon with a positively charged core in its centre and meson (negative for the neutron and positive for the proton) clouds at the periphery which was able to explain all those riddles. However, the existence of the nucleon core was not confirmed, and until now there is no equally obvious model. In recent years, the Cloudy Bag Model of quantum chromodynamics became approaching the Schopper model.

(4) No electric dipole moment heretofore was detected for the neutron, although, as it follows from the experimentally established fact of the CP-invariance violation in K^0-decay, it should exist. True, the comparison of theoretical estimates with findings of modern experiments shows that, apparently, its accuracy is still insufficient in order to 'reach' the most probable theoretical predictions. At any rate, the riddle remains unsolved.

(5) The same considerations on insufficient experimental accuracy can be applied to the fact that neither neutron (and proton) decays with $\Delta B = 1$, nor neutron-antineutron oscillations with $\Delta B = 2$ have been yet detected. Though it is to be mentioned in these cases that the phenomena may not exist, as well, if the baryon charge is exactly conserved.

(6) Finally, concerning the lifetime and angular correlations in β-decay of the neutron, we have paid the most attention in our paper, it can be said that the cause of the discovered puzzle in their behaviour is not any peculiarity in the neutron properties but merely neglected experimental errors and not quite an adequate theoretical description of the interactions in which the neutron takes part. Beyond all manner of doubt, both the neutron lifetime and angular correlations in its β-decay will be measured in a near future much more accurately than they are known at present.

However, for the neutron itself this will be though very important but nevertheless only a *quantitative* more accurate determination of the *known* properties, whereas in the theoretical field this can produce a radical *qualitative* change of its fundamentals, for instance, the prediction of existing the right-handed currents and right-handed W-boson. If not having led to such radical consequences, i.e. this will testify to the classical (V – A) theory being valid, it will also be a remarkable result! Thus, in connection with this puzzle it can be probably said that it will be solved anyhow.

In conclusion, we would like to apologize to those readers who find our review incomplete. We only briefly mentioned, for instance, such important problems as neutron-induced nuclear reactions, moderation of fast neutrons and properties of thermal neutrons, resonance effects and diffraction, etc. An excuse can be that all those problems concern not the properties of the neutron but the processes of its interaction with matter. True, this consideration does not excuse us when the case in point is (more precisely, is not) either the nn-scattering length and its comparison with the pp-scattering length or weak nn-interaction proceeding with the P-parity violation. Here we may be excused only with the known aphorism: "Boundless cannot be grasped".

Studies of the neutron properties are being continued and remain an attractive and promising problem.

References

1. Abov Yu G, Gul'ko A D, Krupchitskiĭ P A *Polyarizovannye Medlennye Neĭtrony* (Polarized Slow Neutrons) (Moscow: Atomizdat, 1966)
2. Aleksandrov Yu A *Fundamental'nye Svoĭstva Neĭtrona* 3rd edition (Fundamental Properties of Neutrons) (Moscow: Energoatomizdat, 1992) [Translated into English (Oxford: Clarendon Press, 1992)]
3. Vlasov N A *Neĭtrony* 2nd edition (Neutrons) (Moscow: Nauka, 1971)

4. Gurevich I I, Tarasov L V *Fizika Neĭtronov Nizkikh Énergiĭ* (Low-Energy Neutrons Physics) (Moscow: Nauka, 1965) [Translated into English (Amsterdam: North-Holland Publ. Co., 1968)]
5. Ignatovich V K *Fizika Ul'trakholodnykh Neĭtronov* (The Physics of Ultracold Neutrons) (Moscow: Nauka, 1986) [Translated into English (Oxford: Clarendon Press, 1990)]; Ignatovich V K, Lushchikov V I *Fiz. Elem. Chastits At. Yadra* **15** (2) 330 (1984) [*Sov. J. Part. Nucl.* **15** 149 (1984)]
6. Krupchitskiĭ P A *Fundamental'nye Issledovaniya s Polyarizovannymi Medlennymi Neĭtronami* (Fundamental Research with Polarized Slow Neutrons) (Moscow: Energoatomizdat, 1985) [Translated into English (Berlin: Springer-Verlag, 1987)]
7. Mukhin K N *Éksperimental'naya Yadernaya Fizika* Kniga 1 Chast' 1: *Svoĭstva Nuklonov, Yader i Radioaktivnykh Izlucheniĭ* 5th edition (Experimental Nuclear Physics, Book 1, Part 1: Properties of Nucleons, Nuclei and Radioactive Radiations) (Moscow: Energoatomizdat, 1993)
8. Frank A I *Usp. Fiz. Nauk* **137** (1) 5 (1982) [*Sov. Phys. Usp.* **25** 280 (1982)]
9. Weinberg S *Physica Scripta* **21** 773 (1980); Weinberg S *Usp. Fiz. Nauk* **134** (2) 333 (1981)
10. Petrov Yu V *Usp. Fiz. Nauk* **123** (3) 473 (1977) [*Sov. Phys. Usp.* **20** 937 (1977)]
11. Rutherford E *Proc. Roy. Soc. A* **97** 374 (1920)
12. Chadwick J, in *Actes du X Congres International d'Histoire des Sciences, Ithaca, New York, 1962* Vol. 1 (Paris: Herman, 1964) p. 159
13. Bothe W, Becker H *Naturwissenschaften* **18** 705 (1930)
14. Curie I *C.R. Comptes Rendus* **193** 1412 (1931)
15. Joliot F *C.R. Comptes Rendus* **193** 1415 (1931)
16. Curie I, Joliot F *C.R. Comptes Rendus* **194** 273 (1932)
17. Chadwick J *Nature* **129** (February 27) 312 (1932)
18. Heisenberg W *Z. Phys.* **77** 1 (1932)
19. Iwanenko D *Nature* **129** (3265) 798 (1932)
20. Iwanenko D *C.R. Comptes Rendus* **195** 439 (1932)
21. Fermi E *Z. Phys.* **88** 161 (1934)
22. Yukawa H *Proc. Phys.-Math. Soc. Japan* **17** (2) 48 (1935)
23. Zel'dovich Ya, Khariton Yu *Zh. Eksp. Teor. Fiz.* **9** 1425 (1939); *Zh. Eksp. Teor. Fiz.* **10** 29 (1940); *Zh. Eksp. Teor. Fiz.* **10** 477 (1940)
24. Fermi E *Nature* **133** (June 16) 898 (1934)
25. Hahn O, Strassmann F *Naturwissenschaften* **27** 11 (1939)
26. McMillan E, Abelson P H *Phys. Rev.* **57** 1185 (1940)
27. Mukhin K N *Éksperimental'naya Yadernaya Fizika* Kniga 1 Chast' 2: *Yadernye Vzaimodeĭstviya* 5th edition (Experimental Nuclear Physics, Book 1, Part 2: Nuclear Interactions) (Moscow: Energoatomizdat, 1993)
28. "Review of Particle Properties" *Phys. Rev. D* **50** 1173 (1994)
29. Pauli W, in *Theoretical Physics in the Twentieth Century* (New York: Interscience Publ., 1960) [Translated into Russian (Moscow, 1962) p. 390]
30. Pontecorvo B M *Usp. Fiz. Nauk* **141** (4) 675 (1983) [*Sov. Phys. Usp.* **26** 1087 (1983)]
31. Reines F, Cowan C L *Phys. Rev.* **92** 830 (1953); Reines F, Cowan C *Nature* **178** 446 (1956) [*Usp. Fiz. Nauk* **62** 391 (1957)]
32. Shapiro F L *Fiz. Elem. Chastits At. Yadra* **2** 973 (1972)
33. Zel'dovich Ya B *Zh. Eksp. Teor. Fiz.* **36** 1952 (1959) [*Sov. Phys. JETP* **36** 1389 (1959)]
34. Vladimirskiĭ V V *Zh. Eksp. Teor. Fiz.* **39** 1062 (1960) [*Sov. Phys. JETP* **12** 740 (1961)]
35. Shapiro F L *Usp. Fiz. Nauk* **95** 145 (1968) [*Sov. Phys. Usp.* **11** 345 (1968)]
36. Lushchikov V I et al. Preprint OIYaI P3-4127 (Dubna, 1968); *Pis'ma Zh. Eksp. Teor. Fiz.* **9** (1) 40 (1969) [*JETP Lett.* **9** 23 (1969)]
37. Groshev L V et al. Preprint OIYaI P3-5392 (Dubna, 1970); *Phys. Lett. B* **34** (4) 293 (1971)
38. Shapiro F L et al. Preprint OIYaI P3-5554 (Dubna, 1970); *Fiz. Elem. Chastits At. Yadra* **2** (4) 973 (1972)
39. Golikov V V, Lushchikov V I, Shapiro F L, Preprint OIYaI P3-6556 (Dubna, 1972); *Zh. Eksp. Teor. Fiz.* **64** (1) 73 (1973) [*Sov. Phys. JETP* **37** 41 (1973)]
40. Groshev L V et al. Preprint OIYaI P3-7282 (Dubna, 1973)
41. Zamyatnin Yu S et al., *Soobshch. OIYaI* P3-7946 (Dubna, 1973)
42. Shapiro F L, Preprint OIYaI P3-7135 (Dubna, 1972); in *Proc. Intern. Conf. Nuclear Structure Study with Neutrons* (London: Plenum Press, 1974) p. 259
43. Steyerl A *Phys. Lett. B* **29** 33 (1969)
44. Steyerl A "Transmissionsmessungen mit ultrakalten Noutronen" Dissertation (München: Technische Universitat München, 1971)
45. Antonov A V et al. *Pis'ma Zh. Eksp. Teor. Fiz.* **24** 387 (1976) [*JETP Lett.* **24** 352 (1976)]
46. Abov Yu G et al., in *Neĭtronnaya Fizika* Tr. Vsesoyuz. Konferentsii Part 1 (Moscow: TsNIIAtominform, 1977) p. 197
47. Kosvintsev Yu Yu, Kushnir Yu A, Morozov V I *Pis'ma Zh. Eksp. Teor. Fiz.* **23** 135 (1976) [*JETP Lett.* **23** 118 (1976)]
48. Abov Yu G et al. Preprint ITEF-16 (Moscow, 1981)
49. Abov Yu G et al. *Yad. Fiz.* **38** 122 (1983) [*Sov. J. Nucl. Phys.* **38** 70 (1983)]
50. Steyerl A, Malik S S *Nucl. Instrum. Methods Phys. Res. A* **284** 200 (1989)
51. Altarev I S et al. *Pis'ma Zh. Eksp. Teor. Fiz.* **44** 269 (1986) [*JETP Lett.* **44** 344 (1986)]
52. Altarev I S et al. *Phys. Lett. A* **80** 413 (1980)
53. Steyerl A et al. *Phys. Lett. A* **116** 347 (1986)
54. Steyerl A *Nucl. Instrum. Methods* (Netherlands) **125** 461 (1975)
55. Scheckenhofer H, Steyerl A *Phys. Rev. Lett.* **39** (21) 1310 (1977)
56. Kügler K J, Paul W, Trinks U *Phys. Lett. B* **72** 422 (1978)
57. Kügler K J et al. *Nucl. Instrum. Methods Phys. Res. A* **228** 240 (1985)
58. Anton F et al. *Nucl. Instrum. Methods Phys. Res. A* **284** 101 (1989)
59. Stoica A D, Strelkov A V, Hetzelt M *Z. Phys. B* (Germ.) **29** 349 (1978); Strelkov A V, Hetzelt M *Zh. Eksp. Teor. Fiz.* **74** 23 (1978) [*Sov. Phys. JETP* **47** 11 (1978)]
60. Kosvintsev Yu Yu, Morozov V I, Terekhov G I *Pis'ma Zh. Eksp. Teor. Fiz.* **36** 346 (1982) [*JETP Lett.* **36** 424 (1982)]
61. Steyerl A, Malik S S, in *Lectures VII School on Neutron Physics, Ratmino, 3 – 22 September 1995* Vol. 1 (Dubna, 1995) p. 109
62. Mampe W et al. *Nucl. Instrum. Methods Phys. Res. A* **284** 111 (1989)
63. Snell A H, Miller L C *Bull. Am. Phys. Soc.* **23** 2 (1948)
64. Snell A H, Miller L C *Phys. Rev.* **74** 1217 (1948)
65. Robson J M *Phys. Rev.* **77** 747 (1950)
66. Robson J M *Phys. Rev.* **78** 311 (1950)
67. Spivak P E et al., in *Doklady Sovetskoĭ Delegatsii na Mezhdunarodnoĭ Konferentsii po Mirnomu Ispol'zovaniyu Atomnoĭ Énergii. Zheneva 1955 Fizicheskie Issledovaniya* (Moscow: Izdatel'stvo Akad. Nauk SSSR, 1955) p. 235
68. Bondarenko L N et al. *Pis'ma Zh. Eksp. Teor. Fiz.* **28** (5) 328 (1978) [*JETP Lett.* **28** 303 (1978)]
69. Spivak P E *Zh. Eksp. Teor. Fiz.* **94** (9) 1 (1988) [*Sov. Phys. JETP* **67** 1735 (1988)]
70. Byrne J et al. *Phys. Rev. Lett.* **65** 289 (1990)
71. Byrne J et al. *Nucl. Instrum. Methods Phys. Res. A* **284** 116 (1989)
72. Christensen C J et al. *Phys. Rev. D* **5** 1628 (1972)
73. Last J et al. *Phys. Rev. Lett.* **60** 995 (1988)
74. Kossakowski R et al. *Nucl. Phys. A* **503** 473 (1989)
75. Mampe V et al. *Pis'ma Zh. Eksp. Teor. Fiz.* **57** (2) 77 (1993) [*JETP Lett.* **57** 82 (1993)]
76. Alfimenkov V P et al. *Pis'ma Zh. Eksp. Teor. Fiz.* **52** (7) 984 (1990) [*JETP Lett.* **52** 373 (1990)]
77. Kosvintsev Yu Yu, Morozov V I, Terekhov G I *Pis'ma Zh. Eksp. Teor. Fiz.* **44** (10) 444 (1986) [*JETP Lett.* **44** 571 (1986)]; Morozov V I *Nucl. Instrum. Methods Phys. Res. A* **284** 108 (1989)
78. Mostovoĭ Yu A *Yad. Fiz.* (in press, vyp. 7 1996)
79. Wilkinson D H *Nucl. Phys. A* **377** 474 (1982)
80. Sirlin A *Phys. Rev. D* **35** 3423 (1987)
81. Hardy J C et al. *Nucl. Phys. A* **509** 429 (1990)
82. Jackson J D, Treiman S B, Wyld H W *Phys. Rev.* **106** 517 (1957)
83. Erozolimskiĭ B G, Mostovoĭ Yu A *Yad. Fiz.* **53** (2) 418 (1991)
84. Trebukhovskiĭ Yu V et al. *Zh. Eksp. Teor. Fiz.* **36** 1314 (1959) [*Sov. Phys. JETP* **36** 931 (1959)]
85. Vladimirskiĭ V V et al. *Izv. Akad. Nauk SSSR Ser. Fiz.* **25** 1121 (1961) [*Bull. Acad. Sci. USSR Ser. Phys.* **25** 1128 (1961)]
86. Grigor'ev V K et al. *Yad. Fiz.* **6** 329 (1967)
87. Balashov S N, Mostovoi Yu A, JINR E3-94-419 ISINN-2 (Dubna, 1994) p. 72
88. Stratowa Chr, Dobrozemsky R, Weinzierl P *Phys. Rev. D* **18** (11) 3970 (1978)

89. Bopp P et al. *Phys. Rev. Lett.* **56** 919 (1986)
90. Erozolimskiĭ B G et al. *Yad. Fiz.* **52** (6) 1583 (1990)
91. Erozolimskiĭ B G et al. *Yad. Fiz.* **30** (3) 692 (1979)
92. Schreckenbach K et al. *Phys. Lett. B* **349** 427 (1995)
93. Bussiere A et al. *J. Phys. E: Sci. Instrum.* **21** 1183 (1988)
94. Erozolimskiĭ B G, Frank A I, Mostovoĭ Yu A, Preprint IAE-3180 (Moscow, 1979)
95. Kuznetsov I A et al. *Pis'ma Zh. Eksp. Teor. Fiz.* **60** (5) 311 (1994) [*JETP Lett.* **60** 315 (1994)]
96. Kuznetsov I A et al. *Phys. Rev. Lett.* **75** (5) 794 (1995)
97. Serebrov A P et al. *Nucl. Instrum. Methods Phys. Res. A* **357** 503 (1995)
98. Erozolimskiĭ B G et al. *Yad. Fiz.* **8** (1) 176 (1968)
99. Steinberg R I et al. *Phys. Rev. Lett.* **33** 41 (1974)
100. Erozolimskiĭ B G et al. *Yad. Fiz.* **28** (1) 98 (1978)
101. Mostovoĭ Yu A *Pis'ma Zh. Eksp. Teor. Fiz.* **38** 42 (1983) [*JETP Lett.* **38** 48 (1983)]
102. Christensen C J, Krohn V E, Ringo G R *Phys. Rev. C* **1** 1693 (1970)
103. Krohn V E, Ringo G R *Phys. Lett. B* **55** 175 (1975)
104. Erozolimskiĭ B G et al. *Yad. Fiz.* **11** (5) 1049 (1970)
105. Mostovoĭ Yu A, Frank A I *Pis'ma Zh. Eksp. Teor. Fiz.* **24** (1) 43 (1976) [*JETP Lett.* **24** 38 (1976)]
106. Gaponov Yu V, Shul'gina N B *Yad. Fiz.* **49** (5) 1359 (1989) [*Sov. J. Nucl. Phys.* **49** 845 (1989)]
107. Gaponov Yu V, Spivak P E, Shul'gina N B *Yad. Fiz.* **52** (6) 1653 (1990)
108. Carnoy A S et al. *Phys. Rev. Lett.* **65** 3249 (1990)
109. Dubbers D, Mampe W, Döhner J *Europhys. Lett.* **11** (3) 195 (1990)
110. Savard G et al. *Phys. Rev. Lett.* **74** (9) 1521 (1995)
111. Serebrov A P, Romanenko N V *Pis'ma Zh. Eksp. Teor. Fiz.* **55** (9) 490 (1992) [*JETP Lett.* **55** 503 (1992)]
112. Bloch F *Phys. Rev.* **50** 259 (1936); *Phys. Rev.* **51** 994 (1937)
113. Schwinger J S *Phys. Rev.* **51** 544 (1937)
114. Landau L D *Zh. Eksp. Teor. Fiz.* **32** 405 (1957) [*Sov. Phys. JETP* **5** 336 (1957)]; *Nucl. Phys.* **3** 127 (1957)
115. Ellis J et al. *Nucl. Phys. B* **304** 205 (1988)
116. Ellis J *Nucl. Instrum. Methods Phys. Res. A* **284** 33 (1989)
117. Sakharov A D *Pis'ma Zh. Eksp. Teor. Fiz.* **5** 32 (1967) *JETP Lett.* **5** 24 (1967)]
118. Ellis J et al. *Phys. Lett. B* **99** 101 (1981)
119. Pendlebury J M *Ann. Rev. Nucl. Part. Sci.* **43** 687 (1993)
120. Bernstein J, Feinberg G, Lee T D *Phys. Rev.* **139** (6B) B1650 (1965)
121. Feinberg G *Phys. Rev.* **140** (5B) B1402 (1965)
122. Arbuzov B A *Usp. Fiz. Nauk* **95** 460 (1968) [*Sov. Phys. Usp.* **11** 493 (1969)]
123. Baird J K et al. *Bull. Am. Phys. Soc.* **12** 1073 (1967)
124. Braaten E, Li C S, Yuan T C *Phys. Rev. Lett.* **64** 1709 (1990)
125. Dress W B et al. *Phys. Rev. D* **15** (1) 9 (1977)
126. Greene G L et al. *Phys. Rev. D* **20** 2139 (1979)
127. Smith K F et al. *Phys. Lett. B* **234** 191 (1990)
128. Altarev I S et al. *Phys. Lett. B* **276** 242 (1992)
129. Rosenbluth M N *Phys. Rev.* **79** (4) 615 (1950)
130. Hofstadter R *Ann. Rev. Nucl. Sci.* **7** 231 (1957)
131. Mukhin K N *Éksperimental'naya Yadernaya Fizika* Kniga 2 *Fizika Élementarnykh Chastits* 5th edition (Experimental Nuclear Physics, Book 2: Physics of Elementary Particles) (Moscow: Energoatomizdat, 1993)
132. Samosvat G S, in *Lectures VII School on Neutron Physics, Ratmino, 3 – 22 September 1995* Vol. 1 (Dubna, 1995) p. 49
133. Leeb H, Teichtmeister C *Phys. Rev. C* **48** 1719 (1993)
134. Alexandrov Yu A, in *Lectures VII School on Neutron Physics, Ratmino, 3 – 22 September 1995* Vol. 1 (Dubna, 1995) p. 9
135. McReynolds A W *Phys. Rev.* **83** (1) 233 (1951)
136. Dabbs J W T et al. *Phys. Rev.* **139** (3B) 756 (1965)
137. McReynolds A W *Bull. Am. Phys. Soc.* **12** (1) 105 (1967)
138. Okonov E O, Podgoretskiĭ M I, Khrustalev O A *Zh. Eksp. Teor. Fiz.* **42** (3) 770 (1962) [*Sov. Phys. JETP* **15** 537 (1962)]
139. Feinberg G, Goldhaber M *Proc. Nat. Acad. Sci. USA* **45** (8) 1301 (1959)
140. Marshak R E, Sudarshan E G *Introduction to Elementary Particle Physics* (New York, London: Interscience Publ., 1961) [Translation into Russian (Moscow: Izd. Inostr. Lit. 1962)]
141. Shapiro I S, Éstulin I V *Zh. Eksp. Teor. Fiz.* **30** (3) 579 (1956) [*Sov. Phys. JETP* **3** 626 (1956)]
142. Shull C G, Billman K W, Wedgwood F A *Phys. Rev.* **153** (5) 1415 (1967)
143. Hughes V W *Phys. Rev.* **105** (1) 170 (1957)
144. King J G *Phys. Rev. Lett.* **5** (12) 562 (1960)
145. Zorn J C, Chamberlain G E, Hughes V W *Phys. Rev.* **129** (6) 2566 (1963)
146. Baumann J et al. *J. Phys. E: Sci. Instrum.* **20** 448 (1987)
147. Borisov Yu V et al. *Kratkie Soobshch. OIYaI* N21-87 (Dubna, 1987) p. 40
148. Landsberg L G *Usp. Fiz. Nauk* **164** (11) 1129 (1994) [*Phys. Usp.* **37** 1043 (1994)]
149. Mukhin K N, Patarakin O O *Usp. Fiz. Nauk* **165** (8) 841 (1995) [*Phys. Usp.* **38** 803 (1995)]
150. Schmiedmayer J et al. *Phys. Rev. Lett.* **66** 1015 (1991)
151. Weinberg S *Sci. Am.* **244** (6) 52 (1981) [*Usp. Fiz. Nauk* **137** (1) 151 (1982)]
152. Segre É *Usp. Fiz. Nauk* **68** (4) 621 (1959)
153. Baldo-Ceolin M et al. *Phys. Lett. B* **236** (1) 95 (1990)
154. Il'inov A S et al. *Tr. III Vsesoyuznogo Seminara, Zvenigorod, 23 – 27 April, 1983* (Moscow: IYaI, 1984) p. 92
155. Okun' L B *Fizika Élementarnykh Chastits* 2nd edition (Physics of Elementary Particles) (Moscow: Nauka, 1988)
156. Strelkov A V, in *Proc. VI Intern. School on Neutron Physics: Proc. Dubna D3*, 14-91-154 (Dubna, 1990) p. 325
157. Alfimenkov V P et al. *Pis'ma Zh. Eksp. Teor. Fiz.* **55** (2) 92 (1992) [*JETP Lett.* **55** 84 (1992)]
158. Nesvizhevskiĭ V V et al. *Zh. Eksp. Teor. Fiz.* **102** (3) 740 (1992) [*Sov. Phys. JETP* **75** 405 (1992)]
159. Ageron P, Mampe W, Kilvington A I *Z. Phys. B* **59** 261 (1985)
160. Kosvintsev Yu Yu, Morozov V I, Terekhov G I *Pis'ma Zh. Eksp. Teor. Fiz.* **44** (10) 444 (1986) [*JETP Lett.* **44** 571 (1986)]
161. Morozov V I *Nucl. Instrum. Methods Phys. Res. A* **284** 108 (1989)
162. Kosvintsev Yu Yu et al. *Zh. Eksp. Teor. Fiz.* **77** (10) 1255 (1979) [*Sov. Phys. JETP* **50** 642 (1979)]
163. Kilvington A J et al. *Phys. Lett. A* **125** 416 (1987)
164. Golub R, Boning K, in *Proc. Workshop on Neutron Scattering Instrumentation for SNQ, Maria Laach, Germany, 3 – 5 Sept. 1984* (Eds R Scherm, H Stiller) (Julich, Germany: KFA-Julich, 1984) p. 489
165. Yoshiki H, Ishimoto S, Utsuro M *Z. Phys. B* **67** 161 (1987)
166. Golub R *J. Phys. Lett.* (Paris) **44** L321 (1983)
167. Novopoltsev M I et al. Preprint JINR R3-84-219 (Dubna, 1984)
168. Brun T O et al. *Phys. Lett. A* **75** 223 (1980)
169. Schreckenbach K, Mampe W *J. Phys. G* **18** 1 (1992)
170. Golub R, Lamoreaux S K *Phys. Rep.* **237** 1 (1994)
171. Doyle J M, Lamoreaux S K *Europhys. Lett.* **26** 253 (1994)
172. Golub R, Pendlebury J M *Rep. Prog. Phys.* **42** 439 (1979)
173. Ageron P et al. *Phys. Lett. A* **66** 469 (1978)
174. Erozolimski B G, in *Lectures VII School on Neutron Physics, Ratmino, 3 – 22 September 1995* Vol. 1 (Dubna, 1995) p. 38
175. Vorobiev A V et al. *Nucl. Instrum. Methods Phys. Res. A* **284** 127 (1989)
176. Schopper H F *Phys. Blätter.* **17** 316 (1961); *Phys. Blätter.* **16** 88 (1961)